


5-2017

ROLE AND REGULATION OF SPHINGOSINE 1-PHOSPHATE IN ERYTHROCYTE

Kaiqi Sun

Follow this and additional works at: http://digitalcommons.library.tmc.edu/utgsbs_dissertations

 Part of the [Biochemistry Commons](#), and the [Medicine and Health Sciences Commons](#)

Recommended Citation

Sun, Kaiqi, "ROLE AND REGULATION OF SPHINGOSINE 1-PHOSPHATE IN ERYTHROCYTE" (2017). *UT GSBS Dissertations and Theses (Open Access)*. 736.

http://digitalcommons.library.tmc.edu/utgsbs_dissertations/736

This Dissertation (PhD) is brought to you for free and open access by the Graduate School of Biomedical Sciences at DigitalCommons@TMC. It has been accepted for inclusion in UT GSBS Dissertations and Theses (Open Access) by an authorized administrator of DigitalCommons@TMC. For more information, please contact laurel.sanders@library.tmc.edu.

ROLE AND REGULATION OF SPHINGOSINE 1-PHOSPHATE IN ERYTHROCYTE

By

Kaiqi Sun, B.S

APPROVED:

Yang Xia, M.D, Ph.D.
Advisory Professor

Rodney E. Kellems, Ph.D.

Dorothy E. Lewis, Ph.D.

Harinder S. Juneja, M.D.

Zheng Chen, Ph.D.

APPROVED:

Dean, The University of Texas
MD Anderson Cancer Center UTHHealth Graduate School of Biomedical Sciences

ROLE AND REGULATION OF SPHINGOSINE 1-PHOSPHATE IN ERYTHROCYTE

A

THESIS

Presented to the Faculty of

The University of Texas

MD Anderson Cancer Center UTHealth

Graduate School of Biomedical Sciences

in Partial Fulfillment

of the Requirements

for the Degree of

DOCTOR OF PHILOSOPHY

by

Kaiqi Sun, B.S

Houston, Texas

May, 2017

Copyright

1. For the publication titled **Elevated adenosine signaling via adenosine A2B receptor induces normal and sickle erythrocyte sphingosine kinase 1 activity** that was published in *Blood* in 2015, the journal does not require permission to reuse publications of the authors for dissertation, as quoted below:

“Specific examples of acceptable author reuse and sharing include:

Using the article in theses and/or dissertation.

Authors reusing their own material in the above ways must include appropriate attribution and do not need to contact Blood for permission.”

2. For the publication titled **Sphingosine-1-phosphate promotes erythrocyte glycolysis and oxygen release for adaptation to high-altitude hypoxia** that was published in *Nature Communications* in 2016, permission to reuse the whole article for thesis was obtained from www.copyright.com with license number: 4051490592058.

Dedication

I dedicate this thesis:

to my parents Hong Sun and Hong Jiang for their continuing unconditional support and love;

to the three grandparents-Qingan Sun, Shulan Li and Xiuqin Xu that I lost during my PhD study for passing on the genes and family legacies;

and to the love of my life-my wife Weixia Yan, for her company and comfort that gave me the strength to overcome the challenges in the past six years!

Acknowledgement

First and foremost, I would like to express the greatest gratitude to my mentor **Dr. Yang Xia**, Professor and McGovern Scholar at the Department of Biochemistry and Molecular Biology, The University of Texas McGovern Medical School, for her invaluable mentoring, which enabled me to make exciting discoveries and develop the critical thinking ability that will benefit me throughout my lifetime. The motto that she gave to me—**“Reject the rejections”** will be memorized and exercised in my whole life.

Second, I am deeply grateful to the helpful suggestions and critiques given by my current and previous advisory committee members: **Dr. Rodney E. Kellems**, **Dr. Dorothy E. Lewis**, **Dr. Harinder S. Juneja**, **Dr. Zheng Chen** and **Dr. Cheng-chi Lee**.

Third, I could not have made these exciting discoveries without the great help from **Dr. Yujin Zhang** and many other current and previous members in the Xia lab, and the great collaborations with **Dr. Angelo D’Alessandro** at The University of Colorado School of Medicine and **Dr. Martin K. Safo** at the Virginia Commonwealth University.

Fourth, I wish to express my sincere acknowledgement to the Department of Biochemistry and Molecular Biology, The University of Texas McGovern Medical School, the Biochemistry and Molecular Biology Graduate Program and The University of Texas Graduate School of Biomedical Sciences at Houston.

ROLE AND REGULATION OF SPHINGOSINE 1-PHOSPHATE IN ERYTHROCYTE

Kaiqi Sun

Advisory Professor: Yang Xia, M.D, Ph.D.

Sphingosine 1-phosphate (S1P) is a bioactive signaling sphingolipid produced in every mammalian cell. It plays a variety of important roles both in and outside of cells. S1P is highly enriched in mature erythrocytes because of the high enzymatic activity of the S1P-generating enzyme Sphingosine Kinase 1 (Sphk1) and the absence of S1P degrading enzymes. Erythrocytes are considered only a major reservoir for S1P because they supply S1P to the circulation for the regulation of various physiological processes which include but are not limited to immune cell trafficking, endothelial integrity and hematopoietic stem cell mobilization. However, if S1P plays a role in the oxygen delivery ability of erythrocyte is unknown. Recent studies using unsupervised metabolomics screening revealed significantly higher S1P levels in Sickle Cell Disease mice. Moreover, the activity of erythrocyte Sphk1 was also higher in SCD and was further increased by hypoxia. Elevated erythrocyte Sphk1 and S1P contribute to sickling and SCD progression, though by an unknown mechanism. Here in this thesis, I provide answers to three key questions regarding S1P and Sphk1 in erythrocytes: i) the regulation of erythrocyte Sphk1 activation; ii) the function of erythrocyte Sphk1/S1P in hypoxia adaptation; iii) the mechanism underlying the detrimental role of

erythrocyte Sphk1/S1P in SCD. Elevated adenosine, a signaling molecule induced by hypoxia, increases erythrocyte Sphk1 activity in normal and sickle erythrocytes by activating the A2B adenosine receptor (ADORA2B) which then leads to activation of protein kinase A (PKA) and Extracellular Signal Regulated Kinase 1/2 (ERK1/2) signaling pathways. Activated erythrocyte Sphk1 and elevated S1P are beneficial to hypoxia adaptation by promoting erythrocyte glycolysis to increase oxygen release. In SCD, erythrocyte Sphk1/S1P mediated elevation of glycolysis is detrimental because of the increased sickling and oxidative stress induced. The discoveries reported in this thesis not only extend human knowledge in understanding erythrocyte physiology and pathology, but also reveal several innovative mechanism-based therapeutic targets that can be harnessed to develop treatments for hypoxia and SCD.

Table of Contents

Approval Sheet	i
Titel page	ii
Copyright	iii
Dedication	iv
Acknowledgement	v
Table of Contents	viii
List of Illustrations	xi
List of Tables	xiii
Abbreviations	xiv
I. Introduction	17
1.1 Extracellular and Intracellular Roles of S1P	18
1.2 Role and Regulation of Sphingosine Kinase 1	19
1.3 Erythrocyte: production and destruction	20
1.4 Erythrocyte: metabolism and function	22
1.5 Response and Adaptation to Hypoxia	24
1.6 Sickle Cell Disease	26
II. Methods	30
2.1 Human subjects	30
2.2 Mice	30
2.3 Polyethylene glycol-modified ADA (PEG-ADA) treatment	31
2.4 Blood collection and preparation from humans and mice	32
2.5 Plasma adenosine analysis	32
2.6 Isolation of total erythrocytes and treatment of human and mouse erythrocytes <i>in vitro</i>	33
2.7 Sphk1 activity assay	33
2.8 Erythrocyte membrane isolation and western blot	34
2.9 Metabolomics profiling	34
2.10 S1P quantification	35
2.11 Metabolic flux analysis	36
2.12 Hypoxyprobe TM detection in multiple tissues <i>in vivo</i>	36
2.13 2,3-BPG analysis and erythrocyte oxygen release capacity (P50) measurement	37
2.14 Irradiation and bone marrow transplant	38

2.15	Isolation of erythrocyte cytoplasm and measurement of Glyceraldehyde 3-phosphate dehydrogenase (GAPDH) activity	38
2.16	Immunofluorescent staining of GAPDH in erythrocytes	38
2.17	S1P beads interaction assay	39
2.18	<i>In vitro</i> reconstitution of ghost membrane	39
2.19	Morphology study of erythrocytes	40
2.20	Hemolytic analysis.....	41
2.21	Mouse organ isolation and histological analysis.....	41
2.22	Measurement of life span of erythrocytes in SCD Tg mice.....	41
2.23	Measurement of Nicotinamide adenine dinucleotide phosphate-reduced (NADPH)	42
2.24	Reactive oxygen species detection.....	42
2.25	Crystal structural studies.....	43
2.26	Statistical analysis.....	44
III.	Results.....	45
3.1	Chapter 1: Regulation of Erythrocyte Sphk1 activity	45
3.1.1	Adenosine induces Sphk1 activity in normal and sickle erythrocyte from both humans and mice	45
3.1.2	Genetic deletion of adenosine deaminase leads to excess plasma adenosine and elevated erythrocyte Sphk1 activity <i>in vivo</i>	47
3.1.3	Adenosine-induced Sphk1 activity in normal and sickle erythrocytes is dependent on adenosine receptor A2B (ADORA2B)	50
3.1.4	Genetic deletion of ADORA2B abolishes excess plasma adenosine-induced erythrocyte Sphk1 activity <i>in vivo</i>	52
3.1.5	PKA mediated ERK1/2 activation functions downstream of ADORA2B and underlies adenosine-induced Sphk1 activity in normal and sickle erythrocytes from both human and mice	54
3.2	Chapter 2: Erythrocyte S1P Promotes Hypoxia Adaptation	58
3.2.1	Altitude induces S1P level and Sphk1 activity in human RBCs.....	58
3.2.2	Sphk1 promotes O ₂ release from mouse erythrocytes to offset hypoxia	61
3.2.3	Intracellular S1P underlies increased 2,3-BPG production.....	67
3.2.4	Glycolysis is induced by high altitude in human RBCs.....	69
3.2.5	Erythrocyte Sphk1 promotes glucose fluxes to glycolysis in hypoxia.....	71
3.2.6	High altitude induces glycolytic enzyme activity in human erythrocytes	74
3.2.7	Hypoxia-induced GAPDH activity is blunted in <i>Sphk1</i> ^{-/-} mice.....	74
3.2.8	S1P underlies hypoxia-induced GAPDH activity	77
3.3	Chapter 3: S1P induces pathogenic metabolic programming in SCD erythrocytes.....	81

3.3.1	Genetic evidence for the pathogenic role of elevated Sphk1 in SCD mice	81
3.3.2	Enhanced erythrocyte pentose phosphate pathway and anti-oxidation capacity in <i>SCD/Sphk1^{-/-}</i> mice.....	86
3.3.3	Reduced erythrocyte glycolysis and Hb-O ₂ binding affinity in <i>SCD/Sphk1^{-/-}</i> mice.....	89
3.3.4	Genetic deletion of Sphk1 channels glucose fluxes to PPP in SCD erythrocytes.....	91
3.3.5	Sphk1 regulates GAPDH localization in SCD erythrocyte.....	92
3.3.6	Co-binding of 2,3-BPG and S1P to Hb is required for S1P-induced decrease in Hb-O ₂ affinity	94
3.4	Chapter 4: X-ray crystallography reveals atomic level insight into S1P-Hb binding.....	96
IV.	Discussion.....	102
4.1	Hypoxic Regulation of Sphk1	106
4.2	Role of Sphk1/S1P in Hypoxia	107
4.3	S1P Regulates Erythrocyte Metabolism	110
4.4	Regulation of Erythrocyte Oxygen Release in Hypoxia	113
4.5	Regulation of GAPDH Activity and Localization	115
4.6	Targeting Adenosine-ADORA2B-Sphk1-S1P Axis for Therapeutics Development	116
4.7	Future Directions	119
V.	References.....	120
	Bibliography	143
	Vita	148

List of Illustrations

Figure 1. Test of potential molecules capable of inducing erythrocyte Sphk1 activity.	46
Figure 2. Adenosine directly increases erythrocyte Sphk1 activity.....	47
Figure 3. Elevated plasma adenosine induce erythrocyte Sphk1 activity increase <i>in vivo</i>	49
Figure 4. Adenosine signaling through ADORA2B to induce erythrocyte Sphk1 activity increase.	51
Figure 5. Elevated plasma adenosine increases erythrocyte Sphk1 activity through ADORA2B.....	53
Figure 6. PKA-mediated activation of ERK1/2 underlies adenosine-ADORA2B mediated erythrocyte Sphk1 activation in WT mice and normal human individuals.....	55
Figure 7. PKA-mediated activation of ERK1/2 underlies adenosine-ADORA2B mediated erythrocyte Sphk1 activation in SCD Tg mice and SCD patients.....	56
Figure 8. Concurrent increase of erythrocyte Sphk1 activity, S1P production and O ₂ delivery ability in human high-altitude study.....	59
Figure 9. Plasma S1P concentration increases in human and mice under hypoxia.	61
Figure 10. Hypoxia-induced Sphk1 and S1P increase regulate 2,3-BPG level, O ₂ delivery ability and tissue hypoxia in mice. Erythrocyte Sphk1 activity.....	63
Figure 11. Arterial hemoglobin oxygen saturation (SaO ₂) in WT and <i>Sphk1</i> ^{-/-} mice under normoxia and hypoxia up to 72 hours.....	64
Figure 12. Bone marrow derived Sphk1 and S1P are responsible for protecting tissue hypoxia by inducing erythrocyte 2,3-BPG levels and O ₂ release capacity.....	66
Figure 13. Erythrocyte Sphk1 activity measurements in bone-marrow transplanted mice.....	67
Figure 14. Regulation of erythrocyte 2,3-BPG production by Sphk1-S1P is independent of S1P receptors.	68
Figure 15. Metabolomic screening revealed time-dependent increase of glycolysis and decrease of PPP in erythrocyte from humans exposed to high-altitude hypoxia.....	70
Figure 16. Alteration of erythrocyte glucose metabolism favoring glycolysis in hypoxia.	73

Figure 17. Sphk1-mediated production of S1P functions intracellularly underlying hypoxia-induced cytosolic GAPDH by inducing GAPDH release from membrane to cytosol .	75
Figure 18. Cytosolic GAPDH activity in erythrocytes isolated from WT and Sphk1 ^{-/-} mice treated with different doses of S1P under normoxia and hypoxia for 6 hours.	76
Figure 19. S1P promotes deoxy-Hb anchoring to the membrane and enhances GPADH release from membrane to cytosol only under hypoxia but not normoxia deoxy-Hb.	78
Figure 20. Generation and confirmation of <i>SCD/Sphk1</i> ^{-/-} mice.	82
Figure 21. Genetic deletion of Sphk1 improves disease conditions in SCD Berkeley mice.	85
Figure 22. Enhanced pentose phosphate pathway and anti-oxidant capacity in <i>SCD/Sphk1</i> ^{-/-} mouse erythrocytes.	88
Figure 23. Genetic deletion of Sphk1 reduces glycolysis and O ₂ release.	91
Figure 24. Genetic deletion of Sphk1 channels glucose flux to PPP in SCD erythrocytes.	92
Figure 25. Sphk1-mediated production of S1P functions intracellularly to regulate GAPDH and Hb localization and subsequent metabolic consequences.	94
Figure 26. Functional evidence of S1P binding to Hb and stabilizing deoxyHb in T-state.	95
Figure 27. Structural evidence of S1P binding to Hb and stabilizing deoxyHb in T-state.	99
Figure 28. Regulation of erythrocyte Sphk1 activity by adenosine signaling.	104
Figure 29. Hypoxia-induced S1P promotes glycolysis for hypoxia adaptation.	104
Figure 30. Erythrocyte Sphk1/S1P induces impaired metabolic reprogramming in SCD.	105
Figure 31. Role and Regulation of Erythrocyte Sphingosine 1-phosphate	106

List of Tables

Table 1. Complete Blood Count of WT, SCD and <i>SCD/Sphk1^{-/-}</i> mice.	84
Table 2. Crystallographic data for deoxyHbA-S1P-2,3-BPG and deoxyHbA-S1P complex structures...	100

Abbreviations

2,3-BPG: 2,3-Bisphosphoglycerate

ADA: Adenosine deaminase

ADORA1: adenosine receptor A1

ADORA2A: adenosine receptor A2A

ADORA2B: adenosine receptor A2B

ADORA3: adenosine receptor A3

ATP: adenosine triphosphate

deoxyHb: deoxygenated-hemoglobin

ERK1/2: Extracellular Signal Regulated Kinase 1/2

FDA: US Food and Drug Administration

GAPDH: Glyceraldehyde 3-phosphate dehydrogenase

GPCRs: G protein coupled receptors

Hb: hemoglobin

HbA: normal hemoglobin

HbS: sickle hemoglobin

HCT: hematocrit

H&E: hematoxylin and eosin

HIF: hypoxia-inducible factors

HIF-1: hypoxia-inducible factors-1

HPLC: High Performance Liquid Chromatography

NADP: Nicotinamide adenine dinucleotide phosphate

NADPH: Nicotinamide adenine dinucleotide phosphate-reduced

NECA: 5'-(N-ethyl-carboxamido) adenosine

NHS: N-hydroxysuccinimide

oxyHb: oxygenated-hemoglobin

PBS: Phosphate-buffered saline

PEG-ADA: Polyethylene glycol-modified adenosine deaminase

PPP: pentose phosphate pathway

PKA: protein kinase A

S1P: sphingosine 1-phosphate

S1P1: sphingosine 1-phosphate receptor 1

S1P2: sphingosine 1-phosphate receptor 2

S1P3: sphingosine 1-phosphate receptor 3

S1P4: sphingosine 1-phosphate receptor 4

S1P5: sphingosine 1-phosphate receptor 5

SCD: sickle cell disease

Sphk1: sphingosine kinase 1

Sphk2: sphingosine kinase 2

Sphks: sphingosine kinases

WT: wild type

I. Introduction

Sphingosine 1-phosphate (S1P) is a lipid mediator derived from sphingosine, named after the Greek mythological creature Sphinx [1]. Since its discovery, important functions of S1P has been found in a variety of physiological and pathophysiological processes in mammalian cells, as well as in plants, worms, flies, mold and yeast [1], suggesting an evolutionally conserved role for S1P. In humans, S1P levels are generally low in other tissues but significantly higher in blood [2, 3]. Erythrocytes, the most abundant cells in circulation, are considered the major source of circulating S1P levels because they store and release large amount of S1P spontaneously [4]. However, little is known about the role and regulation of S1P in erythrocytes.

Recently, through accurately measuring functional phenotypes that are the net results of genomic, transcriptomic and proteomic changes, metabolomics profiling has become a new tool to study mature erythrocytes, where gene expression profiling is not an option due to lack of a nucleus and *de novo* protein synthesis machinery. Substantial metabolic alterations in erythrocytes of humans [5, 6] and mice [7] in various physiological and pathological conditions have been discovered which suggest multiple therapeutic possibilities. Interestingly, metabolomics screening revealed that erythrocyte S1P levels are elevated in patients and mice with Sickle Cell Disease (SCD)[5, 8], as well as in humans exposed to high-altitude hypoxia[9]. Here in this thesis, I report the role and regulation of S1P in normal and SCD erythrocytes.

1.1 Extracellular and Intracellular Roles of S1P

S1P is a versatile bioactive lipid mediator both inside and outside of cells. It is the ligand of five G-protein coupled receptors (GPCRs) named S1P1-S1P5, each with high affinity and K_d at nanomolar (nM) range [1, 10]. Each S1P receptor has its own pattern of tissue distribution and function, though there is some overlapping among the five. For example, S1P1 plays a key role in immune cell trafficking and vascular integrity; S1P2 has a role in vasoconstriction and hearing loss; S1P3 contributes to leukocyte rolling; S1P4 regulates thrombopoiesis during stress-induced accelerated platelet production; and S1P5 mediates the immune suppression of the human brain endothelial barrier [10]. Besides the extracellular signaling role, intracellular S1P regulates histone deacetylation [11], ubiquitin functions [12], mitochondrial assembly and the activity of β -site amyloid precursor protein cleaving enzyme-1 [10].

S1P levels are controlled by the balance of the two generating enzymes and three degrading enzymes-S1P lyase and S1P phosphatase 1 and 2. Due to the high activity of S1P degrading enzymes, S1P levels are generally low in peripheral tissues and in nucleated cells with values below 100nmole/g [13]. Contrary to low tissue S1P levels, the highest S1P concentration in the body is found in blood where concentrations reach approximately 200 nM in human and 700 nM in mouse plasma in normal conditions [14, 15]. The high S1P level in circulation and the concentration gradient between circulation and peripheral tissues is important for various physiological processes, including lymphocyte trafficking[16], vascular integrity[17], bone homeostasis[18], neovascularization[19], and antigen presentation[20], primarily because of activating the five S1P receptors. Mature erythrocytes contain Sphk1 but not

the S1P degrading enzymes, presumably due to the lack of nuclei and other organelles [4, 21]. Because of such unique features, erythrocytes produce and store large amounts of S1P [8] and accounts for nearly all embryonic S1P and approximately 75% of adult plasma S1P in mice [16, 22]. In mouse erythrocytes, S1P level is about 1~2 μM at normal condition but can reach 8~10 μM in SCD [8]. However, since the initial discovery of the enrichment of S1P in erythrocytes, it remains unknown how S1P production is regulated in erythrocytes and if S1P has a role in erythrocyte function.

1.2 Role and Regulation of Sphingosine Kinase 1

Sphingosine Kinase 1 (Sphk1) is one of the two isoenzymes that generate S1P by adding a phosphate to the sphingosine backbone with the consumption of one ATP molecule. The two Sphks have functional redundancy because mice with genetic deficiency of either one can survive and procreate successfully [23]. However, deletion of both enzymes causes embryonic lethality [23]. Although catalyzing the same reaction, the two Sphks originate from different genes and show different substrate specificities, tissue distributions, and subcellular localization patterns [24]. For example, unlike its isoenzyme Sphk2 that is localized to the nucleus, Sphk1 is mainly found in the cytosol, and migrates to the plasma membrane once activated by phosphorylation [25]. During mouse embryonic development, Sphk1 expression reaches the highest at embryonic day 7 and decreases thereafter, whereas Sphk2 expression increases gradually up to embryonic day 17 [26, 27]. Moreover, highly active Sphk1 is found in blood and contributes to the high concentration of circulating S1P. It is also found in the spleen, lungs, brain and liver; whereas SphK2 was predominantly found in brain, liver, heart, and kidney [26-28].

Regulation of Sphk1 occurs at transcriptional, translational and post-translational modification stage. Because of the importance of its product, regulation of Sphk1 has been extensively studied in nucleated cells focusing primarily on transcriptional regulation. Upregulation of Sphk1 expression is found in different types of cancer, including solid tumors of the breast, colon, lung, ovary, stomach, uterus, kidney, and rectum, as well as in leukemia, and has been linked to tumor survival and growth, angiogenesis or lymphangiogenesis and to radiation or chemotherapy resistance [29]. Increased Sphk1 mRNA levels were detected in smooth muscle cells after hypoxia exposure [30]. In addition, at the post-translational level, early observations showed that a diverse range of growth factors, hormones, cytokines and other external stimuli such as tumor necrosis factor- α (TNF- α), interleukin-1 β , PDGF, VEGF, ET-1 and phorbol esters could increase cellular Sphk1 activity rapidly and transiently [29, 31]. Many of these agonists induce extracellular signal regulated kinase (ERK)-dependent Sphk1 phosphorylation at serine 225, leading to the translocation of Sphk1 from the cytosol to the plasma membrane where it can access the substrate sphingosine [32, 33]. However, all of these studies were performed in nucleated cells. Although erythrocytes possess high Sphk1 activity and are the major contributor to circulating S1P, factors that regulate erythrocyte Sphk1 activity remain unknown.

1.3 Erythrocyte: production and destruction

Erythrocytes are the most abundant host cells in most vertebrate animals with numbers in the trillions. They are pivotal to the development and survival of all stages in human life: embryonic, fetal, neonatal, adolescent, and adult. In adults, erythrocytes are terminally-differentiated cells with no nuclei or other cellular organelles and are

specifically evolved for oxygen (O_2) delivery. In the embryo stage, erythrocytes come from fetal liver and are nucleated and carry the fetal hemoglobin; whereas in adult stage, erythrocytes are produced mainly in the bone marrows and express the adult hemoglobin and become enucleated before entering the circulation. Erythrocytes in the embryos, also named primitive erythrocytes, are relatively larger than the adult erythrocytes. The primitive cells express embryonic globins ($\epsilon\gamma$, β^H1 , and ζ in the mouse; ϵ , γ , and ζ in man) and form a variety of distinguishable hemoglobin tetramers in man ($\zeta_2\epsilon_2$, $\alpha_2\epsilon_2$, $\zeta_2\gamma_2$, $\zeta_2\beta_2$)[34]. At mouse embryo day 11.5 (E11.5), newly emigrating erythro-myeloid progenitors differentiate in the fetal liver to produce the first definitive erythrocytes with an immediate switch to fetal/adult globins. In humans, a specific fetal β -like globin (γ -globin) is expressed of and forms HbF. These hemoglobins enable the developing fetus to extract oxygen more efficiently from the maternal blood. Mammalian definitive erythrocytes expel their nucleus before they enter the circulation and are smaller in size than primitive erythrocytes [35]. Shortly before birth, the site of erythropoiesis switches to the bone marrow and the spleen. Humans rely mainly on the bone marrow for steady-state adult erythropoiesis, but in mice the spleen remains an important erythropoietic organ during adult life. Under erythroid stress conditions, for example, low oxygen pressure or anemia, the spleen of both mouse and man is used to produce erythrocytes[36]. In adult, fetal globin gene is silenced. Hemoglobin tetramers composed of α - and β -globin ($\alpha_2\beta_2$, HbA1) account for $\sim 97\%$ of all hemoglobin in adult erythrocytes, HbA2 ($\alpha_2\delta_2$) and HbF account, respectively, for $\sim 2\%$ and $\sim 1\%$ of total hemoglobin in most adults. However, in conditions when the β -globin expression is inhibited, fetal globin gene can be re-activated[37]. Hydroxyurea, the only FDA-

approved drug for treating SCD, induces the expression of fetal globin and decreases the concentration of the mutated sickle Hb in erythrocytes, and thereby decreases sickling.

In general, human blood contains about 5 million erythrocytes per μl (normal range 4.7 million to 6.1 million for males and 4.2 million to 5.4 million for females). The average life span of erythrocytes is 120 days in humans and 55 days in mice. Under steady-state conditions, $\sim 1\%$ of the erythrocytes are cleared every day and replaced by new cells. Erythrocytes that are at the end of their lifespan or have sustained damage beyond repair will be cleared in the spleen by residential macrophages[38]. Aged erythrocytes are characterized with a decline in metabolic activity and progressive membrane remodeling, mostly due to oxidative stress and vesiculation. The programmed death of erythrocytes is termed “eryptosis”[39]. Signals that indicate the readiness of aged and damaged erythrocytes for clearance include the increased binding of natural occurring antibodies with erythrocyte membrane protein Band3, expose of the inner membrane phosphatidylserine on erythrocyte surface, decreased expression of the immunoreceptor signal regulatory protein alpha (namely CD47), and the activation of complement receptor 1 on erythrocyte membrane [40]. The tightly regulated erythropoiesis and eryptosis collectively maintain the stability and dynamics of erythrocyte number under various physiological and pathological conditions.

1.4 Erythrocyte: metabolism and function

Erythrocyte is only cell type capable of carrying oxygen from the lungs to the other organs and tissues. In real life, the body faces various challenges that require constant and swift modulation of erythrocyte O_2 delivery. Currently, there are three

factors known to regulate O₂ delivery: temperature; pH; and the levels of 2,3-Bisphosphoglycerate (2,3-BPG) in erythrocyte. In most circumstances, body temperature and pH are strictly controlled to maintain normal functions of the vital organs such as the brain and heart. However, levels of 2,3-BPG fluctuate more in response to changes of O₂ availability [41]. 2,3-BPG is the only known allosteric modulator of hemoglobin (Hb)-O₂ binding affinity. With a much higher affinity to deoxygenated-hemoglobin (deoxyHb), it binds to the deoxyHb tetramer and cause conformational change. This stabilizes the deoxyHb and shifts the oxy-deoxyHb equilibrium towards deoxyHb and thereby enables increased oxygen release[42]. Concentrations of 2,3-BPG is at millimolar with a nearly one-to-one ratio to the Hb tetramers in normal conditions; in response to hypoxia challenges, 2,3-BPG concentrations can be doubled[41].

In erythrocytes, 2,3-BPG is generated in the Rapoport-Luebering shunt of the glycolysis pathway of glucose metabolism. Glucose can be metabolized either through the glycolysis or the pentose phosphate pathway (PPP). Due to lack of mitochondria, erythrocytes rely solely on the glycolysis pathway to generate the energy currency adenosine triphosphate (ATP) from glucose. However, highly overloaded oxygen molecules are useless to erythrocytes and cause severe oxidative stress which requires the production of large amount of anti-oxidant through the pentose phosphate pathway of glucose metabolism. Therefore, erythrocytes maintain a delicate balance between glycolysis, which generates ATP and 2,3-BPG, and PPP, which produces neutralizing anti-oxidant. Studies over the past two decades have revealed an oxygen-linked mechanism that modulates erythrocyte glucose metabolism[43]. In normoxia, the glycolytic enzymes in erythrocytes were found mostly on the membrane where they bind

to the most abundant membrane protein Band3. In low oxygen conditions, deoxyHb increases and binds to Band3, which causes the release of glycolytic enzymes, such as the Glyceraldehyde 3-phosphate dehydrogenase (GAPDH), to the cytosol where they become fully active and catalyze glycolysis. Although this machinery is well-accepted, how it is regulated is unknown.

1.5 Response and Adaptation to Hypoxia

Hypoxia is defined as inadequate O₂ supply to the whole body or a region of the body. Hypoxia frequently occurs in healthy individuals exposed to a low-O₂-content environment, such as high altitude [44, 45]. At any point 1-5 days following ascent to altitudes higher than 2500 m, individuals are at risk of developing one of three forms of acute altitude illness: acute mountain sickness, high-altitude cerebral edema and high-altitude pulmonary edema, all of which can be fatal if not recognized and treated promptly[46]. Humans differ in the ability to adapt to high-altitude hypoxia [45, 47-49]. Failure to quickly adapt can result in pulmonary edema, stroke, cardiovascular dysfunction and even death [44, 50, 51]. Hypoxia is also commonly seen in patients with cardiovascular [50, 52, 53], respiratory [54, 55] and hemolytic diseases[56], which frequently promote multiple end-organ damage and failure. Thus, it is imperative to understand how human body responds and adapts to hypoxia. A myriad of studies on hypoxic responses have focused on the transcriptional and translational machineries centered around the transcription factors hypoxia-inducible factors (HIF), which are master regulators of hypoxic responses at the organ level such as heart and lung function, to the cellular level such as increased erythropoiesis and immune responses, to the molecular level including altered metabolic pathways[57]. In addition, over the last

century, a large body of clinical, genetic and demographic evidence collected in humans that colonize multiple high-altitude locales, including the Tibetan Plateau, the Andean Altiplano, and the Semien Plateau of Ethiopia [58], have shed light on the adaptation to high-altitude hypoxia. However, most of these studies focused largely on nucleated cells. Mature erythrocytes, as the only cell type capable of delivering oxygen yet without active transcriptional and translational machineries, have been neglected. There is an enormous gap in our understanding of the specific factors and signaling pathways involved in the role of erythrocytes in hypoxia adaptation and an even larger one in identifying strategies to reduce hypoxia-induced tissue damage by targeting erythrocyte oxygen release capability.

Erythrocytes quickly respond to hypoxia by increasing O₂ release, but detailed molecular mechanisms underlying such quick response remains largely obscure. A previous study from our lab revealed that erythrocyte Sphk1 activity is elevated in both patients and mice with SCD, the most prevalent hemolytic genetic disease affecting millions worldwide[8]. Intriguingly, hypoxia also significantly induces erythrocyte Sphk1 activity in SCD mice and in human sickle erythrocytes [8]. Thus, it is likely that sickle cells have a higher Sphk1 activity than normal erythrocytes in both human and mice with SCD because they constantly face hypoxia and Sphk1 activity is further increased in response to hypoxia conditions. Adenosine, a potent signaling molecule induced by hypoxia, increases in the circulation of SCD human and mice and plays detrimental effects[7]. As a building block and a critical intermediate of nucleic acids and energy metabolism, adenosine is produced and metabolized in and out of almost every cell type. Out of the cells, adenosine can be generated from ATP through two consecutive

enzymatic reactions that requires ecto-nucleoside triphosphate diphosphohydrolases CD39, which converts ATP to ADP/AMP and ecto-5'-nucleotidase CD73, which converts AMP to adenosine[59]; inside the cells, adenosine is a byproduct of the Methionine Cycle. Because adenosine is the ligand of four G-protein coupled receptors that regulate various important cellular functions, extracellular adenosine levels are finely regulated by the generating enzymes, degrading enzymes and the transporters[60]. Adenosine can be deaminized to inosine by the critical enzyme-Adenosine Deaminase (ADA), the genetic deficiency of which causes lethal immunodeficiency[61]. In addition, extracellular adenosine can be up-taken through a family of equilibrative nucleoside transporters (ENTs). Therefore, it is interesting to investigate if elevated erythrocyte Sphk1 and S1P is regulated by adenosine signaling. More intriguingly, the function of elevated S1P in erythrocytes exposed to hypoxia remains a big puzzle.

1.6 Sickle Cell Disease

Sickle Cell Disease (SCD) is a devastating genetic disorder affecting millions of people worldwide. In the United States alone, about one out of every 500 African-American children and one in every 36,000 Hispanic-American children are affected by SCD[62]. At the genetic level, SCD is caused by a point mutation at the sixth codon of the β -Hb chain that replaces glutamate with valine. This single amino acid change causes polymerization of the sickle Hb (HbS) in deoxygenated conditions. The HbS polymer then leads to erythrocyte sickling, hemolysis and vaso-occlusion, which underlie the other life-threatening complications including stroke and acute chest syndrome. Although SCD was discovered more than a century ago and identified as the “first molecular disease” in 1949 [63], and the genetic and molecular principle behind

this devastating disease has been revealed for decades, it is extremely disappointing that hydroxyurea is currently the only FDA-approved treatment. Notably, increased oxidative stress is also found in sickle erythrocytes and linked with hemolysis and disease progression [64]. Therefore, identifying specific factors and signaling pathways that contribute to sickling and oxidative stress is essential to advance our understanding of this pathogenic process and to develop novel strategies for the treatment. Using metabolomics profiling in SCD transgenic mice, our lab has revealed that both humans and mice with SCD contain significantly elevated intra-erythrocyte and circulating S1P levels [8]. Further studies using pharmacological and siRNA inhibition of Sphk1 demonstrated that elevated intracellular S1P due to increased SphK1 activity directly contributes to sickling, a central pathogenesis of the disease[8], and disease progression as well. However, the exact underlying mechanism remains unknown.

In a view of the above findings, I sought to identify: 1) specific factors and signaling pathways related to hypoxia that contribute to increased SphK1 activity in sickle and normal erythrocytes; 2) roles and mechanisms of S1P in the normal erythrocyte in response to hypoxia; 3) mechanisms underlying the pathologic effects of elevated Sphk1 and S1P in SCD erythrocytes.

Here, I report that elevated adenosine, a signaling molecule induced by hypoxia, induces erythrocyte Sphk1 activity in normal and sickle erythrocytes by activating the A2B adenosine receptor and the downstream PKA and ERK1/2 signaling pathways. Also, metabolomics profiling and functional analyses of erythrocytes of blood samples

collected from 21 young and healthy lowland individuals at sea level and at 5260 meters for up to 16 days, showed that erythrocyte S1P levels were elevated in all lowland volunteers when brought to 5260 m high altitude. Translating results from the human high-altitude study to a mouse model of hypoxia, I demonstrate that elevated erythrocyte Sphk1 activity underlies increased S1P production within erythrocytes in high altitude hypoxia conditions and that elevated erythrocyte S1P counteracts tissue hypoxia independent of S1P receptors. Mechanistically, I further revealed that erythrocyte S1P is an important hypoxia-responsive biolipid functioning intracellularly to promote erythrocyte glycolysis and trigger O₂ delivery. One step further, I demonstrated the functional and metabolic mechanisms underlying why the beneficial adaptation to high altitude in healthy individuals via the induction of S1P in normal erythrocytes is detrimental in sickle erythrocytes. Genetic deletion of Sphk1 in SCD has potent anti-sickling and anti-hemolysis effects by correcting pathogenic metabolic reprogramming, channeling glucose to the pentose phosphate pathway relative to glycolysis, lowering 2,3-BPG production and rewiring NADPH/glutathione-mediated detoxification. Moreover, the atomic level details of S1P binding to Hb were also revealed in collaboration with a group at the Virginia Commonwealth University which showed that S1P binds to the surface of deoxyHb in the presence of 2,3-BPG and induces further oxygen release and conformational change. These findings significantly enrich our understanding of the role of erythrocytes in hypoxia and the molecular regulation behind. They also open new promising scenarios in the development of innovative mechanism-based therapies for hypoxic conditions and SCD.

II. Methods

2.1 Human subjects

Individuals with sickle cell disease were identified by hematologists on the faculty of The University of Texas Medical School at Houston. Subjects participating in this study had no blood transfusion for at least 6 months before blood samples were collected. Normal human subjects were of African descent and were free of hematological disease. The research protocol, which included informed consent from the subjects, was approved by The University of Texas Health Science Center at Houston Committee for the Protection of Human Subjects.

The human high-altitude study was conducted as part of the AltitudeOmics project examining the integrative physiology of human responses to hypoxia [65]. In brief, all procedures conformed to the Declaration of Helsinki and were approved by the Universities of Colorado and Oregon Institutional Review Boards and the US Department of Defense Human Research Protection office. After written informed consent recreationally active sea-level habitants participated in the study. The participants were non-smokers, free from cardiorespiratory disease, born and raised at <1500 m, and had not travelled to elevations >1000 m in the 3 months prior to investigation.

2.2 Mice

Adenosine deaminase (ADA) deficient mice (*Ada*^{-/-}) were generated and genotyped as previously described [61, 66]. Control mice, designated *Ada*^{+/-}, were littermates that were heterozygotes for the null *Ada* allele. *Ada*^{-/-}/*Adora2b*^{-/-} mice were

generated by crossing *Ada*^{-/-} mice with *Adora2b*^{-/-} mice [67]. Mice on a mixed 129sV/C57BL/6J background were backcrossed at least 10 generations on the C57BL/6 background. Four adenosine receptor deficient mice were initially transferred from Dr. Michael R. Blackburn and later bred in our lab. Berkley SCD transgenic mice expressing exclusively human sickle hemoglobin (HbS) were purchased from The Jackson Laboratory [68]. Eight to ten-week-old male and female C57BL/6 wild-type (WT) mice were purchased from Harlan Laboratories (Indianapolis, IN). Sphingosine Kinase 1-deficient mice were initially acquired from Dr. Richard L. Proia at the National Institute of Diabetes and Digestive and Kidney Diseases, NIH (Bethesda, MD) and bred in the University of Texas Health Science Center at Houston.

All phenotypic comparisons were performed using littermates. Animal care was in accordance with National Institutes of Health guidelines and the Animal Welfare Committee at The University of Texas Health Science Center at Houston.

2.3 Polyethylene glycol-modified ADA (PEG-ADA) treatment

PEG-ADA was generated by the covalent modification of purified bovine ADA with activated polyethylene glycol as described previously [69-71]. Different dosages of PEG-ADA were delivered weekly by intra-peritoneal injection to reduce adenosine levels. Specifically, the *Ada*^{-/-} mice were maintained on enzyme therapy at 5 U/week for 8 weeks to allow for normal development. After 8 weeks, the mice were either stopped or continued given PEG-ADA for 2 weeks. For the rescue group, the enzyme therapy were paused for 11 days and then 5 units PEG-ADA were given back three days before the mice were sacrificed.

2.4 Blood collection and preparation from humans and mice

Approximately 4 ml blood was withdrawn from forearm veins of normal individuals and patients with SCD and collected in Sodium Heparin or Ethylenediaminetetraacetic acid- potassium salt (K_2EDTA) coated tubes. For mouse, 1 ml blood was collected in a 1.5-ml tube with in Sodium Heparin or K_2EDTA . For mouse blood collected for adenosine analysis (see below), blood was collected in 1.5 ml tubes containing 17 units of Sodium Heparin, 10 μM dipyridamole, 10 μM α,β -methylene ADP and 10 μM 5'-deoxycoformycin (DCF); plasma was immediately separated and placed in liquid nitrogen and stored at $-80^\circ C$. RBCs were then purified via Percoll density purification (Sigma) to remove white blood cells.

2.5 Plasma adenosine analysis

Adenosine concentration in plasma was measured by High Performance Liquid Chromatography (HPLC) as previously described[72]. In brief, 200 μl plasma was added to 200 μl 0.6 M cold perchloric acid on ice, vortexed and centrifuged at 20,000 x g for 10 min at 4 $^\circ C$. The supernatant (about 220 μl) was transferred to a new tube and neutralized with 16.5 μl 3 M $KHCO_3$ /3.6 N KOH. Phenol red (1 μl of 0.2 mg/ml) was added as indicator. The sample was acidified with 2.3 μl 1.8 M ammonium dihydrogen phosphate (pH 5.1) and 5.5 μl phosphoric acid (30%). Finally, the sample was centrifuged at 20,000 x g for 5 min and the supernatant was transferred to a new tube and stored at $-20^\circ C$. Before HPLC assay, the sample was thawed on ice, and centrifuged at 20,000 x g for 10 min. The supernatant was transferred to a new tube for HPLC analysis as described previously [66, 73].

2.6 Isolation of total erythrocytes and treatment of human and mouse

erythrocytes *in vitro*

Blood collected in heparin as an anti-coagulant was centrifuged at 240 x g for 10 min at room temperature, followed by aspiration of plasma and buffy coat. Packed erythrocytes were washed 3 times with culture media (F-10 nutrients mix, Life Technology) and re-suspended to 4% hematocrit (HCT). One ml of pelleted erythrocytes were added to each well of a 12-well plate and treated with different compounds including 5'-(N-ethyl-carboxamido) adenosine (NECA, R&D system), ADORA2B antagonist MRS 1754, PKA inhibitor H89, PKA activator Forskolin, ERK1/2 inhibitor PD 98059 (R&D system), S1P (Sigma, USA) at the concentrations indicated in respective experiments.

2.7 Sphk1 activity assay

Erythrocyte Sphk1 activity was measured using previously described methods [74, 75] with a few modifications. Briefly, RBCs were lysed in a pH7.4 Tris-HCl buffer containing 1mM EDTA, 1mM β -Mercaptoethanol, 0.3% Triton X-100, 50% glycerol and protease and phosphatase inhibitors. Then, the lysates were assayed using 250 μ M D-erythro-sphingosine in bovine serum albumin (0.4%) and [γ -³²P]ATP (10 μ Ci, 20 mM) containing 200 mM MgCl₂. Lipids were extracted and then resolved by TLC on silica gel G60 with 1-butanol/methanol/acetic acid/water (80:20:10:20, v/v). The plates were then exposed to phosphor-imaging screening (Bio-Rad) and scanned for radioactive signals as indications of the amount of S1³²P synthesized.

2.8 Erythrocyte membrane isolation and western blot

Pelleted erythrocytes were frozen and thawed in a 20-fold volume of 5mM phosphate buffer containing 150mM NaCl, protease inhibitor cocktails (Roche) and phosphatase inhibitor cocktails (Sigma), and then centrifuged with 20,000g for 20 min. Supernatant were removed and pellets were washed four times before dissolving in the same buffer with 1% Triton X-100. Protein concentration was quantified using Pierce BCA protein concentration assay (Thermo Scientific). 50µg of membrane protein were loaded for western blot detection of membrane bound Sphk1 and Sering225-phosphorylated Sphk1 with anti-Sphk1 antibody (LifeSpan) and anti-Ser225 p-Sphk1 antibody (ECM Bioscience).

2.9 Metabolomics profiling

Metabolomics extraction. Erythrocytes (100µl) and plasma samples (20µl) were immediately extracted in ice-cold lysis/extraction buffer (methanol:acetonitrile:water 5:3:2) at 1:9 and 1:25 dilutions, respectively. Samples were agitated at 4°C for 30 min, and then centrifuged at 10,000g for 15 min at 4°C. Protein pellets were discarded, and supernatants were stored at -80°C prior to metabolomics analyses[76].

Metabolomics analysis. Ten µl of erythrocyte extracts were injected into a UHPLC system (Ultimate 3000, Thermo, San Jose, CA, USA) and run on a Kinetex XB-C18 column (150 x 2.1mm, 1.7 µm particle size - Phenomenex, Torrance, CA, USA) using a 3 min isocratic flow (5% acetonitrile, 95% water, 0.1% formic acid) at 250 µl/min or a 9 min linear gradient (5-95% acetonitrile with 0.1% formic acid at 400 µl/min). The UHPLC system was coupled online with a Q Exactive mass spectrometer (Thermo, Bremen, Germany), scanning in Full MS mode (2 µscans) at 70,000 resolution in the

60-900 m/z range, 4 kV spray voltage, 15 sheath gas and auxiliary gas, operated in negative and then positive ion mode (separate runs). Calibration was performed before each analysis using positive and negative ion mode calibration mixes (Pierce, Rockford, IL, USA) to ensure sub ppm error of the intact mass. Metabolite identifications were assigned using the software Maven (Princeton, NJ, USA), upon conversion of raw files into mzXML format through MassMatrix (Cleveland, OH, USA). The software allows for peak picking, feature detection and metabolite assignment against the KEGG pathway database. Assignments were further confirmed against chemical formula determination (as gleaned from isotopic patterns and accurate intact mass), and retention times against a >750 standard compound library (Sigma-Aldrich, St. Louis, MO, USA; IROA Tech, Bolton, MA, USA)[76].

2.10 S1P quantification

Validation and quantitative analyses for S1P were performed using a Thermo Vanquish HPLC system coupled to a Thermo Q Exactive mass spectrometer and determined against commercial standard compounds S1P (>95% pure - no. S9666, Sigma Aldrich, St. Louis, MO, USA) and S1P-d7 (>99% pure - no. 860659P – Avanti Polar Lipids Inc, Alabaster, AL, USA) within the linear range, as determined through external calibration curves across 7 orders of magnitude. Samples were diluted 1:10 with methanol:acetonitrile:water (5:3:2) containing 100nmole·l⁻¹ S1P-d7, then agitated and centrifuged as described above. Supernatant (10µl per injection) was analyzed using a 4 minute gradient of 50-95% acetonitrile containing 0.1% formic acid (400µl/min) and a Kinetex C18 column (150 x 2.1 mm, 1.7 µm – Phenomenex) held at 35 °C. The

mass spectrometer was operated in positive ion mode at 70,000 resolution, scan range of 90-1350 m/z, sheath gas 25, auxiliary gas 5.

Quantification was performed by exporting integrated peak area values for endogenous and heavy S1P. Absolute quantitation was determined according to the formula: [light] = Peak Area (Light)/(Heavy)*[Heavy]*dilution factor (10 for red blood cells, 10 for plasma).

2.11 Metabolic flux analysis

Erythrocytes were cultured in HEPES buffer with 6 mmole·l⁻¹ D-Glucose-1,2,3-¹³C₃ (Sigma Aldrich)[77, 78] and extracted and processed as described above. Packed mature erythrocytes were washed 3 times with HEPES buffer and re-suspended to 4% hematocrit (HCT). One ml of erythrocytes were added to each well of a 12-well plate and pretreated with for 30 min before sample collection started. Flux analysis was performed by determining the integrated peak areas of isotopologues +2.0068 and +3.0102 Da of lactate, glucose, and Glyceraldehyde 3-phosphate in negative ion mode through the software Maven (Princeton University).

2.12 HypoxyprobeTM detection in multiple tissues *in vivo*

Tissue hypoxia levels were assessed by HypoxyprobeTM immunofluorescence as described before [79, 80]. Briefly, animals were administered HypoxyprobeTM (Pimonidazole HCl) (Hypoxyprobe, Inc.) via intraperitoneal injection (60 mg/kg body weight). In hypoxia (pO₂ < 10 mmHg), Pimonidazole HCl forms adducts with thiol groups in proteins, peptides and amino acids in a way that all atoms of the ring and side-chain of the 2-nitroimidazole are retained. Thirty min after injection, tissues were

harvested, fixed overnight in 4% buffered formalin, and embedded in paraffin. Tissue sections were deparaffined, rehydrogenated and incubated with anti-Hypoxyprome™ (rabbit anti-PAb2627AP, 1:200 dilution Hypoxyprome, Inc.) overnight at 4°C. Hypoxia signaling was detected by applying Alexa Fluor® 488-conjugated donkey anti-rabbit IgG antibody (1:1000 dilution, Life technologies). Quantification of the fluorescent signaling was performed using the Image-Pro Plus software (Media Cybernetics, Bethesda, MD). The density of the fluorescence was measured. The average densities of 20 areas per samples were determined and the SEM is indicated.

2.13 2,3-BPG analysis and erythrocyte oxygen release capacity (P50)

measurement

2,3-BPG in 20 µl erythrocyte pellet was isolated with 100 µl 0.6 M cold perchloric acid on ice, vortexed, and subsequently sonicated for 10 seconds with output 6 (W-220F, Heat systems-ultrasonic, Inc). The homogenate was centrifuged at 20,000 x g for 10 min). 80 µl supernatant was transferred to a new tube and neutralized with 10 µl 2.5 M K₂CO₃, then centrifuged at 20,000 x g for 5 min. 20 µl supernatant was used to quantify 2,3-BPG using a commercially available kit (Roche, Nutley, NJ) [72, 81] [72, 81]. For human samples, arterial blood gases were measured and the Hill equation was used to calculate P50[82]. For mouse samples, 10 µl of whole blood aliquot were mixed with 4.5ml Hemox Buffer (TCS Scientific Corporation, PA), 10 µl anti-foaming reagent [(TCS Scientific Corporation, PA) and 20 µl 22% BSA in PBS. The mixture was then injected in the Hemox Analyzer (TCS Scientific Corporation, PA)] for measurement of oxygen equilibrium curve at the temperature of 37°C.

2.14 Irradiation and bone marrow transplant

The day before irradiation, recipient mice (8 to 10 weeks of age) were treated with neomycin at 2 µg/ml in drinking water, as described previously[8]. The next day, mice were exposed to 5 Gy irradiation by RS X-ray irradiator (Rad Source Technologies, Suwanee, GA). Four hours later, the mice were exposed to the same dose of irradiation. Bone marrow cells were isolated from femur of donor mice and injected retro-orbitally into irradiated recipient mice (1×10^6 bone marrow cells per mouse). After transplant, the mice were treated with 2 µg/ml neomycin in drinking water for 2 weeks. Mice were used 8–10 weeks later for experiments.

2.15 Isolation of erythrocyte cytoplasm and measurement of Glyceraldehyde 3-phosphate dehydrogenase (GAPDH) activity

Erythrocytes were lysed by freeze and thaw in 10 volume of $5\text{mmole}\cdot\text{l}^{-1}$ cold phosphate buffer (pH 8.0) and vortexed. Erythrocyte membrane was removed by centrifuged at 20,000g for 20 minutes at 4°C. The supernatant was saved and used to measure cytosolic GAPDH activity by KDaAlert GAPDH assay kit (Life technologies)[83].

2.16 Immunofluorescent staining of GAPDH in erythrocytes

Mouse erythrocytes were fixed with 100% ice-cold methanol for 10 minutes. The fixed cells were washed two times with Phosphate-buffered saline (PBS), blocked by 1% BSA in PBS (Blocking buffer, pH 7.4.) for one hour at room temperature. Cells were incubated with monoclonal anti-GAPDH antibody (Sigma-aldrich, 1:100 in blocking buffer) at 4°C for overnight. The cells were washed three times with PBS, incubated with Alexa fluor 594 donkey anti-mouse IgG(H+L) (1:1000 dilution) or Alexa fluor 488 donkey anti-rabbit IgG(H+L) (1:1000 dilution) (Life technologies) for one hour at room

temperature in dark, then washed 3 times and re-suspended in PBS. Cell-smear were made and dried in dark. The slides were mounted with cover glass by mounting medium (VECTASHIELD H-1400, Vector, CA). Pictures were taken under Zeiss LSM 780 confocal microscope (Carl Zeiss Inc, Jena, Germany).

2.17 S1P beads interaction assay

Two μg of total erythrocyte lysate from normal individual was adjusted to $100\mu\text{L}$ using lysis buffer [20mM PIPES, $150\text{ mmole}\cdot\text{l}^{-1}$ NaCl, $1\text{ mmole}\cdot\text{l}^{-1}$ EGTA, 1% V/V Triton-X-100, $1.5\text{ mmole}\cdot\text{l}^{-1}$ MgCl_2 and $1\text{ mmole}\cdot\text{l}^{-1}$ Naorthovanidate, 0.1% SDS, 1X protease inhibitors (Roche Applied), pH7.4]. Approximately $100\mu\text{l}$ of various lipids conjugated to agarose beads including S1P-agarose beads, lysophosphatic acid-beads or sphingosine-beads (Echelon Biosciences Inc, Salt Lake City, UT) were washed twice with lysis buffer. The lysates were incubated with beads overnight at 4°C with constant gentle rotation. Protein-bound beads were washed by wash buffer ($10\text{ mmole}\cdot\text{l}^{-1}$ HEPES pH 7.4, $150\text{ mmole}\cdot\text{l}^{-1}$ NaCL, 0.25% NP-40) for 6 times. Washed beads were added $50\mu\text{L}$ of 2 x Laemmli buffer (Sigma-Aldrich) and heated at 100°C for 5 minutes. Beads were centrifuged at 5000g for 5 minutes and supernatants (eluted proteins) were separated by SDS-PAGE, trans-blotted to nitrocellulose membrane. Hemoglobin was probed with anti-human hemoglobin antibody (Santa Cruz, CA). Immuno-reactive bands were visualized by ECL using secondary antibodies conjugated with horseradish peroxidase and Super-signal West Pico chemiluminescence substrate (Piere).

2.18 *In vitro* reconstitution of ghost membrane

Nonporous silicon beads with $3.15\text{ }\mu\text{m}$ diameter (Bangs Laboratories, IN) were pretreated with 6ml specific buffer (30% $\text{H}_2\text{O}_2/30\%$ $\text{NH}_4\text{OH}/\text{H}_2\text{O}$: $1/1/5$) and sonicated

for 5 minutes, incubated at 60⁰C for 30 minutes. The beads are washed with pH5.5 millipore water for 5 times and washed with 5 mM PS for 3 times. Human or mouse ghost cells were prepared as follows: heparin-blood was centrifuged at 2,400g for 5 minutes. The plasma and buffy coat were removed. The pellet was washed twice with PBS. The cells were lysed in 5mmole·l⁻¹ phosphate buffer (pH8.0), centrifuged at 18,000g for 15 minutes. The supernatant was removed and the pellet was washed in phosphate buffer for 7 times to obtain ghost cells. The beads were coated by ghost cells to produce inside-out membrane (IOM). The IOM was washed 6 times with 5mmole·l⁻¹ phosphate buffer (PB, pH 8.0). Packed 5x10⁹ IOM beads were added 100 µl 5mmole·l⁻¹ PB (pH7.4) with 100 µM hemoglobin, varied concentrations of S1P. Beads were incubated at 37⁰C for 10 minutes, centrifuged at room temperature for 1 minute at 500g. The supernatant was transferred to new tube for GAPDH activity assay. Pellet beads were washed 6 times with PB (pH7.4). Beads were added to 100 µl of concentrated formic acid (Sigma-Aldrich), vortexed for 5 minutes. The beads were centrifuged at 2000rpm for 2 minutes. 80 µl of the supernatant was transferred to a new 1.5 ml tube and added 400µl 5M NaOH. The heme concentration was determined at 398 nm wavelength as described[84] and normalized to protein concentration. Human Hb A was used as standards for heme assay. For hypoxia condition, PB was bubbled by 8% oxygen, 92% nitrogen for 10 minutes, then beads and PB were transferred to glove box. All the steps were performed in glove box until beads were ready for heme assay.

2.19 Morphology study of erythrocytes

Blood smears were made using 1% glutaraldehyde fixed human blood or mouse tail blood from bone marrow transplanted mice. Blood smears were stained by WG16-

500ml kit (Sigma-Aldrich). Blood smears were observed using the 40x objective of an Olympus BX60 microscope. Areas where red blood cells do not overlap were randomly picked, at least 10 fields were observed and 1000 red blood cells including sickle cells were counted. The percentages of sickle cells in red blood cells were calculated.

2.20 Hemolytic analysis

The hemoglobin in mouse plasma was quantified by ELISA kits following instructions provided by the vendor (BioAssay Systems, Hayward, CA).

2.21 Mouse organ isolation and histological analysis

Mice were anesthetized and organs were isolated and fixed with 10% paraformaldehyde in PBS overnight at 4°C. Fixed tissues were rinsed in PBS, dehydrated through graded ethanol washes, and embedded in paraffin. 5µm sections were collected on slides and stained with hematoxylin and eosin (H&E).

2.22 Measurement of life span of erythrocytes in SCD Tg mice

Erythrocytes were labeled in vivo by using N-hydroxysuccinimide (NHS) biotin and the life span of circulating red blood cells was measured as described[8]. Specifically, 50 mg/kg of NHS biotin was injected into the retro-orbital plexus of SCD mice (prepared in 100µl sterile saline just prior to injection; initially dissolved at 50 mg/mL in dimethyl sulfoxide). Blood samples (5 µl) were collected the first day after biotin-injection from tail vein by venipuncture to determine the percentage of erythrocytes labeled with biotin. Subsequently, 5µl of blood were obtained by tail vein venipuncture on day 1, 3, 5 and 7 for measurement of biotinylated erythrocytes. The percentage of biotinylated erythrocytes was calculated by determining the fraction of

peripheral blood cells labeled with Ter-119 (to identify erythrocytes) that were also labeled with a streptavidin-conjugated fluorochrome by flow cytometry with a Gallios Flow Cytometer and analyzed with Kaluza software (Beckman-Coulter) at Dr. Dorothy Lewis's lab.

2.23 Measurement of Nicotinamide adenine dinucleotide phosphate-reduced (NADPH)

Erythrocyte NADPH was quantified by a commercially available kit (Sigma-Aldrich). Briefly, 10 μ l erythrocytes were used for each assay. NADPH was extracted with 800 μ l of NADP/NADPH Extraction Buffer and placed on ice for 10 minutes, then centrifuged the samples at 10,000 g for 10 minutes to remove insoluble material. Then, 10KDa molecular weight cut-off columns were used to filter out enzymes in the lysate. The filtered solution was then applied to the measurement of NADPH through a chain colorimetric reaction and the read-outs were detected by spectrophotometer.

2.24 Reactive oxygen species detection

One μ l RBC pellet was added to 1.73 μ M Dichlorodihydrofluorescein Diacetate (H₂DCFDA) in 100 μ l PBS, (Thermo Scientific) and incubated for 30~60 min in dark at 37°C. After incubation, cells were washed 3 times with 1 ml PBS each time. Afterwards, supernatant was removed and cells were re-suspended in 200 μ l PBS for flow cytometry [Gallios Flow Cytometer with Kaluza software (Beckman-Coulter)] detection and analysis of fluorescent signals at 488nm.

2.25 Crystal structural studies

Freshly prepared solution of S1P in methanol was incubated with deoxygenated Hb (40 mg/mL deoxyHb) with and without freshly prepared solution of 2,3-BPG in water for 60 minutes at Hb tetramer: 2,3-BPG:S1P molar ratio of 1:5:5 or Hb tetramer:S1P molar ratio of 1:5. The binary (deoxyHb-S1P) and ternary (deoxyHb-S1P-2,3-BPG) complex solutions were then crystallized with 0.2 M sodium acetate trihydrate, 0.1 mole·l⁻¹ sodium cacodylate trihydrate, pH 6.5 and 30% PEG 8000 using the batch method as previously described[85]. Crystals were cryo-protected with mother liquor and glycerol (3:1 ratio) prior to diffraction data collection at 100 K with a Rigaku IV ++ image plate detector using a CuK α X-rays ($\lambda = 1.54 \text{ \AA}$) from a MicroMax-007 source fitted with Varimax Confocal optics (Rigaku, The Woodlands, TX). The two complexes crystallized in orthorhombic space group P2₁2₁2, each with one tetramer per asymmetric unit. The datasets were processed with the d*trek software (Rigaku) and the CCP4 suite of programs[86].

The deoxyHb-S1P structure was first determined using molecular replacement method with Phenix v.1.8 [87], with the native deoxyHb structure, deoxyHb (2DN2)[88] and refined with both Phenix[87] and the CNS programs[89]. Model building and correction were carried out using the graphic programs COOT[90]. The refined-S1P structure was then used as a starting model to refine the deoxyHb-S1P-BPG complex structure. The deoxyHb-S1P refines to Rfactor/Rfree of 22.4/27.9% at 2.4 \AA , while deoxyHb-S1P-2,3-BPG refines to 18.2/21.1% at 1.8 \AA . A significant number of the low-resolution reflections in the ternary deoxyHb-S1P-BPG complex were characterized by high mosaicity, which could have contributed to the large difference in the Rfactor and

Rfree. The atomic coordinate and structure factor files have been deposited in the RCSB Protein Data Bank with accession codes 5KSJ for deoxyHb-S1P and 5KSI for deoxyHb-S1P-2,3-BPG. Detailed crystallographic and structural analysis parameters are reported in Table 2.

2.26 Statistical analysis

All data were presented as mean \pm SEM (standard error of mean) and analyzed statistically using GraphPad Prism 5 software (GraphPad Software). The significance of differences among two groups was assessed using Two-tailed Student's *t*-test (paired or unpaired as appropriate). Differences between the means of multiple groups were compared by one-way analysis of variance (ANOVA) or two way ANOVA, followed by a Turkey's multiple comparisons test. A *P* value of less than 0.05 was considered significant.

III. Results

3.1 Chapter 1: Regulation of Erythrocyte Sphk1 activity

This chapter is based upon: Sun K, Zhang Y, Bogdanov MV, Wu H, Song A, Li J, Dowhan W, Idowu M, Juneja HS, Molina JG, Blackburn MR, Kellems RE, Xia Y: **Elevated adenosine signaling via adenosine A2B receptor induces normal and sickle erythrocyte sphingosine kinase 1 activity**. *Blood* 2015, 125(10):1643-1652. [91], with permission from the journal *Blood* for the usage in thesis.

The highest level of extracellular S1P is found in plasma where it reaches close to the micromolar range. Even higher levels of S1P are found in erythrocytes at about 2 μ M under normal condition but can reach 8 μ M in SCD. Erythrocytes were considered to be merely an S1P reservoir before recent studies indicating potentially important functions of S1P in inducing sickling of SCD erythrocytes. Although regulation of Sphk1 at both translational and post-translational levels has been studied in nucleated cells, the question remains regarding how Sphk1 is regulated in mature erythrocytes.

3.1.1 Adenosine induces Sphk1 activity in normal and sickle erythrocyte from both humans and mice

To identify specific molecules that can induce Sphk1 activity in erythrocytes, I screened a series of molecules known to regulate Sphk1 in other cell types, including angiotensin II[92], tumor necrosis factor- α (TNF- α)[93, 94], endothelin 1 (ET-1)[95, 96] and even S1P[97], the product of Sphk1. However, none of them activated Sphk1 in wild type (WT) mouse erythrocytes (Figure 1a). Next, I decided to focus on hypoxia-induced molecules since erythrocytes Sphk1 activity is further increased in response to hypoxia[8] in SCD. Of note, early non-biased metabolomic screening showed the

accumulation of the potent hypoxia signaling molecule adenosine in the circulation of SCD mice. Like S1P, adenosine also contributes to sickling[72]. Therefore, I hypothesized that adenosine can induce erythrocyte Sphk1 activity. To test this hypothesis, I treated WT mouse erythrocytes with the potent non-metabolizable adenosine analog 5'-N-ethylcarboxamidoadenosine (NECA). NECA significantly increased Sphk1 activity, indicating that adenosine can directly induce Sphk1 activity in normal mouse erythrocytes in a time (Figure 1b) and dose (Figure 1c) dependent manner.

Figure 1

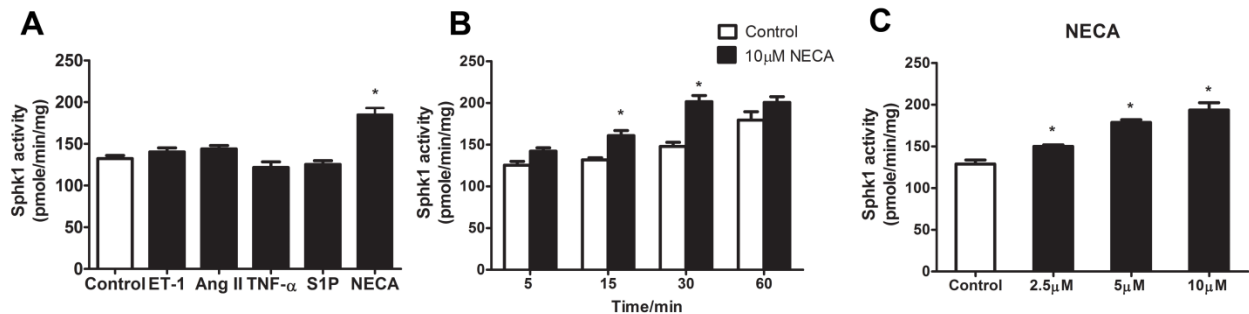


Figure 1. Test of potential molecules capable of inducing erythrocyte Sphk1 activity. (A) Sphk1 activity in primary erythrocytes from WT mice treated with endothelin-1 (100nM), angiotensin II (100nM), tumor necrosis factor- α (50 ng/ml), sphingosine 1-phosphate (100nM) and NECA (10 μ M). (B) Induction of erythrocyte Sphk1 activity by NECA in a time-dependent manner. (C) Dose-dependent erythrocyte Sphk1 activation by NECA treatment for 30 min. Values shown represents the mean \pm SEM (n=3~5 for each group).

To determine if adenosine can induce Sphk1 activity in normal human erythrocytes, I treated normal human erythrocytes with NECA and found that NECA significantly induced Sphk1 activities in normal human erythrocytes (Figure 2a). Extending to sickle human and mouse erythrocytes, similarly, I observed that the adenosine analog, NECA, can induce Sphk1 activity in both mouse and human sickle

erythrocytes (Figure 2b-c). Together, these data suggest that adenosine is a common signaling molecule responsible for increased Sphk1 activity in normal and sickle erythrocytes from both humans and mice.

Figure 2

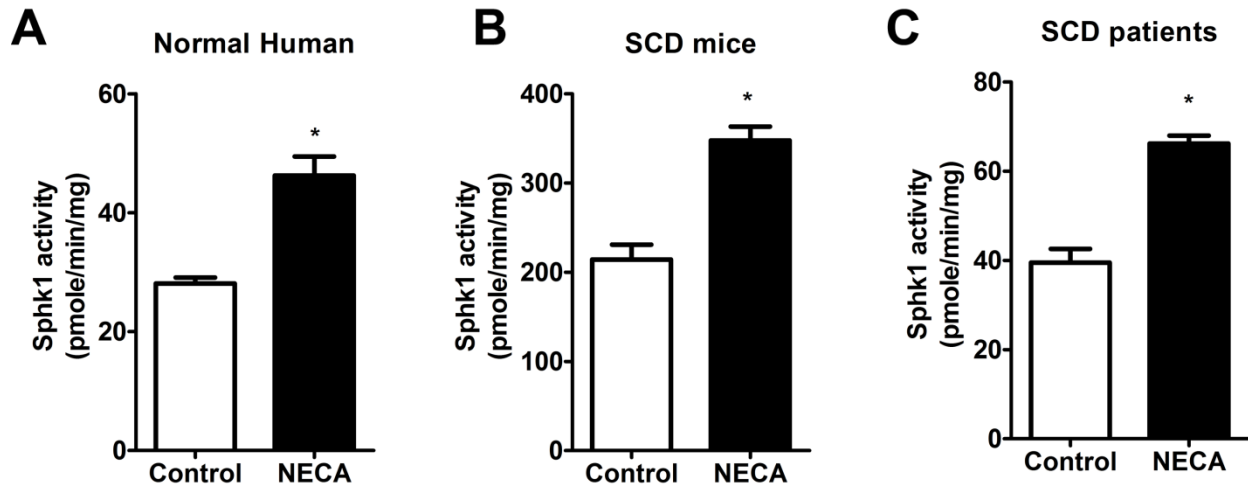


Figure 2. Adenosine directly increases erythrocyte Sphk1 activity. Sphk1 activity in primary erythrocytes from normal human subjects (A), SCD transgenic mice (B) and SCD patients (C) after NECA (10 μ M) treatment for 30 min. Values shown represent the mean \pm SEM (n=5 for SCD patients and normal human subjects; n=6 for SCD transgenic mice and WT mice). * $P < 0.05$ NECA versus control.

3.1.2 Genetic deletion of adenosine deaminase leads to excess plasma

adenosine and elevated erythrocyte Sphk1 activity *in vivo*

Although the *in vitro* data showed that adenosine induces Sphk1 activity in normal and sickle erythrocytes, I sought to extend to *in vivo* using adenosine deaminase-deficient mice (*Ada*^{-/-}). Adenosine deaminase (ADA) catalyzes the irreversible deamination of adenosine to inosine. ADA deficiency mice accumulate high levels of adenosine in the circulation and in all tissues examined [61]. Though a lethal

condition in human and mice, with regularly injected exogenous polyethylene glycol-modified adenosine deaminase (PEG-ADA) enzyme, $Ada^{-/-}$ mice and humans can maintain a low plasma adenosine level and prolong life indefinitely. Once stopping the injection, $Ada^{-/-}$ mice accumulate large amount of plasma adenosine within days [61]. Thus, using PEG-ADA enzyme therapy to regulate adenosine levels in $Ada^{-/-}$ mice is a powerful experimental strategy to investigate the role of adenosine on erythrocyte Sphk1 activity *in vivo*. Specifically, first, $Ada^{-/-}$ mice were treated with PEG-ADA till 8-week-old to ensure normal development. Then, the mice were divided into four groups as showing in Figure 3a: Group 1-control- $Ada^{-/+}$ mice; Group 2-prevention group with continuous PEG-ADA treatment; Group 3-phenotype group with PEG-ADA treatment withdrawn for two weeks to allow adenosine accumulation; Group 4-rescued group with PEG-ADA treatment suspended for 11 days and then resumed with an additional injection before sacrifice. As expected, with PEG-ADA treatment withdrawn, $Ada^{-/-}$ mice (phenotype group) accumulated dramatically higher plasma adenosine compared to the control $Ada^{-/+}$ (Figure 3b).

Interestingly, significantly increased erythrocyte Sphk1 activity was also seen in the phenotype group (Figure 3c). In contrast, elevation of plasma adenosine was not seen in the $Ada^{-/-}$ mice (prevention group) that were continuously treated with PEG-ADA (Figure 3b). As such, Sphk1 activity was not induced in the erythrocytes of the prevention group (Figure 3c). Moreover, when the plasma adenosine level in rescued group was decreased by re-administrating PEG-ADA (Figure 3b), the erythrocyte Sphk1 activity was also reduced (Figure 3c). Therefore, these data provided solid genetic evidence that increased plasma adenosine levels causes erythrocyte Sphk1 activation

in vivo and that PEG-ADA is a safe and effective drug to regulate adenosine levels and subsequently control erythrocyte Sphk1 activity.

Figure 3

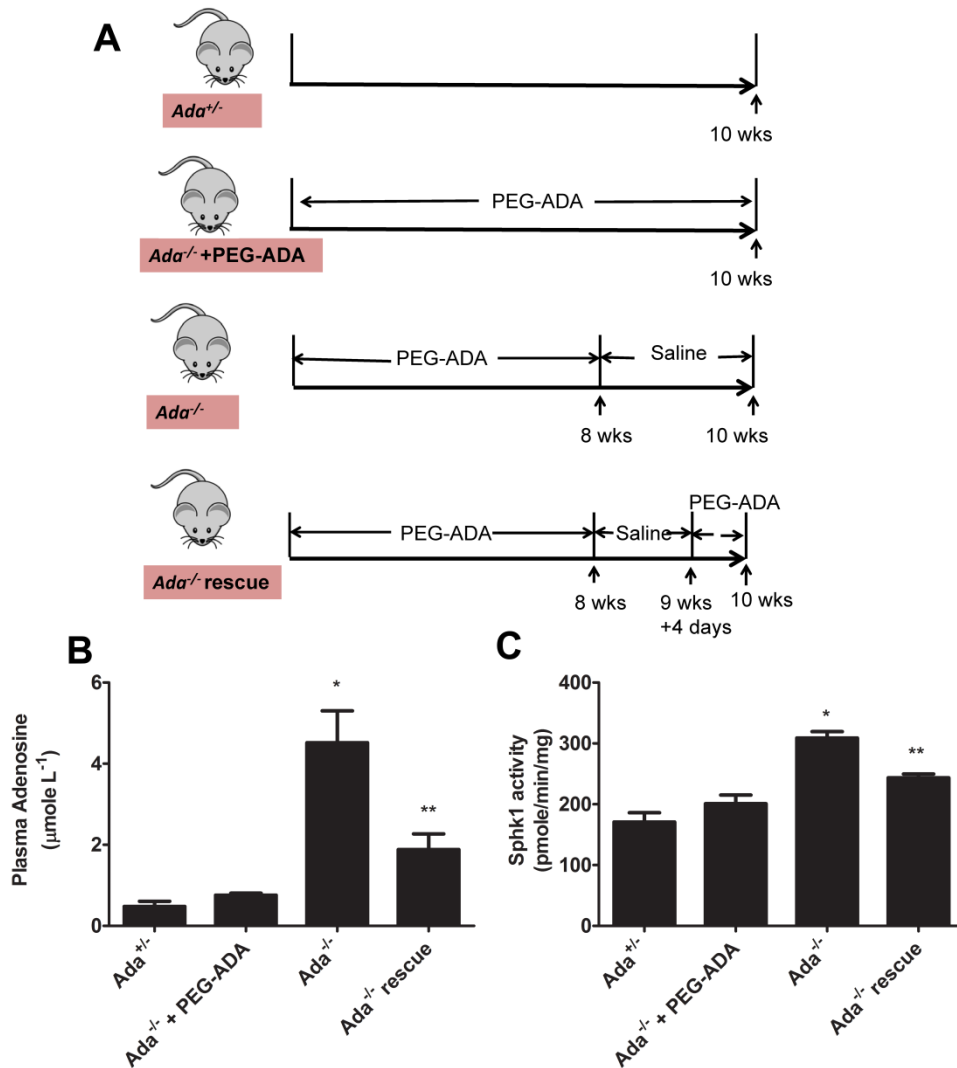


Figure 3. Elevated plasma adenosine induce erythrocyte Sphk1 activity increase *in vivo*.

(A) Schematic representation of mouse treatment strategy. (B-C) Plasma adenosine (B) and erythrocyte SphK1 activity (C) in *Ada*^{+/-}, *Ada*^{-/-} with PEG-ADA treatment, *Ada*^{-/-} without PEG-ADA treatment and *Ada*^{-/-} rescue. Values shown represent the mean \pm SEM (n=6 for each group). **P* < 0.05 *Ada*^{+/-} versus *Ada*^{+/-} + PEGADA; ***P* < 0.05 *Ada*^{+/-} versus *Ada*^{+/-} rescue.

3.1.3 Adenosine-induced Sphk1 activity in normal and sickle erythrocytes is dependent on adenosine receptor A2B (ADORA2B)

As a signaling molecule, adenosine executes its many functions primarily by activating its four G protein–coupled receptors-ADORA1, ADORA2A, ADORA2B and ADORA3—each with a distinct affinity for the ligand and a distinct cellular and tissue distribution[98-100]. To determine which of the four adenosine receptors regulates erythrocyte Sphk1 activity, I isolated erythrocytes from wild type mice and four adenosine receptor deficient mice and treated them with NECA. NECA induced Sphk1 activity in erythrocytes from *Adora1*^{-/-}, *Adora2a*^{-/-} and *Adora3*^{-/-} mice similar to WT mice but not in erythrocytes isolated from *Adora2b*^{-/-} mice (Figure 4a), indicating that ADORA2B is essential for adenosine-induced Sphk1 activity in normal mouse erythrocytes.

Next, to extend our genetic studies, I also tested the effects of pharmacologically blocking ADORA2B signaling with specific antagonist MRS1754[101]. MRS1754 completely blunted the induction of erythrocyte Sphk1 activity by NECA (Figure 4b-c). Thus, genetic and pharmacological studies combined demonstrate that ADORA2B signaling underlies adenosine-induced erythrocyte Sphk1 activity in normal mouse and human erythrocytes. In addition, pharmacological studies in sickle erythrocytes isolated from patients and mice were also conducted and revealed similar effects of MRS1754 in blocking NECA induced Sphk1 activation (Figure 4d-e). Altogether, I have provided both human and mouse evidence that ADORA2B is required for adenosine-induced Sphk1 activity in normal and sickle erythrocytes and that blocking ADORA2B signaling effectively inhibits adenosine-induced erythrocyte Sphk1 activity.

Figure 4

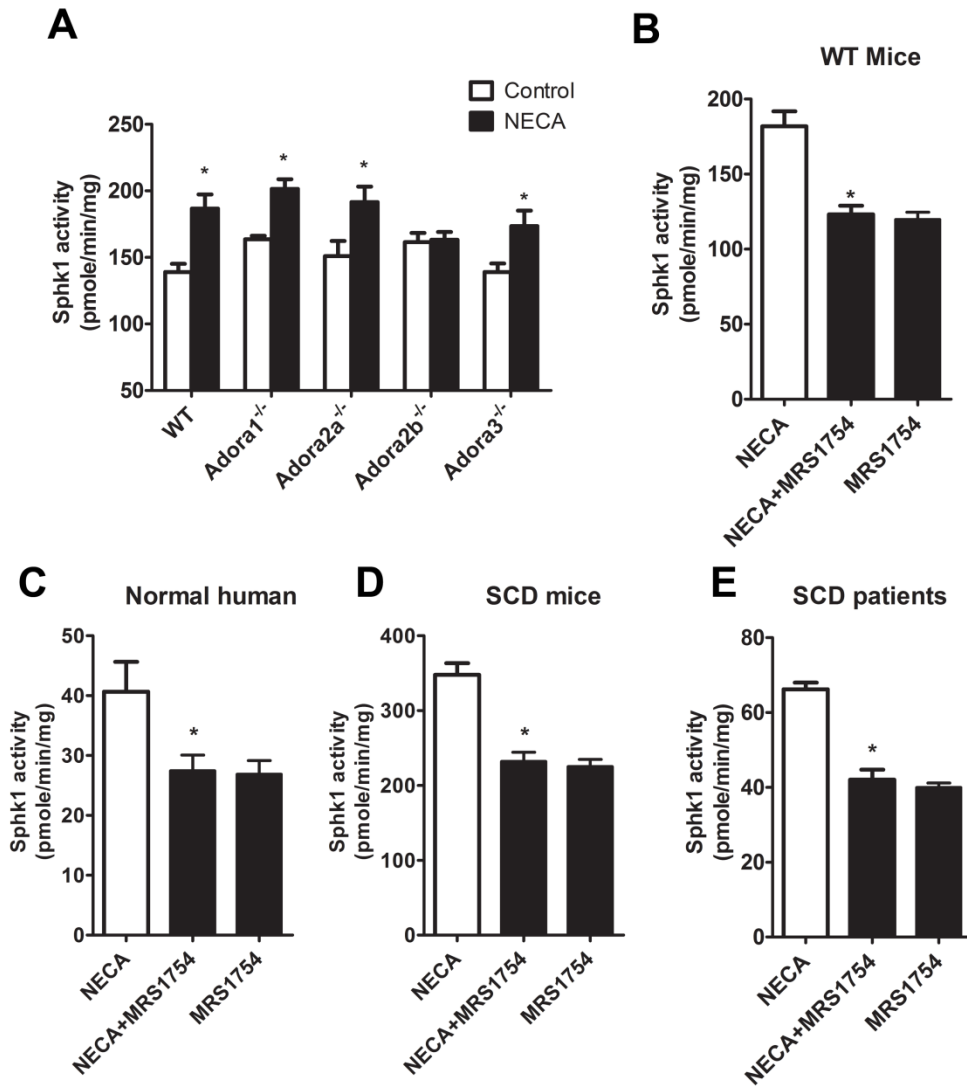


Figure 4. Adenosine signaling through ADORA2B to induce erythrocyte Sphk1 activity increase.

(A) Sphk1 activity in primary erythrocytes from four adenosine receptor deficient mice after NECA (10 μ M) treatment for 30 min. (B~E) Sphk1 activity in cultures of primary erythrocytes from WT mice (B), normal human subjects (C), SCD transgenic mice (D) and SCD patients (E) after NECA (10 μ M) treatment with and without ADORA2B antagonist MRS1754 (10 μ M). Values shown represent the mean \pm SEM (n=5 for SCD patients and normal human subjects; n=6 for SCD transgenic mice and WT mice). * P < 0.05 NECA or NECA + MRS 1754 versus NECA versus control.

3.1.4 Genetic deletion of ADORA2B abolishes excess plasma adenosine-induced erythrocyte Sphk1 activity *in vivo*

The *in vitro* studies demonstrated ADORA2B is required for adenosine induced erythrocyte Sphk1 activity. To confirm the results *in vivo*, I used ADA and ADORA2B-double deficient mice ($Ada^{-/-}/Adora2b^{-/-}$)[67]. Similarly, PEG-ADA enzyme therapy was used to regulate adenosine levels in these mice. As shown in Figure 5a, I treated both $Ada^{-/-}/Adora2b^{-/-}$ and $Ada^{-/-}/Adora2b^{+/+}$ mice with PEG-ADA till 8-week old. Some of the mice were continuously treated with PEG-ADA while the others were terminated two weeks before sacrifice. After stopping PEG-ADA treatment for two weeks, plasma adenosine significantly increased in both $Ada^{-/-}/Adora2b^{-/-}$ and $Ada^{-/-}/Adora2b^{+/+}$ mice compared to the treated groups (Figure 5b and d). When both on PEG-ADA enzyme therapy, $Ada^{-/-}/Adora2b^{+/+}$ and $Ada^{-/-}/Adora2b^{-/-}$ mice had similar level of erythrocyte Sphk1 activity (Figure 5c and e). However, two weeks after the enzyme therapy withdrawn, although adenosine levels went up in both mice (Figure 5b and d), only $Ada^{-/-}/Adora2b^{+/+}$ showed significantly increased erythrocyte Sphk1 activity while the Sphk1 activity in $Ada^{-/-}/Adora2b^{-/-}$ mice erythrocyte remained unchanged (Figure 5c and e). These results validated our *in vitro* studies and provided strong *in vivo* genetic evidence that ADORA2B is required for adenosine mediated induction of erythrocyte Sphk1 activity in $Ada^{-/-}$ mice.

Figure 5

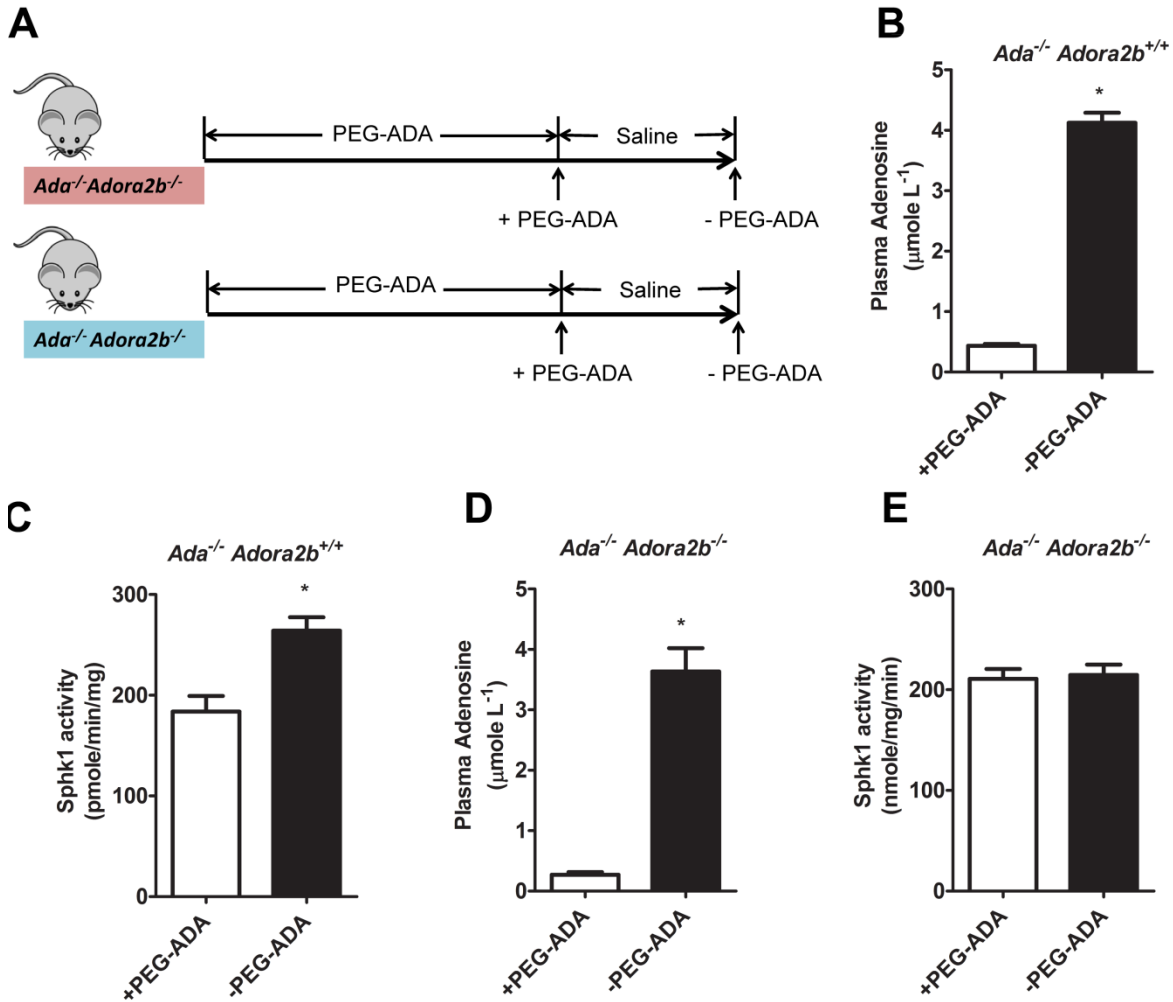


Figure 5. Elevated plasma adenosine increases erythrocyte Sphk1 activity through ADORA2B.

(A) Schematic representation of mouse treatment strategy. (B, C) Plasma adenosine levels (B) and erythrocyte Sphk1 activity (C) in *Ada*^{-/-} *Adora2b*^{+/-} mice before (+PEG-ADA) and after PEG-ADA treatment withdrawn (-PEG-ADA). (D, E) Plasma adenosine levels (D) and erythrocyte Sphk1 activity (E) in *Ada*^{-/-} *Adora2b*^{-/-} mice before (+PEG-ADA) and after PEG-ADA treatment withdraw (-PEG-ADA). Values shown represent the mean ± SEM (n=6 for each group). **P* < 0.05 -PEG-ADA versus +PEG-ADA.

3.1.5 PKA mediated ERK1/2 activation functions downstream of ADORA2B and underlies adenosine-induced Sphk1 activity in normal and sickle erythrocytes from both human and mice

The Gs-coupled ADORA2B signaling involves many downstream components including PKA[102] and the extracellular-signal regulated kinase 1 and 2 (ERK1/2) [103]. Previous study showed PKA underlies adenosine-ADORA2B mediated induction of 2, 3-bisphosphoglycerate in erythrocyte[72]. Also, ERK1/2 can directly phosphorylate and activate Sphk1 [32]. Therefore, I sought to test if PKA and ERK1/2 are important intracellular signaling molecules functioning downstream of ADORA2B responsible for adenosine-induced Sphk1 activity in erythrocytes. First, I treated erythrocytes isolated from normal human and mice with or without NECA in the presence or absence of specific PKA inhibitor, H89 or ERK1/2 inhibitor, PD98059. NECA-induced Sphk1 activity was significantly reduced by either H89 or PD98059 as MRS1754, a specific ADORA2B inhibitor (Figure 6a-b). PKA and ERK inhibitors each prevented NECA-mediated induction of erythrocyte Sphk1 activity, suggesting that PKA and ERK1/2 work in an upstream and downstream manner. To further test this intriguing possibility, I treated normal human and mouse erythrocytes with forskolin, a potent and specific PKA agonist, in the presence or absence of PD98059. Forskolin treatment directly induced Sphk1 activity and PD98059 significantly attenuated forskolin-induced Sphk1 activity in normal human and mouse erythrocytes (Figure 6a-b).

It is known that Sphk1 in the cytosol moves to the plasma membrane once phosphorylated [32]. Therefore, it is not surprising to see that NECA and forskolin treatment increased phosphorylation and membrane localization of Sphk1 in normal

human and mouse erythrocytes, and these inductions can be blunted by ADORA2B antagonist, PKA inhibitor and ERK1/2 inhibitor (Figure 6 c-d). These results indicate that ADORA2B-mediated PKA activation signals via ERK1/2 in the adenosine-induced signaling pathway to activate Sphk1 activity in normal human and mouse erythrocytes. Thus, PKA and ERK1/2 function in a linear sequence rather than parallel pathways downstream from of adenosine induced ADORA2B signaling.

Figure 6

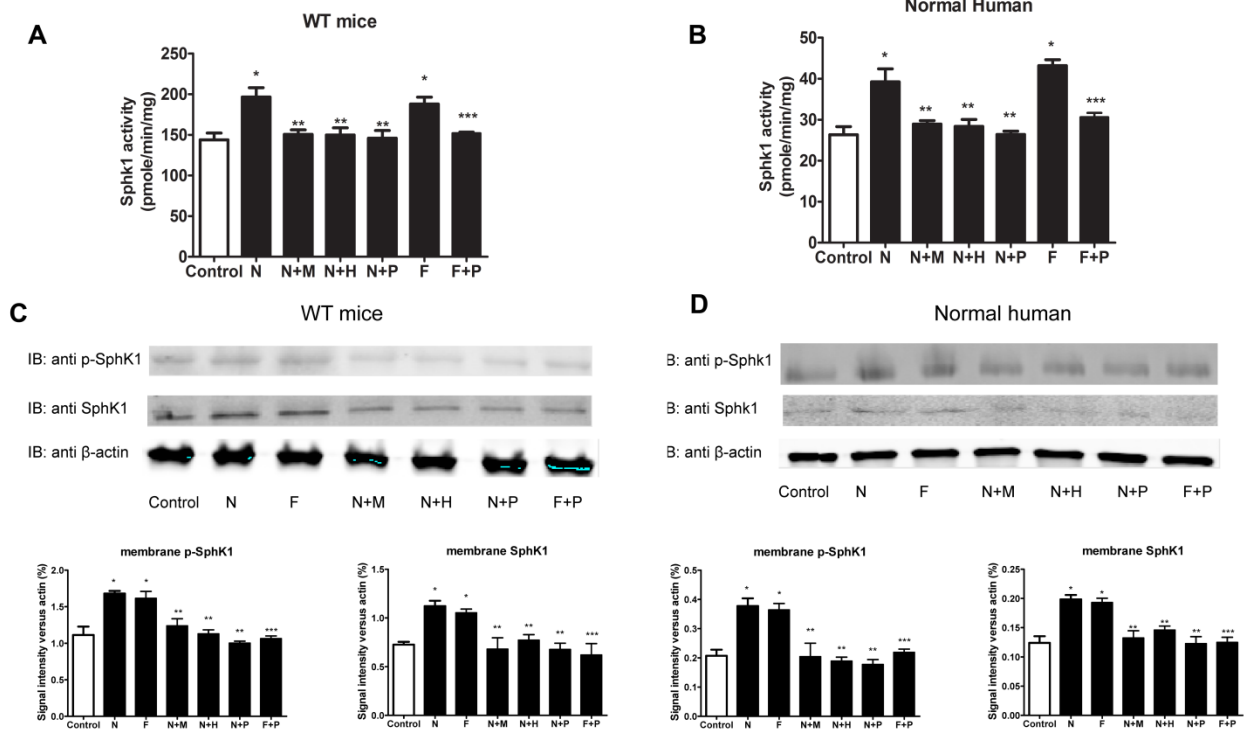


Figure 6. PKA-mediated activation of ERK1/2 underlies adenosine-ADORA2B mediated erythrocyte Sphk1 activation in WT mice and normal human individuals.

Sphk1 activity, membrane bound total and phosphorylated Sphk1 in primary erythrocytes from WT mice (A and C), normal human subjects (B), SCD transgenic mice (C) and SCD patients (and D) after treatment of N (10 μ M NECA), N+M (10 μ M NECA + 10 μ M MRS1754), N+H (10 μ M NECA + 10 μ M H89), N+P (10 μ M NECA + 20 μ M PD98059), F (10 μ M Forskolin) and F+P (10 μ M Forskolin+ 20 μ M PD98059) for 30 min. Values shown represent the mean \pm SEM (n=5 for normal human subjects and n=4 for WT mice). * P < 0.05 N or F versus control; ** P < 0.05 N+M, N+H, N+P versus N; *** P < 0.05 F+P versus F.

Next, I extend the study to sickle erythrocytes. Similarly, NECA-induced Sphk1 activities (Figure 18), membrane bound Sphk1 and phosphorylated Sphk1 (Figure 19) were significantly reduced by H89 or PD98059 in sickle erythrocytes from both patients and mice. Moreover, forskolin directly induced erythrocyte Sphk1 activation, phosphorylation and membrane translocation, and PD98059 blocked forskolin-mediated the activation of Sphk1 (Figure 7). Thus, the data suggest that ADORA2B-mediated activation of PKA responsible for induced Sphk1 activity in an ERK1/2-dependent manner in both normal and sickle erythrocytes.

Figure 7

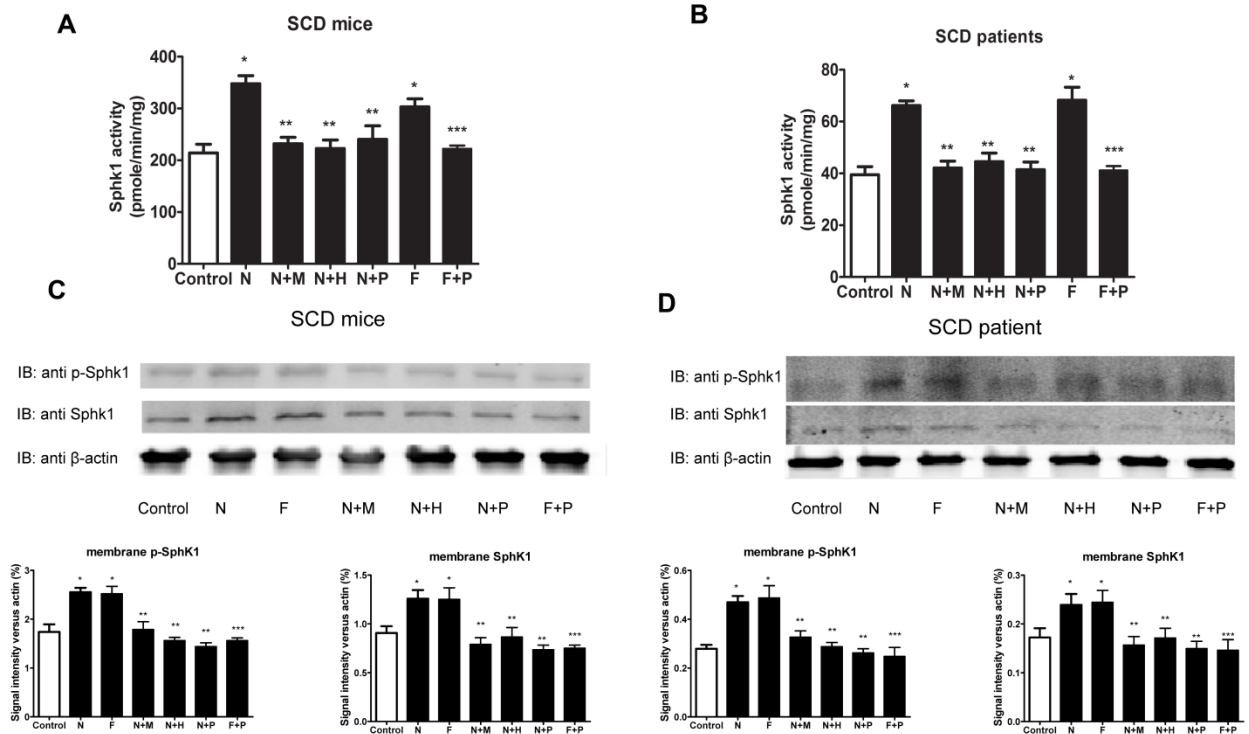


Figure 7. PKA-mediated activation of ERK1/2 underlies adenosine-ADORA2B mediated erythrocyte Sphk1 activation in SCD Tg mice and SCD patients.

Sphk1 activity, membrane bound total and phosphorylated Sphk1 in primary erythrocytes from SCD transgenic mice (A and C) and SCD patients (B and D) after treatment of N (10μM NECA), N+M (10μM NECA + 10μM MRS1754), N+H (10μM NECA + 10μM H89), N+P (10μM NECA + 20μM PD98059), F (10μM Forskolin) and F+P (10μM Forskolin+ 20μM PD98059) for 30 min. Values shown represent the

mean \pm SEM (n=3 for SCD patients and n=5 for normal human subjects; n=3 for SCD transgenic mice and n= 4 for WT mice). * $P < 0.05$ N or F versus control; ** $P < 0.05$ N+M, N+H, N+P versus N; *** $P < 0.05$ F+P versus F.

To summarize, I have identified that adenosine-ADORA2B is a previously unrecognized signaling pathway that activates Sphk1 in normal and sickle erythrocytes. I also provided *in vivo* evidence that excess plasma adenosine induces erythrocyte Sphk1 activity in ADA-deficient mice. ADA enzyme therapy or genetic deletion of ADORA2B completely abolishes excess adenosine-induced erythrocyte Sphk1 activity in ADA-deficient mice. Finally, I demonstrated that ADORA2B activation-mediated PKA signaling is responsible for adenosine-induced Sphk1 activity in an ERK1/2-dependent manner in both normal and sickle erythrocytes. Taken together, I have revealed the novel role of adenosine signaling in erythrocyte physiology and pathology by regulating Sphk1 activity and thereby identified a new means to regulate Sphk1 activity in normal and SCD.

3.2 Chapter 2: Erythrocyte S1P Promotes Hypoxia Adaptation

This chapter is based upon: Sun K, Zhang Y, D'Alessandro A, Nemkov T, Song A, Wu H, Liu H, Adebiyi M, Huang A, Wen YE, Bogdanov MV, Vila A, O'Brien J, Kellems RE, Dowhan W, Subudhi AW, Jameson-Van Houten S, Julian CG, Lovering AT, Safo M, Hansen KC, Roach RC, Xia Y: **Sphingosine-1-phosphate promotes erythrocyte glycolysis and oxygen release for adaptation to high-altitude hypoxia.** *Nat Commun* 2016, **7**:12086.[9], with permission from the journal for usage in thesis.

After discovering that erythrocyte Sphk1 can be activated by hypoxia-induced adenosine signaling in both normal and sickle cell disease, the next question is the function of elevated Sphk1 and S1P. Erythrocytes used to be considered as a reservoir to supply S1P to the circulation before a recent study recognized that elevated S1P induces sickling in SCD erythrocytes. However, the role of S1P in normal erythrocytes remains a mystery. Because the most important function of erythrocytes is to deliver O₂, which increases significantly in response to hypoxia, I hypothesize that elevated S1P in hypoxia regulates erythrocyte O₂ delivery capacity.

3.2.1 Altitude induces S1P level and Sphk1 activity in human RBCs

To determine how human erythrocytes respond to hypoxia, a multinational collaborative project was conducted in which 21 young and healthy lowland individuals were brought to high altitude at 5260 meters for a total of 16 days. Nonbiased metabolomic profiling was performed on the erythrocytes isolated from these volunteers at sea level (SL), and after 12 hours (HA1), 7 days (HA7) and 16 days (HA16) at 5260m altitude. Additionally, their erythrocyte O₂ releasing capacity were monitored by

measuring P50, the partial O₂ pressure required to reach 50% Hb-O₂ saturation, from human subjects at SL and at high altitude[104] (illustration in Figure 8a).

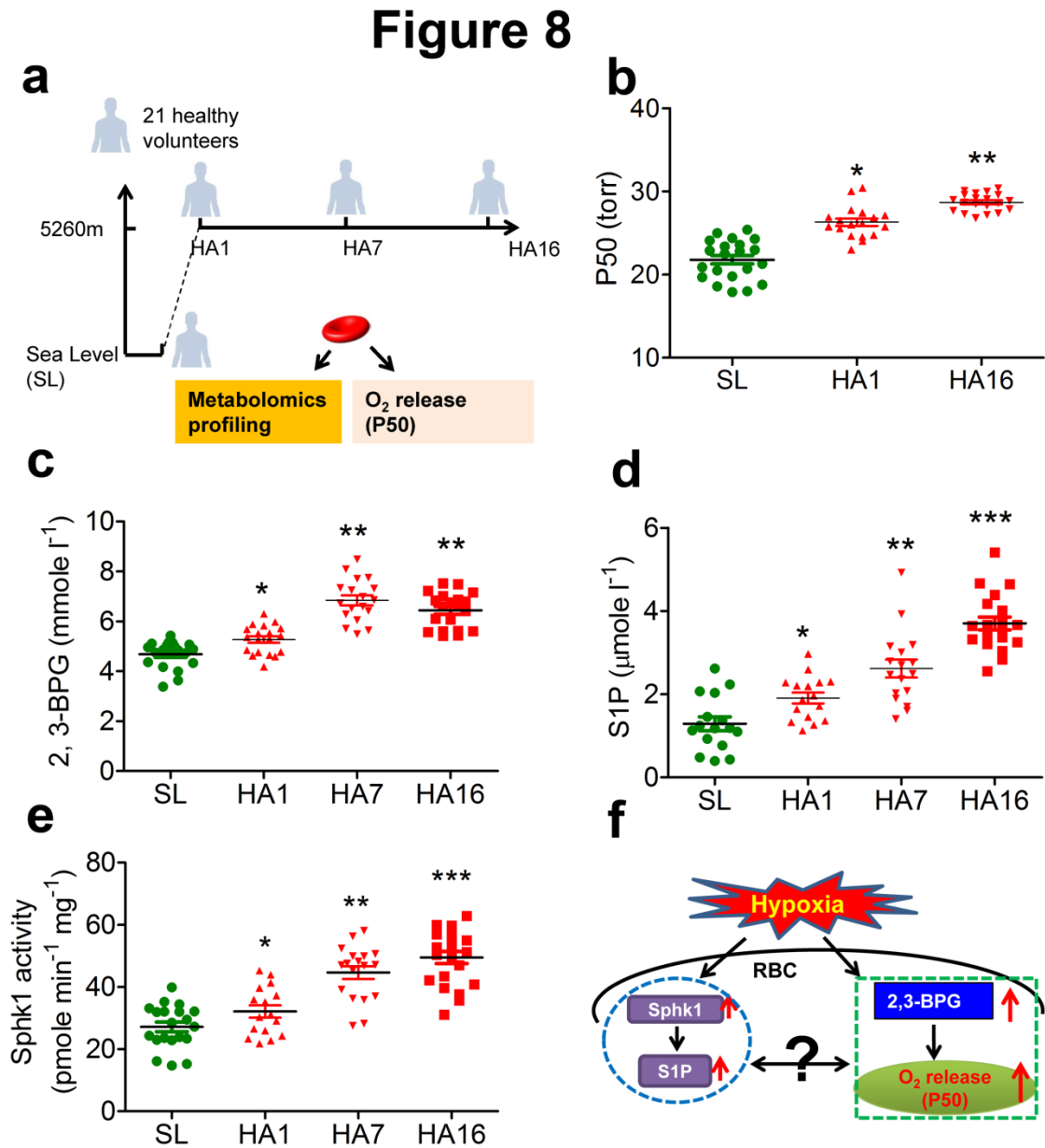


Figure 8. Concurrent increase of erythrocyte Sphk1 activity, S1P production and O₂ delivery ability in human high-altitude study.

(a) Schematic representation of human high-altitude study: nonbiased metabolomic profiling coupled with erythrocyte function analysis was performed on the erythrocytes isolated from 21 human volunteers at sea level (SL), and after 12 hours (HA1), 7 days (HA7) and 16 days (HA16) at 5260m altitude. (b) Erythrocyte O₂ release capacity was measured as P50. 2,3-BPG level (c) and S1P level (d) were

quantified in human high-altitude samples. (e) Erythrocyte Sphk1 activity in human high-altitude samples. (f) Schematic representation showing concurrent increase of erythrocyte S1P metabolism with O₂ delivery identified in human high-altitude study. Mean ± s.e.m; n = 16–21 per group; **P* < 0.05 versus SL, ***P* < 0.01 versus HA1, ****P* < 0.01 versus HA7, two way ANOVA.

Consistent with previous high altitude studies[105], erythrocyte O₂ releasing capacity (P50) was significantly increased by approximately 20% as rapidly as 12 hours at high altitude, and continued increasing to day 16 in human volunteers (Figure 8b). Moreover, among 233 erythrocyte metabolites identified by metabolomic profiling, the levels of erythrocyte 2,3-bisphosphoglycerate (2,3-BPG), a specific allosteric modulator promoting O₂ release from hemoglobin, increased in response to high-altitude hypoxia on day 1 and was maintained at high level until day 16, as quantified by spectrophotometric assays (Figure 8c). Notably, erythrocyte S1P levels rapidly increased within 12 hours at high altitude and further increased to approximately two fold on day 7 and three fold on day 16, consistent with trends observed for 2,3-BPG and P50 (Figure 8d). Sphk1 is the major enzyme responsible for the production of S1P in erythrocytes[22]. Reassuringly, I found that erythrocyte Sphk1 activity was significantly induced at high altitude as well (Figure 8e). Consistent to the notion that erythrocyte is the major cell source of circulating S1P[106], plasma S1P levels were also increased in humans after 16-day stay in high-altitude (Figure 9a). Thus, we demonstrated that Sphk1 activity and S1P levels are induced in mature human erythrocytes by high altitude (Figure 8f).

Figure 9

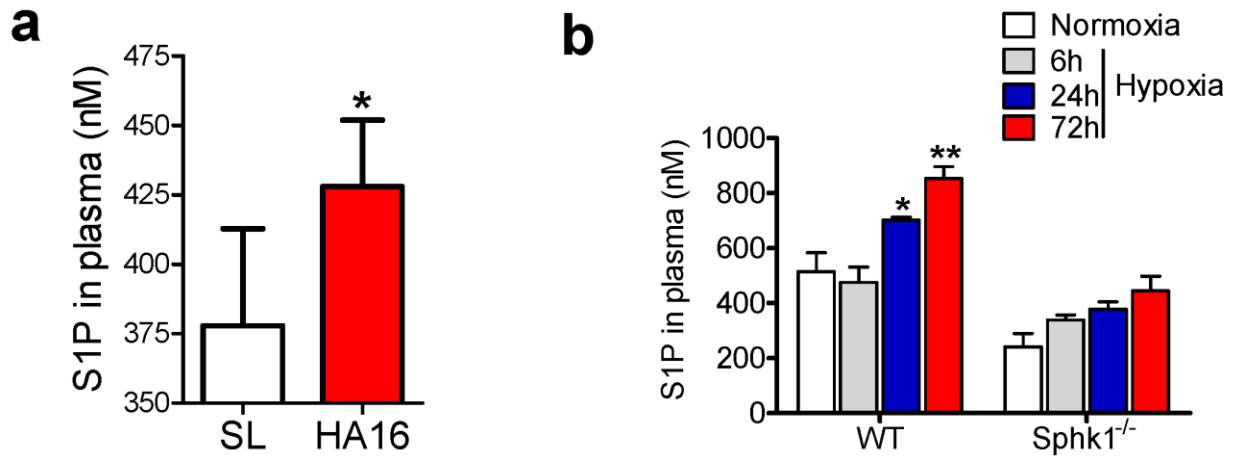


Figure 9. Plasma S1P concentration increases in human and mice under hypoxia. (a) Plasma S1P concentration in human volunteers at sea level and after 16-day at high-altitude. (b) Plasma S1P concentration in WT and *Sphk1*^{-/-} mice under normoxia and hypoxia at different time points. Mean \pm s.e.m; N=16~21 for human samples; n=5 for mouse samples, * p <0.05 versus SL or 6h, ** p <0.05 versus 24h, Student's t -test and one way ANOVA

3.2.2 Sphk1 promotes O₂ release from mouse erythrocytes to offset hypoxia

Since 2,3-BPG is one the most important regulators of erythrocyte O₂ release capacity[105], the above findings raise an intriguing possibility that elevated erythrocyte Sphk1-mediated increase in S1P production could induce erythrocyte 2,3-BPG production and thereby increase O₂ release to adapt to high altitude hypoxia. To further investigate this possibility in vivo, I exposed wild-type (WT) and Sphk1-deficient (*Sphk1*^{-/-})[107] mice to hypoxic environment (10% oxygen, close to oxygen level at 5260m altitude) for up to 72 hours. Similar to the human high-altitude studies, erythrocyte Sphk1 activity and S1P levels increased in a time dependent manner (Figure 10a). Moreover, erythrocyte 2,3-BPG levels and P50 were significantly elevated in WT mice similar to the human studies (Figure 10b). By contrast, Sphk1 activity is undetectable and erythrocyte S1P levels are only approximately 1/50 that of WT mice in *Sphk1*^{-/-} mice.

Moreover, hypoxia-mediated increase of erythrocyte S1P, 2,3-BPG and P50 were significantly impaired in *Sphk1*^{-/-} mice (Figure 10a-d). Similar to the human data, plasma S1P levels were induced by hypoxia in WT mice in a time-dependent manner but blunted in *Sphk1*^{-/-} mice (Figure 9b). These results indicate that elevated Sphk1-mediated S1P production is required for hypoxia-induced elevation of mouse erythrocyte 2,3-BPG levels and subsequent O₂ releasing capacity.

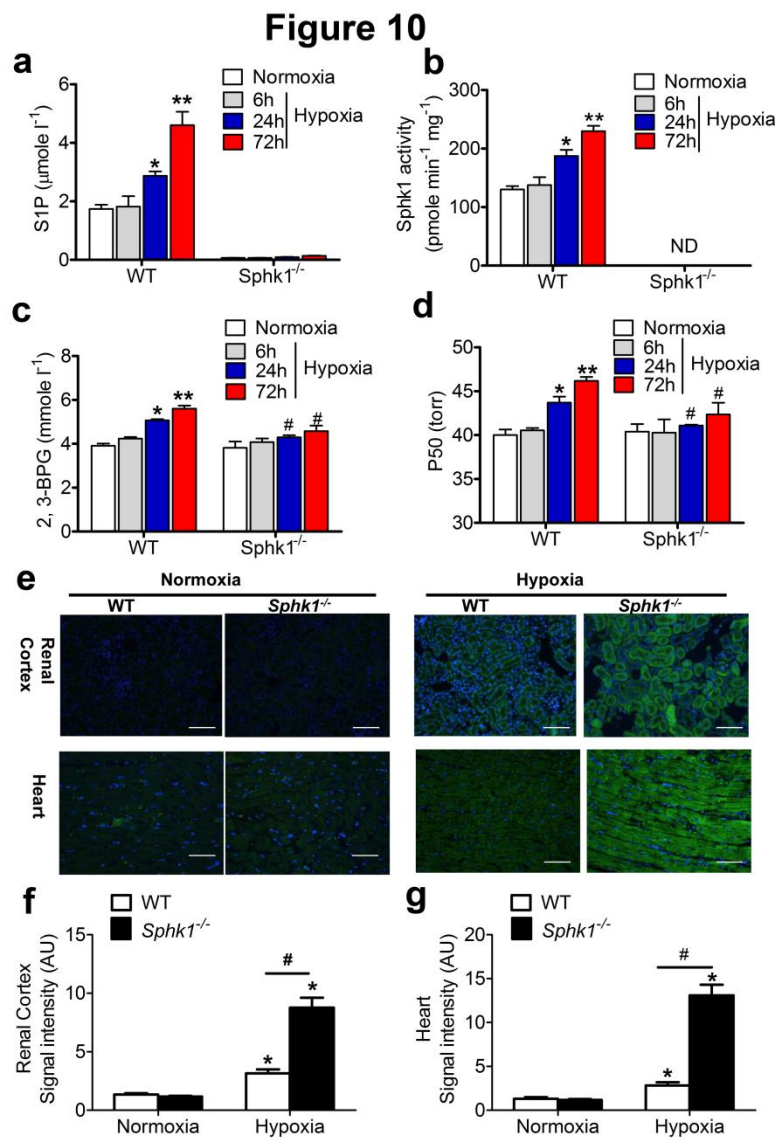


Figure 10. Hypoxia-induced Sphk1 and S1P increase regulate 2,3-BPG level, O₂ delivery ability and tissue hypoxia in mice. Erythrocyte Sphk1 activity.

(a), S1P level (b), 2,3-BPG level (c) and P50 (d) in WT and *Sphk1*^{-/-} mice in normoxia and hypoxia for different treatment time. (e) Tissue hypoxia signals measured by HypoxyprobeTM in renal cortex and heart in WT and *Sphk1*^{-/-} mice in normoxia and hypoxia for 72h. Quantification of hypoxia signals in renal cortex (f) and heart (g). Mean ± s.e.m; n = 6–8 per treatment time point; **P* < 0.05 versus 6h or normoxia, ***P* < 0.05 versus 24h, # *P* < 0.05 versus WT, Student's *t*-test and one way ANOVA.

Next, I assessed the severity of hypoxia at tissue level using HypoxyprobeTM to examine the kidneys and heart since these are the most susceptible organs to hypoxia[53, 108]. No HypoxyprobeTM signals were detected in the tissue sections of WT or *Sphk1*^{-/-} mice in normoxia (Figure 10e). However, in hypoxia, immunofluorescence (IF) analysis of the HypoxyprobeTM signals showed elevated staining in kidneys and hearts after 72 hours in hypoxia compared to normoxia in WT mice (Figure 10e). In contrast, much more severe hypoxia in kidney and heart was observed in *Sphk1*^{-/-} mice after 72 hours in hypoxia (Figure 10e). Image quantification analysis demonstrated that the intensity of HypoxyprobeTM signals in the kidney and heart of *Sphk1*^{-/-} mice was more than two fold of that of WT mice (Figure 10f and g). Since differences in pulmonary function in hypoxia could also affect O₂ availability and thereby tissue hypoxia, I measured arterial Hb-O₂ saturation (SaO₂) to assess lung function in WT and *Sphk1*^{-/-} mice in normoxia and hypoxia. Although a significant decrease of SaO₂ in both WT and *Sphk1*^{-/-} mice in hypoxia was observed, there were no significant differences between WT and *Sphk1*^{-/-} mice under either normoxia or hypoxia for up to 72 hours (Figure 11), indicating that the increased HypoxyprobeTM signals in the kidney and heart of *Sphk1*^{-/-} mice were not due to decreased lung uptake of O₂ under hypoxia.

Figure 11

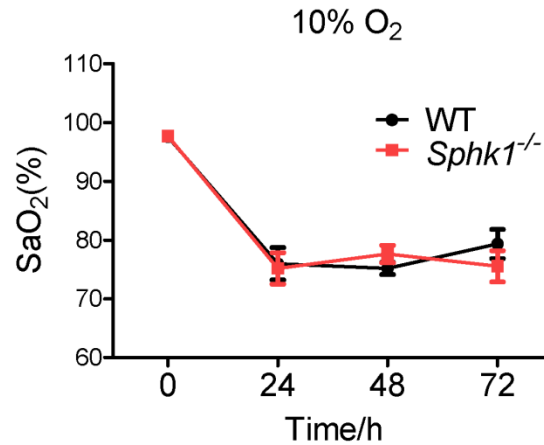


Figure 11. Arterial hemoglobin oxygen saturation (SaO₂) in WT and *Sphk1*^{-/-} mice under normoxia and hypoxia up to 72 hours. Mean ± s.e.m; N=3~5 for each time point; No significant difference, Student's *t*-test.

Erythrocytes are derived from hematopoietic stem cells in the bone marrow and the vast majority of BM-derived cells in the circulation are erythrocytes. To rule out the effect of tissue Sphk1, I conducted reciprocal bone-marrow transplantation (BMT) between WT and *Sphk1*^{-/-} mice. Specifically, three groups of mice were generated: 1) 'WT-to-*Sphk1*^{-/-}' group was designed to critically determine if Sphk1 expressed only in hematopoietic derived cells could rescue severe tissue hypoxia in *Sphk1*^{-/-} mice transplanted with WT mouse BM; 2) '*Sphk1*^{-/-}-to-WT' group was generated by transplanting BM of *Sphk1*^{-/-} mice to WT mice to examine if Sphk1 deficiency only in BM-derived cells is sufficient to cause severe tissue hypoxia; 3) 'WT-to-WT' group is WT mouse BM transplanted to WT mice (Figure 12a). Eight weeks after BMT, Sphk1 activity in mature erythrocytes was detected as an indicator of chimerism (Figure 13). Three groups of mice with more than 95% chimerism were subjected to hypoxia

challenge for 72 hours, respectively (Figure 12a). As expected, the basal levels of erythrocyte Sphk1 activity in the '*WT-to-Sphk1^{-/-}*' group were similar to the '*WT-to-WT*' mice, while it was undetectable in '*Sphk1^{-/-}-to-WT*' mice as in the global *Sphk1^{-/-}* mice under normoxia condition, indicating successful BMT (Figure 12b). Similarly, erythrocyte S1P levels in the '*WT-to-Sphk1^{-/-}*' group were no different compared to the '*WT-to-WT*' mice, while it was 20-fold higher than that in '*Sphk1^{-/-}-to-WT*' mice (Figure 12c). Consistent to global knockouts, no obvious difference in erythrocyte 2,3-BPG and P50 were observed under normoxia condition (Figure 12d and e). However, after 72 hour-hypoxia exposure, '*WT-to-Sphk1^{-/-}*' group showed a 30% increase in Sphk1 activity, one fold induction of S1P levels, 50% increase in 2,3-BPG levels and 6 torr elevation in P50 in the erythrocytes as with the *WT to WT* group (Figure 13d and 3). In contrast, Sphk1 activity was undetectable and 2,3-BPG and P50 were not induced by 72 hour-hypoxia in *WT* mice transplanted with *Sphk1^{-/-}* mouse BM (Figure 12d and e). No obvious HypoxyprobeTM signals were detected in those three groups of mice under normoxia (Figure 13f). However, after 72 hour-hypoxia exposure, severe hypoxia were observed in the kidneys and hearts from '*Sphk1^{-/-}-to-WT*' mice similar to global *Sphk1^{-/-}* mice, indicating that deficiency of Sphk1 in BM-derived cells is sufficient to mimic the severe tissue hypoxia as seen in global *Sphk1^{-/-}* mice. By contrast, the '*WT-to-Sphk1^{-/-}*' group mice showed significantly less HypoxyprobeTM signals in the kidneys and hearts compared with that of '*Sphk1^{-/-}-to-WT*' mice after 72 hour exposure to hypoxia (Figure 12 f-h). Thus, Sphk1 in BM-derived cells but not in other tissues is responsible for adaptation to hypoxia by inducing erythrocyte S1P production, 2,3-BPG levels and O₂ release.

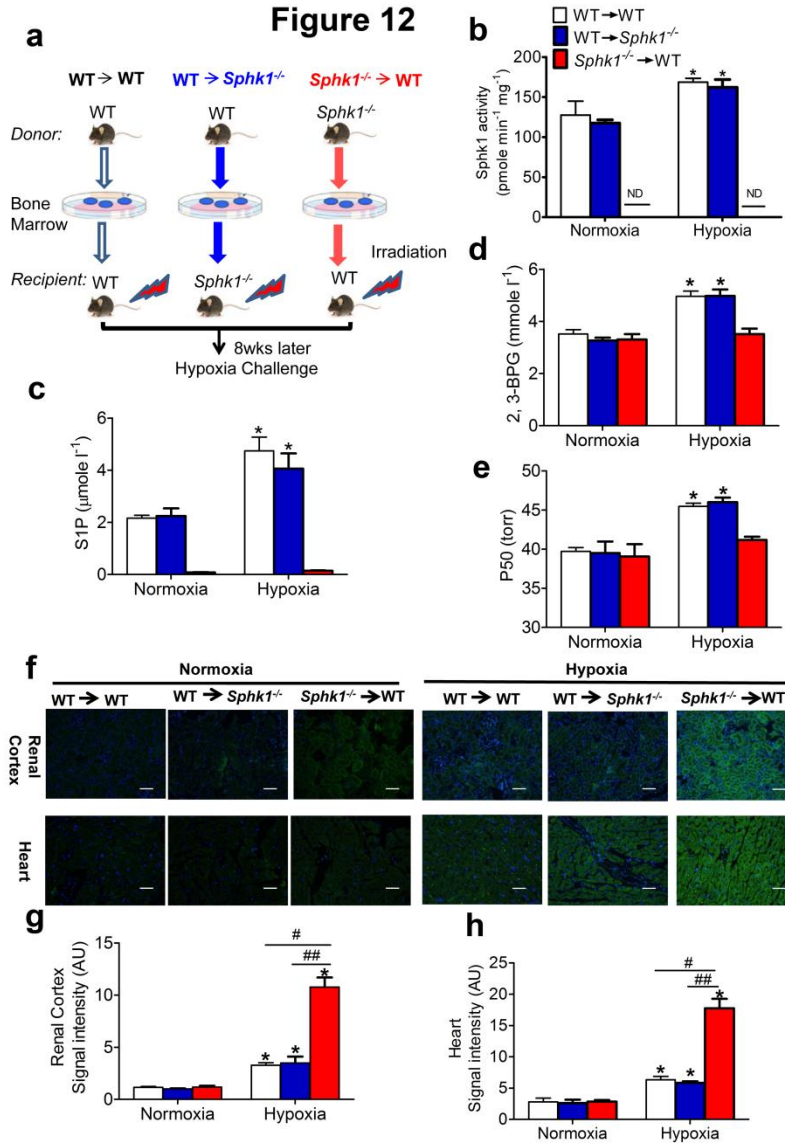


Figure 12. Bone marrow derived Sphk1 and S1P are responsible for protecting tissue hypoxia by inducing erythrocyte 2,3-BPG levels and O₂ release capacity.

(a) Schematic illustration of reciprocal bone-marrow transplantation (BMT) between WT and *Sphk1*^{-/-} mice. Erythrocyte Sphk1 activity (b), S1P (c), 2,3-BPG level (d) and P50 (e) in each group of mice in normoxia and hypoxia for different treatment time. (f) Tissue hypoxia signals measured by HypoxyprobeTM in renal cortex and heart in each group of mice in normoxia and hypoxia for 72h. Quantification of hypoxia signals in renal cortex (g) and heart (h). Mean ± s.e.m; n = 8 per group of mice; **P* < 0.05 versus normoxia, # *P* < 0.05 versus WT to WT, ## *P* < 0.05 versus WT to *Sphk1*^{-/-}, Student's *t*-test and one way ANOVA.

Figure 13

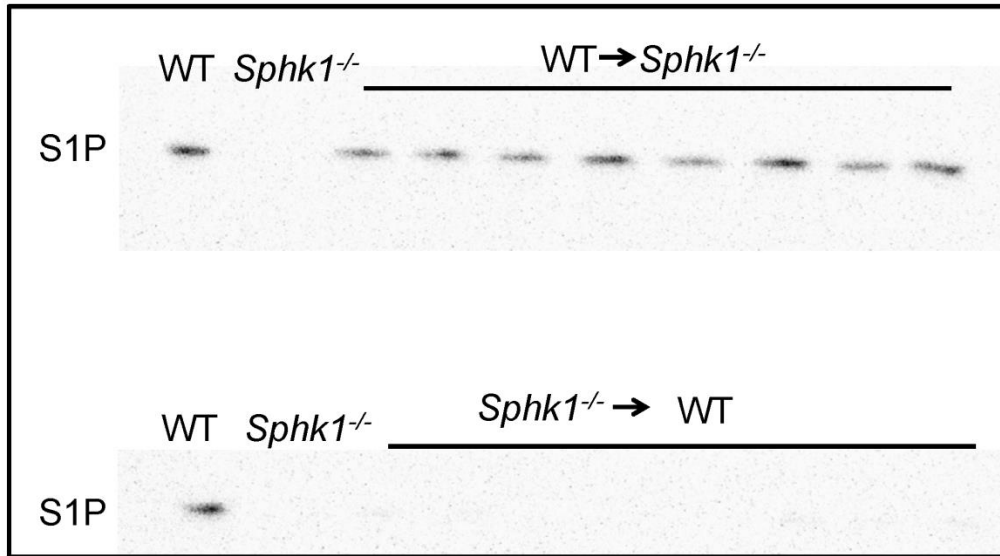


Figure 13. Erythrocyte Sphk1 activity measurements in bone-marrow transplanted mice. Data indicate a high chimerism with nearly 100% of circulating cells donor derived in receipts. Erythrocyte Sphk1 activity were assayed using D-erythro-sphingosine and [γ -³²P]ATP. Lipids were extracted and then resolved by TLC on silica gel G60. The plates were then exposed to phosphor-imaging screening (Bio-Rad) and scanned for radioactive signals as indications of the amount of S1P synthesized. The bands in the figure indicate radio-labeled S1P detected in the Sphk1 assay.

3.2.3 Intracellular S1P underlies increased 2,3-BPG production

S1P is a versatile signaling molecule that plays many important roles by binding to five G-protein coupled receptors. Therefore, I sought to test if the above mentioned function of S1P in regulating erythrocyte 2,3-BPG levels can be attributed to the extracellular signaling roles of S1P. Consistent with human and mouse findings, hypoxia induced Sphk1 activity in erythrocytes from WT mice, but no detectable activity in erythrocytes isolated from *Sphk1*^{-/-} mice under both normoxia and hypoxia conditions (Figure 14a). Moreover, hypoxia directly induced 2,3-BPG levels in erythrocytes from WT mice but not *Sphk1*^{-/-} mice (Figure 14 b and c), indicating that erythrocyte Sphk1 is required for hypoxia-induced 2,3-BPG production in mouse erythrocytes.

Next, to determine if extracellular S1P signaling via its surface receptors directly induces 2,3-BPG production in erythrocytes, I isolated erythrocytes from both WT and *Sphk1*^{-/-} mice and pretreated them with exogenous S1P up to 250 nmole·l⁻¹, which activates all of five S1PRs[109] but does not increase intracellular S1P, under normoxia and hypoxia conditions. However, S1P pretreatment with up to 250 nmole·l⁻¹ failed to further increase 2,3-BPG levels in WT erythrocytes under either normoxia or hypoxia conditions (Figure 14b). Moreover, S1P pretreatment could not rescue the lack of 2,3-BPG induction under both normoxia and hypoxia condition in *Sphk1*^{-/-} erythrocytes (Figure 14c). Thus, these studies provided direct evidence that S1P functions independently of S1P receptors to mediate hypoxia-induced 2,3-BPG level increase in the erythrocytes.

Figure 14

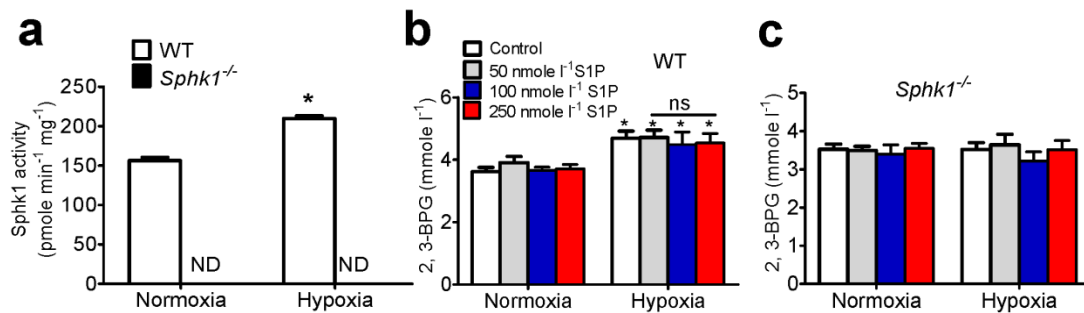


Figure 14. Regulation of erythrocyte 2,3-BPG production by Sphk1-S1P is independent of S1P receptors. (a) Sphk1 activity in cultured erythrocytes isolated from WT mice under normoxia and hypoxia. (b-c) 2,3-BPG concentration in cultured erythrocytes isolated from WT (b) and *Sphk1*^{-/-} (c) mice treated with vehicle or different doses of S1P under normoxia and hypoxia for 6 hours. Mean \pm s.e.m; N=6~8 for each group; * p <0.05 versus normoxia, Student's t -test and one way ANOVA.

3.2.4 Glycolysis is induced by high altitude in human RBCs

Since 2,3-BPG is generated through glycolysis, to investigate the mechanism underlying S1P-mediated 2,3-BPG production increase in hypoxia, I revisited the metabolomic profiling data and noticed that levels of representative glycolytic metabolite glyceraldehyde-3-phosphate (G3P) and downstream intermediate of 2,3-BPG, were significantly elevated in hypoxia after 12 hours and continued to increase to day 16 (Figure 15). In contrast, all of the upstream intermediates of G3P, including glucose-6-phosphate and fructose 1,6-bisphosphate and the two most immediate intermediates downstream of 2,3-BPG including 2/3-phosphoglycerate and phosphoenolpyruvate (PEP), were significantly reduced in response to high altitude hypoxia in a time dependent manner. These findings suggest that the glycolytic pathway prior to shunting to the erythrocyte-specific Rapoport-Luebering Shunt, which is a diversion of main glycolytic pathway for production of 2,3-BPG, is significantly induced (Figure 15).

Figure 15

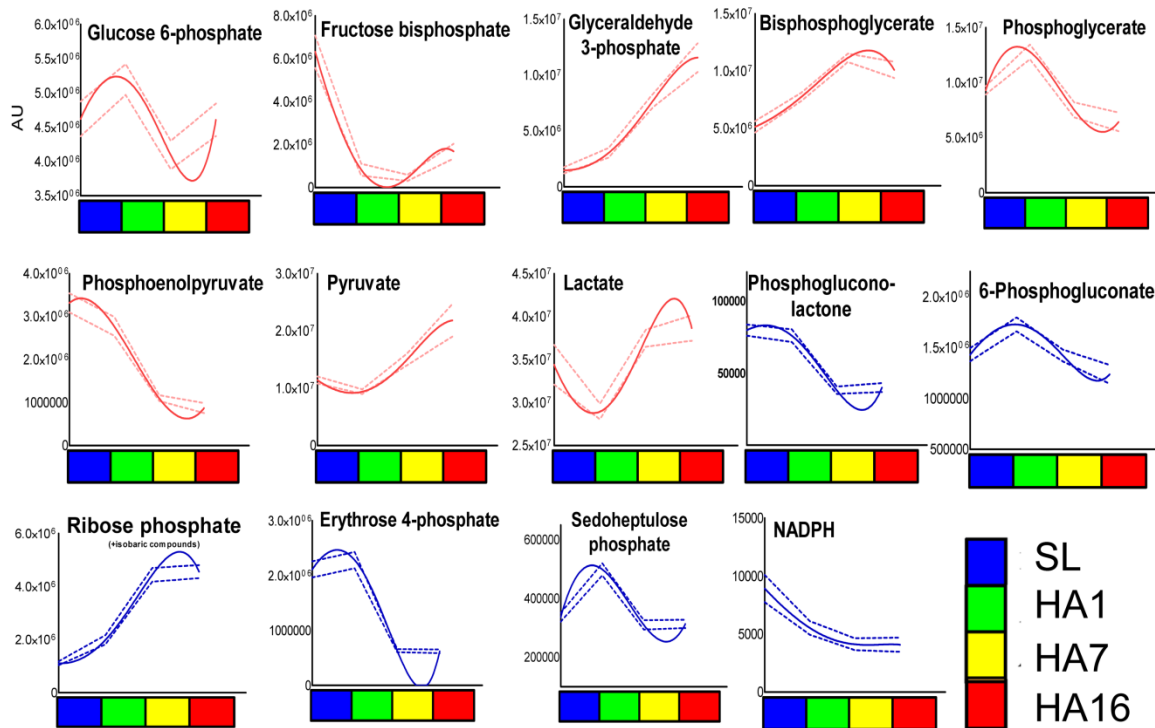


Figure 15. Metabolomic screening revealed time-dependent increase of glycolysis and decrease of PPP in erythrocyte from humans exposed to high-altitude hypoxia. (Data obtained by Dr. Angelo D'Alessandro of The University of Colorado School of Medicine, use with permission)

There are two major glucose metabolism pathways in erythrocytes: the Embden-Meyerhof glycolytic pathway that generates energy and glycolytic intermediates such as 2,3-BPG to promote O₂ release; and the pentose phosphate pathway (PPP) that produces reducing equivalents to regenerate NADPH-dependent antioxidant glutathione and enzymes to protect against oxidative stress[110]. In support of the observation that induction of glycolytic pathways favors 2,3-BPG induction under hypoxia, steady state levels of PPP intermediates, such as phosphogluconolactone, 6-phosphogluconate, erythrose 4-phosphate and sedoheptulose phosphate (Figure 15), were found to be significantly decreased in hypoxia compared to sea level. As such, nicotinamide

adenine dinucleotide phosphate-reduced (NADPH), the PPP derived reducing equivalent, was significantly decreased in high altitude hypoxia in a time-dependent manner (Figure 15). These observations implicate that erythrocytes adapt to high altitude hypoxia by enhancing glucose flux through glycolytic pathway and decreasing its flux through the PPP and thus facilitating 2,3-BPG production.

3.2.5 Erythrocyte Sphk1 promotes glucose fluxes to glycolysis in hypoxia

The above results suggest the possibility that hypoxia-induced erythrocyte Sphk1 activity regulates glucose metabolism. To test this hypothesis, I conducted glucose flux experiments in collaboration with Dr. Angelo D'Alessandro of The University of Colorado School of Medicine using isotopic $^{13}\text{C}_{1,2,3}$ -glucose to trace the fraction of glucose metabolized to glycolysis and PPP, respectively, in erythrocytes isolated from WT and *Sphk1*^{-/-} mice treated under normoxia and hypoxia at different time points (for detail see Methods). As shown in Figure 16a, if $^{13}\text{C}_{1,2,3}$ -glucose is metabolized directly through glycolysis, $^{13}\text{C}_3$ -lactate will be generated; whereas if glucose is metabolized through PPP, $^{13}\text{C}_2$ -lactate will be produced, owing to the release of the first carbon atom of glucose in the form of CO_2 during glucose catabolism at the oxidative branch of the PPP. Ratios of $^{13}\text{C}_3$ -lactate/ $^{13}\text{C}_2$ -lactate isotopologue indicate glucose fluxes to glycolysis over PPP. First, $^{13}\text{C}_3$ -lactate/ $^{13}\text{C}_2$ -lactate ratios were significantly induced in cultured WT mouse erythrocytes under hypoxia compared to normoxia in a time dependent manner (Figure 16b), indicating that hypoxia promoted significant increases in metabolic switch of glucose fluxes toward glycolysis in WT mouse erythrocytes and supporting the findings from *in vivo* human erythrocyte metabolomic profiling in response to high altitude (Figure 16b). Unexpectedly, ratios of $^{13}\text{C}_3$ -lactate/ $^{13}\text{C}_2$ -lactate isotopologue

were also significantly induced in WT mouse erythrocytes under normoxia in a time dependent manner, implicating that other factors besides hypoxia likely involved in switch of glucose fluxes to glycolysis in WT mouse erythrocytes in culture system under normoxia (Figure 16b). And S1P appears to be such a factor because ratios of $^{13}\text{C}_3$ -lactate/ $^{13}\text{C}_2$ -lactate isotopologue under hypoxia to normoxia was significantly induced approximately 1.5 fold from 1 hour until 6 hours in WT mouse erythrocytes (Figure 16c); while the fold induction of the ratios of $^{13}\text{C}_3$ -lactate/ $^{13}\text{C}_2$ -lactate isotopologue under hypoxia to normoxia was significantly attenuated in *Sphk1*^{-/-} mouse erythrocytes compared (Figure 16c), indicating that hypoxia-induced switch of fluxes of glucose from PPP to glycolysis is compromised in *Sphk1*^{-/-} mouse erythrocytes. Altogether, these data indicate that erythrocyte Sphk1 contributes to the regulation of the hypoxia-dependent metabolic switch that promotes glucose metabolic fluxes through glycolysis.

Figure 16

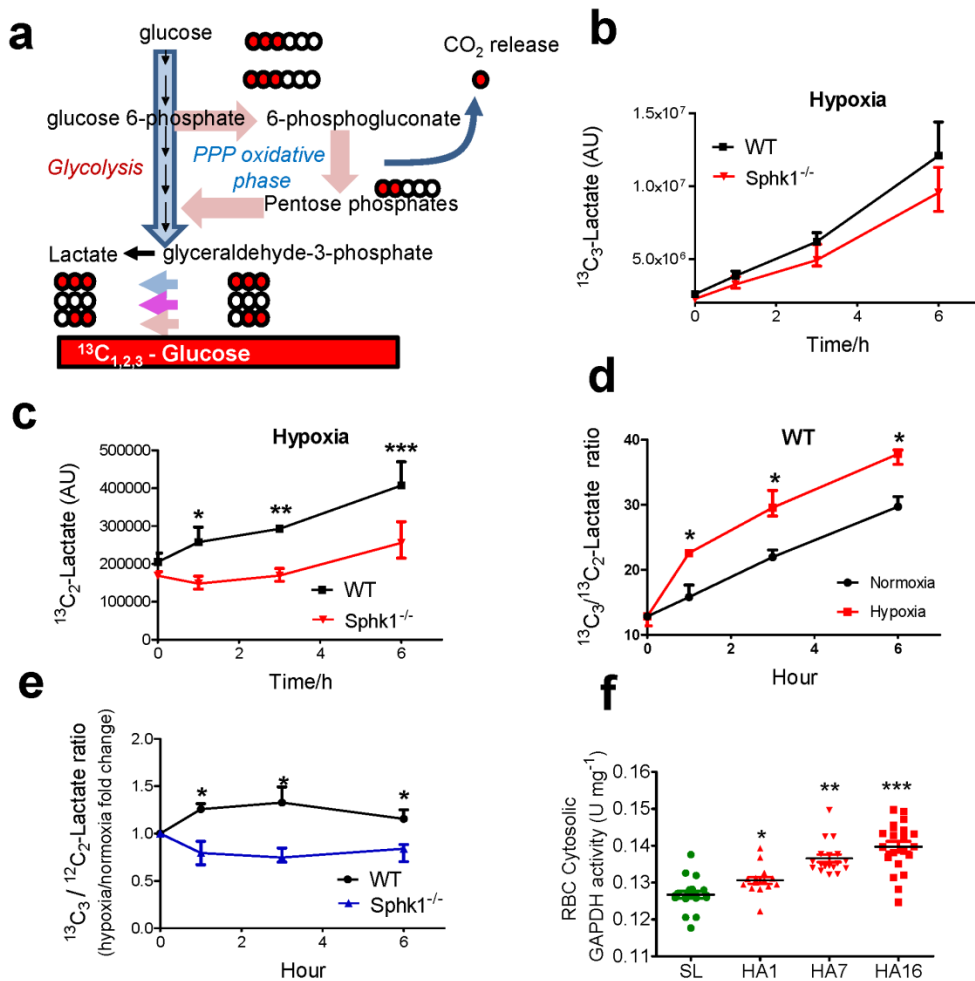


Figure 16. Alteration of erythrocyte glucose metabolism favoring glycolysis in hypoxia. (a) Schematic illustration of glucose metabolism flux detection using $^{13}\text{C}_{1,2,3}$ -Glucose. Changes of $^{13}\text{C}_3$ -lactate (b) and $^{13}\text{C}_2$ -lactate (c) in hypoxia in WT and $Sphk1^{-/-}$ erythrocytes. (d) $^{13}\text{C}_3/^{13}\text{C}_2$ -lactate ratio determined in WT erythrocytes in normoxia and hypoxia. Fold change of $^{13}\text{C}_3/^{13}\text{C}_2$ -lactate ratio (e) in WT and $Sphk1^{-/-}$ erythrocytes in hypoxia to normoxia. (f) Erythrocyte cytosolic GAPDH activity in erythrocyte from humans exposed to high-altitude hypoxia. Mean \pm s.e.m. For human studies, $n = 16-21$ per group; for mouse studies $n=4$ per group; * $P < 0.01$ versus SL, normoxia or $Sphk1^{-/-}$, ** $P < 0.01$ versus HA1, *** $P < 0.001$ versus HA7, Student's t -test, two way ANOVA and one way ANOVA.

3.2.6 High altitude induces glycolytic enzyme activity in human erythrocytes

Glycolysis is limited by the availability of glycolytic enzymes such as glyceraldehyde-3-phosphate dehydrogenase (GAPDH) in cytosol, since most of the rate-limiting glycolytic enzymes are bound to membrane and partially inhibited under normoxia [102, 103]. In hypoxia, deoxygenated Hb (deoxyHb) binds to the cytosolic domain of band 3 at the membrane and releases the glycolytic enzymes to the cytosol to become more active and enhance glycolysis [111-113]. The above findings suggest that S1P may be a key regulatory contributor to the oxygen-dependent metabolic modulation model. Therefore, I tested if S1P affects the binding of deoxy-Hb to membrane, which could result in the release and activation of glycolytic enzymes from membrane. The cytosolic activity of GAPDH is measured in human volunteers at sea level and at high altitude. Supporting the hypothesis and metabolomic profiling result, erythrocyte cytosolic GAPDH activity was significantly increased in a time-dependent manner in response to high altitude hypoxia compared to sea level (Figure 16d).

3.2.7 Hypoxia-induced GAPDH activity is blunted in *Sphk1*^{-/-} mice

Next, to provide genetic evidence, I first measured cytosolic GAPDH activity in WT and *Sphk1*^{-/-} mice under normoxia and hypoxia at different time points. Consistent with the results in humans, hypoxia gradually induced cytosolic GAPDH activity up to three folds after 72 hours exposure (Figure 17a). However, hypoxia-induced elevation of erythrocyte cytosolic GAPDH activity was significantly reduced in *Sphk1*^{-/-} mice compared to WT mice (Figure 17a). Meanwhile, confocal microscopy showed significant increase of cytosolic GAPDH in WT mice erythrocyte after 72 hours hypoxia treatment while to a much less extent in *Sphk1*^{-/-} mice using (Figure 17b). Thus, Sphk1 is essential

for hypoxia-induced release of GAPDH from membrane to cytosol and subsequent elevated cytosolic GAPDH activity under hypoxia condition.

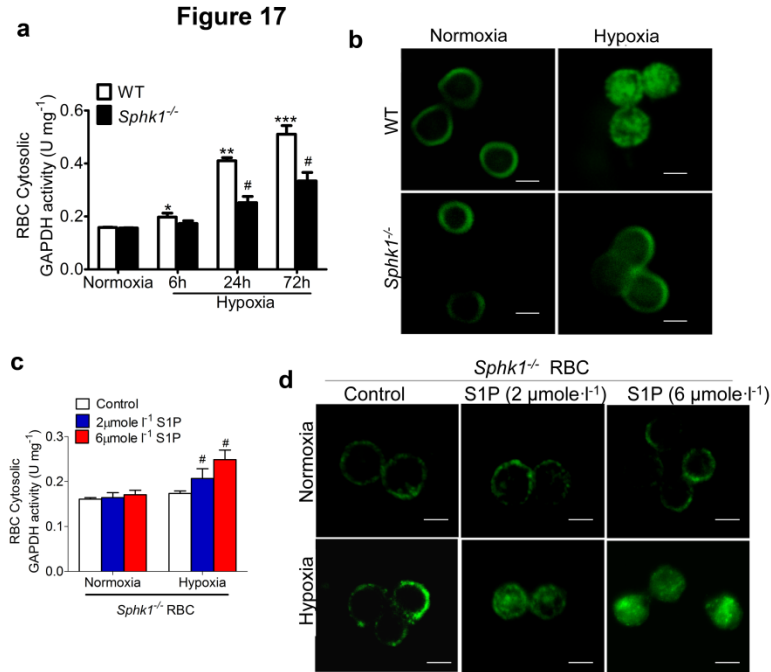


Figure 17. Sphk1-mediated production of S1P functions intracellularly underlying hypoxia-induced cytosolic GAPDH by inducing GAPDH release from membrane to cytosol .
(a) Erythrocyte cytosolic GAPDH activity in WT and *Sphk1*^{-/-} mice treated in normoxia and hypoxia (10% O₂) for different time. **(b)** Representative con-focal images demonstrating GAPDH localization in erythrocytes from WT and *Sphk1*^{-/-} mice treated in normoxia and hypoxia for 72 hours. **(c-d)** Cytosolic GAPDH activity **(c)** and representative con-focal images in primary cultures of *Sphk1*^{-/-} mouse erythrocyte pretreated with DMSO, 2 and 6 μmole·l⁻¹ S1P in normoxia and hypoxia (4% O₂) for 6 hours. Mean ± s.e.m; n = 4-6 per group; **P* < 0.05 versus normoxia, ***P* < 0.05 versus 6h, ****P* < 0.05 versus 24h, # *P* < 0.05 versus control, Student's *t*-test and one way ANOVA. (Confocal data obtained by Dr. Yujin Zhang and use with permission)

Next, to determine if function of Sphk1 is mediated by S1P surface receptors, erythrocytes from WT and *Sphk1*^{-/-} mice were isolated and pretreated with exogenous S1P up to 250 nmole·l⁻¹ under normoxia and hypoxia conditions. S1P pretreatment up to 250 nmole·l⁻¹ had no effect on cytosolic GAPDH activity in cultured erythrocytes from WT under either normoxia or hypoxic conditions (Figure 44). Moreover, S1P pretreatment could not rescue cytosolic GAPDH induction under both normoxia and

hypoxia condition in cultured erythrocytes isolated from *Sphk1*^{-/-} mice (Figure 44). Thus, these studies provided evidence that Sphk1 underlies hypoxia-induced GAPDH activity independent of S1P receptors in the erythrocytes.

Figure 18

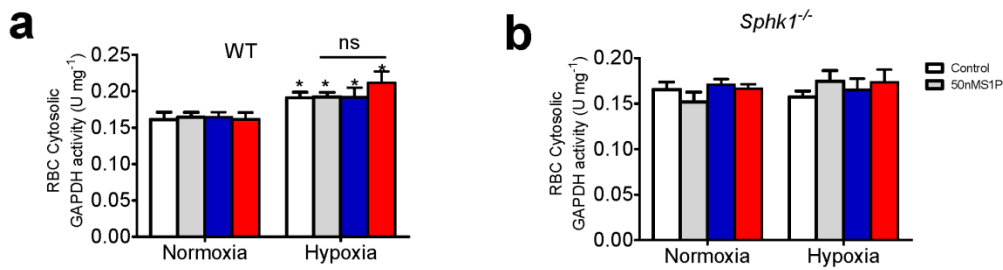


Figure 18. Cytosolic GAPDH activity in erythrocytes isolated from WT and *Sphk1*^{-/-} mice treated with different doses of S1P under normoxia and hypoxia for 6 hours.

Mean ± s.e.m; N=6~8 for each group; *p<0.05 versus normoxia, Student's t-test and one way ANOVA.

Erythrocytes can readily uptake exogenous S1P up to 5μmole·l⁻¹ in an *in vitro* system[4]. Thus, I chose to test if exogenous S1P at μmole·l⁻¹ concentrations known to be taken up by erythrocytes can restore hypoxia-induced GAPDH activity by releasing membrane anchored GAPDH to the cytosol in isolated *Sphk1*^{-/-} mouse erythrocytes. First, under normoxia, pretreatment with S1P up to 6 μmole·l⁻¹ had no effect on cytosolic GAPDH activity in *Sphk1*^{-/-} erythrocytes (Figure 17c). However, under hypoxia, S1P pretreatment at 2 μmole·l⁻¹ began to induce erythrocyte cytosolic GAPDH activity and reached higher level with 6 μmole·l⁻¹ S1P pretreatment (Figure 17c). Consistently, confocal image analysis revealed that S1P treatment significantly induced translocation of membrane anchored GAPDH to the cytosol of *Sphk1*^{-/-} mouse erythrocytes in a dosage-dependent manner under hypoxia but not normoxia condition (Figure 17d). These studies provided genetic evidence that S1P at μmole·l⁻¹

concentrations restored hypoxia-induced cytosolic GAPDH activity by promoting translocation of GAPDH from the membrane to the cytosol in *Sphk1*^{-/-} mouse erythrocytes.

3.2.8 S1P underlies hypoxia-induced GAPDH activity

Previous studies showed that organic phosphates (such as 2,3-BPG) can bind to Hb[42, 114-117]. S1P, also an organic phosphate, is produced and stored at relative high concentrations in erythrocytes. Thus, it is possible that S1P directly binds to Hb. Indeed, S1P-beads, but not lysophosphatic acid (LPA)-beads or sphingosine (Sph)-beads, successfully pulled down Hb from erythrocyte lysates of normal humans (Figure 19a). This is important evidence that S1P directly interacts with Hb in the erythrocyte lysates. These findings raise an intriguing possibility that interaction of S1P with Hb can promote deoxy-Hb anchoring to the membrane thereby enhancing release of glycolytic enzymes (such as GAPDH) from membrane to the cytosol under hypoxic conditions. To test this hypothesis, membrane anchored Hb was assayed by measuring heme content in isolated *Sphk1*^{-/-} mouse erythrocytes treated with or without S1P at μM concentrations, which is known to increase intracellular S1P levels. S1P treatment significantly increased membrane heme content under hypoxia but not under normoxia (Figure 19b). Thus, S1P treatment can restore hypoxia-induced deoxygenated Hb anchoring to the membrane and subsequent release of GAPDH from membrane to cytosol.

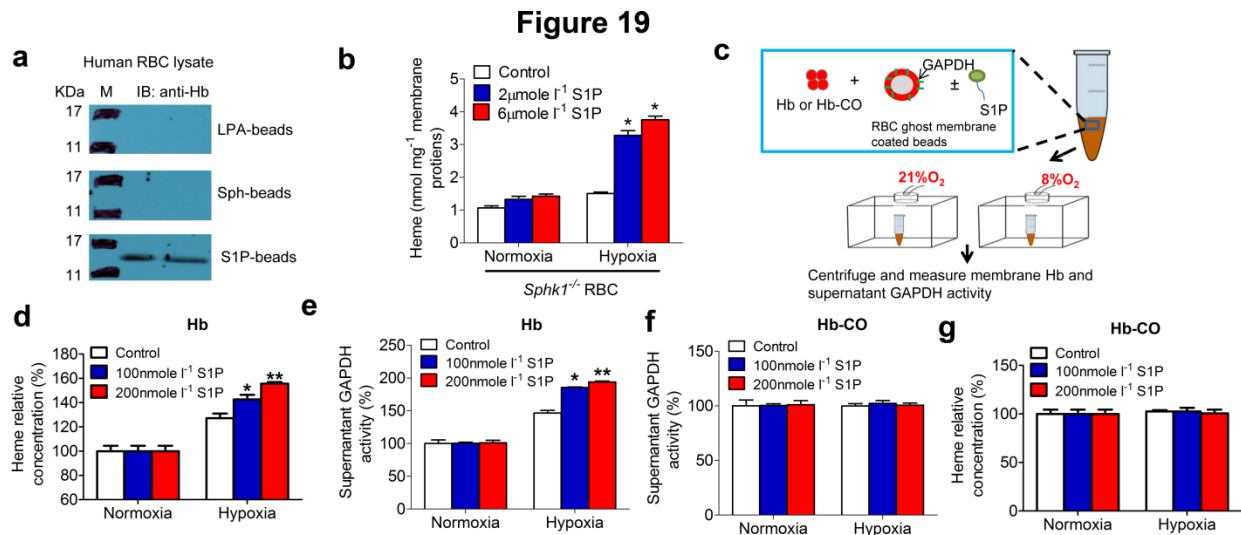


Figure 19. S1P promotes deoxy-Hb anchoring to the membrane and enhances GAPDH release from membrane to cytosol only under hypoxia but not normoxia deoxy-Hb. (a) Pull-down of Hb by LPA, Sphingosine and S1P beads from normal human RBC lysates. (b) Membrane heme concentrations in isolated *Sphk1*^{-/-} mouse erythrocyte pretreated with DMSO, 2 and 6 $\mu\text{mole}\cdot\text{l}^{-1}$ S1P in normoxia and hypoxia (4% O₂) for 6 hours. (c) Schematic drawing illustrates functional experiments to monitor translocation of GAPDH from membrane isolated from human erythrocytes. Hb binding to membrane (d) and GAPDH release from membrane to the cytosol (e) in human erythrocyte membrane ghost treated with Hb and different concentration of S1P under normoxia and hypoxia. Hb binding to membrane (f) and GAPDH release from membrane to the cytosol (g) in human erythrocyte membrane ghost treated with Hb-CO and different concentration of S1P under normoxia and hypoxia. Mean \pm s.e.m; n = 6 per group, * $P < 0.05$ versus normoxia, ** $P < 0.05$ versus 2 $\mu\text{mole}\cdot\text{l}^{-1}$ or 100 nmole l⁻¹, Student's *t*-test and one way ANOVA. (Pulldown data obtained by Dr. Yujin Zhang and use with permission)

Finally, to validate the mouse findings, I conducted functional experiments to directly monitor 1) the alteration of membrane anchored Hb and 2) the translocation of GAPDH from human erythrocyte membranes under normoxia and hypoxia. First, human erythrocyte ghost membranes were inversely coated on silicon beads to expose the inner layer. Then, the silicon beads were coated with inverted erythrocyte ghost membranes with 100 $\mu\text{mole}\cdot\text{l}^{-1}$ Hb in the absence or presence of S1P at 100 nmole l⁻¹, to mimic the physiological molar ratio of Hb:S1P from 1000:1 under different concentration of O₂ ranging from fully oxygenated (21% O₂) to hypoxia (8%). After 10-

min incubation followed by brief centrifugation, supernatant GAPDH activity and membrane anchored Hb were quantified, respectively (Figure 19c). Membrane anchored heme significantly increased under hypoxia compared to normoxia (Figure 19d). Moreover, once Hb was fully oxygenated under normoxia condition (21% O₂), S1P failed to induce oxy-Hb anchoring to membrane (Figure 19d). However, under hypoxia condition, S1P further enhanced deoxy-Hb anchoring to the membrane (Figure 19d). Next, the functional kinetics of S1P on membrane anchored deoxy-Hb under 8% O₂ was measured with different concentrations of S1P ranged from 0 to 200 nmole·l⁻¹. S1P increased membrane anchored deoxy-Hb but not oxy-Hb in a dose-dependent manner (Figure 19d). Thus, these studies provide direct evidence that S1P forms a complex with Hb and promotes deoxy-Hb anchoring to the membrane in a hypoxia-dependent manner.

In parallel, the release of GAPDH from the membrane under normoxia and hypoxia was also monitored, in presence of different doses of S1P as detailed above. Supernatant GAPDH activity was significantly induced under hypoxia in a S1P dose-dependent manner in comparison to normoxia (Figure 19e). In contrast, S1P had no effect on supernatant GAPDH activity under normoxia (Figure 19e). Since CO was reported to highly stabilize R-state of Hb to inhibit glycolysis, I examined if treatment with CO cancels effects of S1P on hypoxia-induced anchoring of Hb and GAPDH activity. In the CO-treated groups, we found that S1P had no effect on membrane anchoring of Hb (Figure 19f) and GAPDH activity (Figure 19g). Altogether, these data provide human evidence that S1P functions intracellularly as a hypoxia modulator promoting deoxy-Hb anchoring to the membrane and subsequently enhancing

membrane bound GAPDH releasing to the cytosol, which in turn leads to increased cytosolic GAPDH activity under hypoxia.

In this chapter, first, S1P is found significantly induced in humans following ascent to high altitude or mice expose to hypoxia. Then, beneficial role of Sphk1-dependent elevation of erythrocyte S1P by promoting 2,3-BPG production and O₂ release to counteract tissue hypoxia was revealed in animal experiments. Moreover, S1P functions intracellularly by binding directly to Hb, promoting deoxy-Hb anchoring to the membrane and subsequently enhancing the release of membrane bound glycolytic enzymes to the cytosol. Together, I found that increased erythrocyte S1P directs metabolic fluxes through glycolysis to generate more 2,3-BPG and thereby promoting O₂ release to protect against tissue hypoxia

3.3 Chapter 3: S1P induces pathogenic metabolic programming in SCD erythrocytes

Metabolomics screening revealed that circulating S1P is elevated in patients and mice with SCD[7, 8]. Additional studies showed that pharmacologic inhibition or shRNA knockdown of Sphk1 significantly attenuated sickling and other deadly complications [8]. Moreover, the previous chapter showed that increased S1P induces O₂ delivery to counteract tissue hypoxia by inducing 2,3-BPG production in healthy individuals at high altitude and in normal mice exposed to hypoxia, revealing the beneficial role of elevated erythrocyte S1P in normal individuals. However, it is puzzling why elevated S1P is detrimental in SCD. Here, functional, metabolic and structural studies solve the puzzle. In contrast to normal erythrocytes, genetic deletion of Sphk1 in SCD has potent anti-sickling and anti-hemolysis effects by correcting pathogenic metabolic reprogramming, channeling glucose to pentose phosphosphate pathway relative to glycolysis, lowering 2,3-BPG production and rewiring NADPH/glutathione-mediated detoxification. The findings open new scenarios for the development of innovative mechanism-based therapies.

3.3.1 Genetic evidence for the pathogenic role of elevated Sphk1 in SCD mice

To precisely assess the detrimental role and mechanisms of elevated S1P in SCD, I generated a strain of mice with humanized sickle Hb and Sphk1 deficiency by crossing the SCD Berkeley mice[68] with *Sphk1*^{-/-} mice[107] (Figure 20a). The *SCD/Sphk1*^{-/-} offspring were viable and lived to adulthood. PCR analysis confirmed that the *Sphk1* gene was deleted (Figure 20 a); analysis of Hb composition demonstrates the presence of only HbS in *SCD/Sphk1*^{-/-} erythrocyte; and Sphk1 activity is undetectable (Figure 20b;

erythrocyte and plasma S1P levels also decreased dramatically (Figure 20 c-e). The remaining plasma S1P is presumably derived from the Sphk2 isoform expressed in a variety of cells[106], but not in mature erythrocytes due to lack of a nucleus.

Figure 20

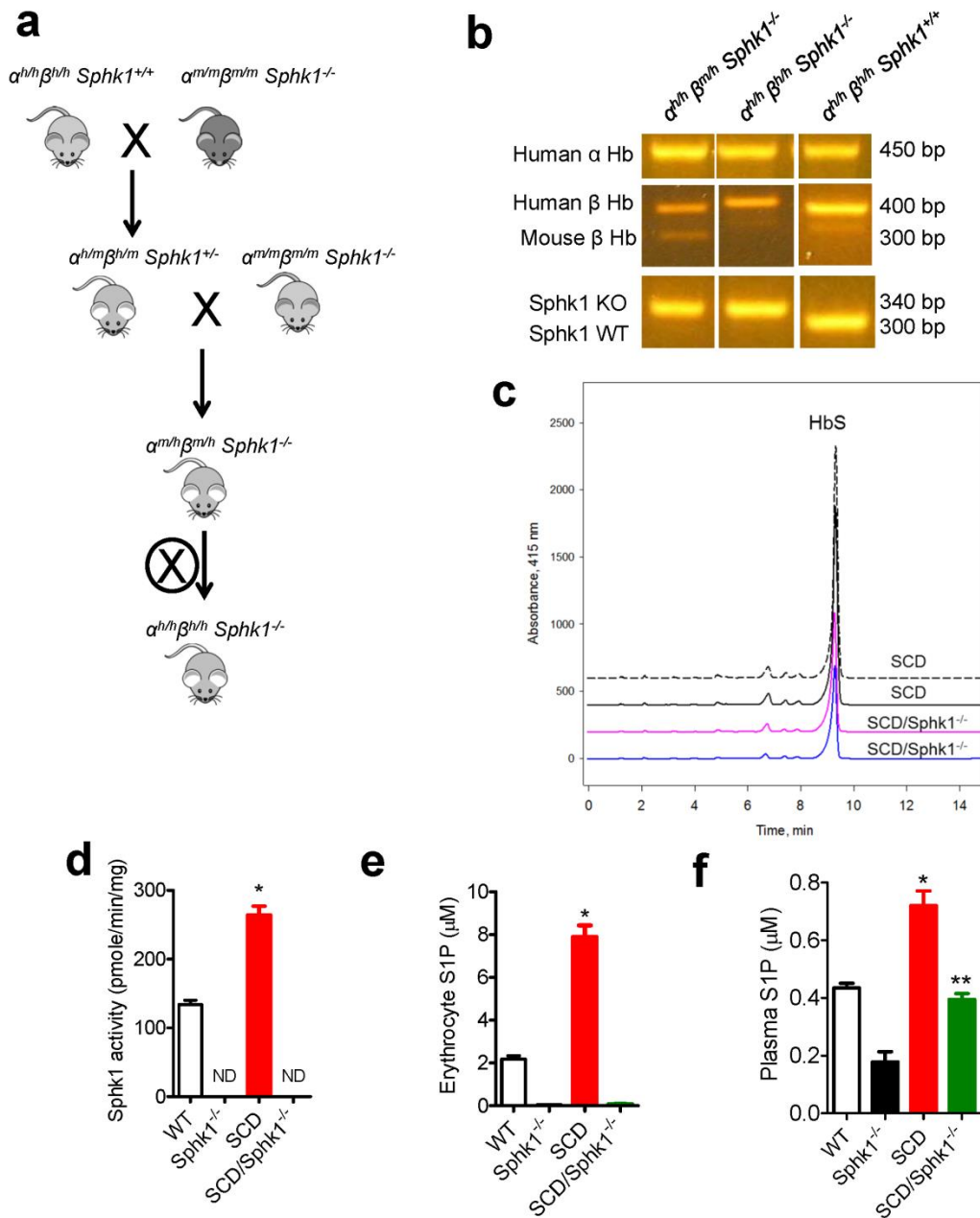


Figure 20. Generation and confirmation of *SCD/Sphk1*^{-/-} mice.

(a) Schematic plot demonstrating the mating strategy employed to generate *SCD/Sphk1^{-/-}* mice. (b) PCR analysis of genomic DNA detecting α,β Hb genes and *Sphk1* gene. (c) HPLC analysis of Hb composition in SCD and *SCD/Sphk1^{-/-}* mice. Erythrocyte Sphk1 activity (c), erythrocyte (d) and plasma (e) S1P levels in WT, *Sphk1^{-/-}*, SCD and *SCD/Sphk1^{-/-}* mice. Mean \pm s.e.m; N=5 for each group; * p <0.05 versus WT, ** p <0.05 versus SCD, Student's *t*-test.

Next, I compared sickling in age and gender matched *SCD/Sphk1^{-/-}* mice and SCD mice. Erythrocyte shape was much more uniform and organized in *SCD/Sphk1^{-/-}* mice (Figure 21a), and the percentage of irreversible sickle-shaped erythrocytes was significantly reduced (Figure 21b). Because intravascular hemolysis is one of the major complications of SCD[118], I assayed erythrocyte hemolysis by measuring plasma Hb concentrations, which are significantly lower in *SCD/Sphk1^{-/-}* mice (Figure 21c). Improvement of erythrocyte life-span in *SCD/Sphk1^{-/-}* mice was observed (Figure 21d). Because of severe anemia, there is a large number of reticulocytes in SCD mice[68], which were significantly reduced in *SCD/Sphk1^{-/-}* mice (Figure 21e). Complete blood count (CBC) analysis revealed higher total erythrocyte number, Hb concentration and hematocrit in *SCD/Sphk1^{-/-}* mice (Table 1). Moreover, the erythrocyte distribution width was also significantly reduced (Table 1). Because S1P is a potent immune regulator[119], the peripheral white blood cell count was dramatically decreased in *SCD/Sphk1^{-/-}* mice with both neutrophil and lymphocyte counts in the normal range (Table 1). Splenomegaly and multiple organ damage are the hallmarks of SCD progression[118]. Consistent with the above findings of improvements in *SCD/Sphk1^{-/-}* mice, splenomegaly (Figure 21f), congestion and damage in spleen, lungs and liver were also significantly improved in *SCD/Sphk1^{-/-}* mice (Figure 21g and h). Albumin levels in the bronchoalveolar lavage fluid were also significantly reduced (Figure 21h), indicating less vascular leakage in the lungs of *SCD/Sphk1^{-/-}* mice. Taken together,

these data provide solid genetic and clinic evidence indicating that deletion of Sphk1 is beneficial in SCD.

Table 1. Complete Blood Count of WT, SCD and *SCD/Sphk1^{-/-}* mice. Values shown represent the mean \pm SEM (n = 5); * $p < 0.05$ versus SCD, Student's *t*-test.

	WT	SCD	<i>SCD/Sphk1^{-/-}</i>
Erythrocyte			
RBC (M/ μ l)	9.42 \pm 0.78	5.26 \pm 0.39	6.79 \pm 0.59*
Hb (g/dl)	14.5 \pm 0.36	7.15 \pm 0.26	9.83 \pm 0.55*
HCT (%)	44.8 \pm 1.05	28.53 \pm 0.98	34.55 \pm 0.47*
MCV (fl)	49.8 \pm 2.33	44.53 \pm 0.97	50.60 \pm 3.47*
MCH (pg)	15.23 \pm 0.17	10.83 \pm 0.31	14.06 \pm 0.70*
MCHC (g/dl)	29.9 \pm 1.22	25.33 \pm 1.21	26.68 \pm 0.88
RDW (%)	18.5 \pm 4.35	32.47 \pm 5.47	23.58 \pm 3.54*
Leukocyte			
WBC (k/ μ l)	4.90 \pm 2.98	18.56 \pm 5.10	5.12 \pm 2.16*
NE (k/ μ l)	1.44 \pm 1.74	11.25 \pm 2.37	2.57 \pm 1.49*
LY (k/ μ l)	4.55 \pm 3.13	6.81 \pm 2.04	2.15 \pm 1.50*
MO (k/ μ l)	0.41 \pm 0.10	0.45 \pm 0.40	0.35 \pm 0.24
EO (k/ μ l)	0.14 \pm 0.05	0.04 \pm 0.006	0.05 \pm 0.03
BA (k/ μ l)	0.03 \pm 0.005	0.013 \pm 0.005	0.006 \pm 0.008

Figure 21

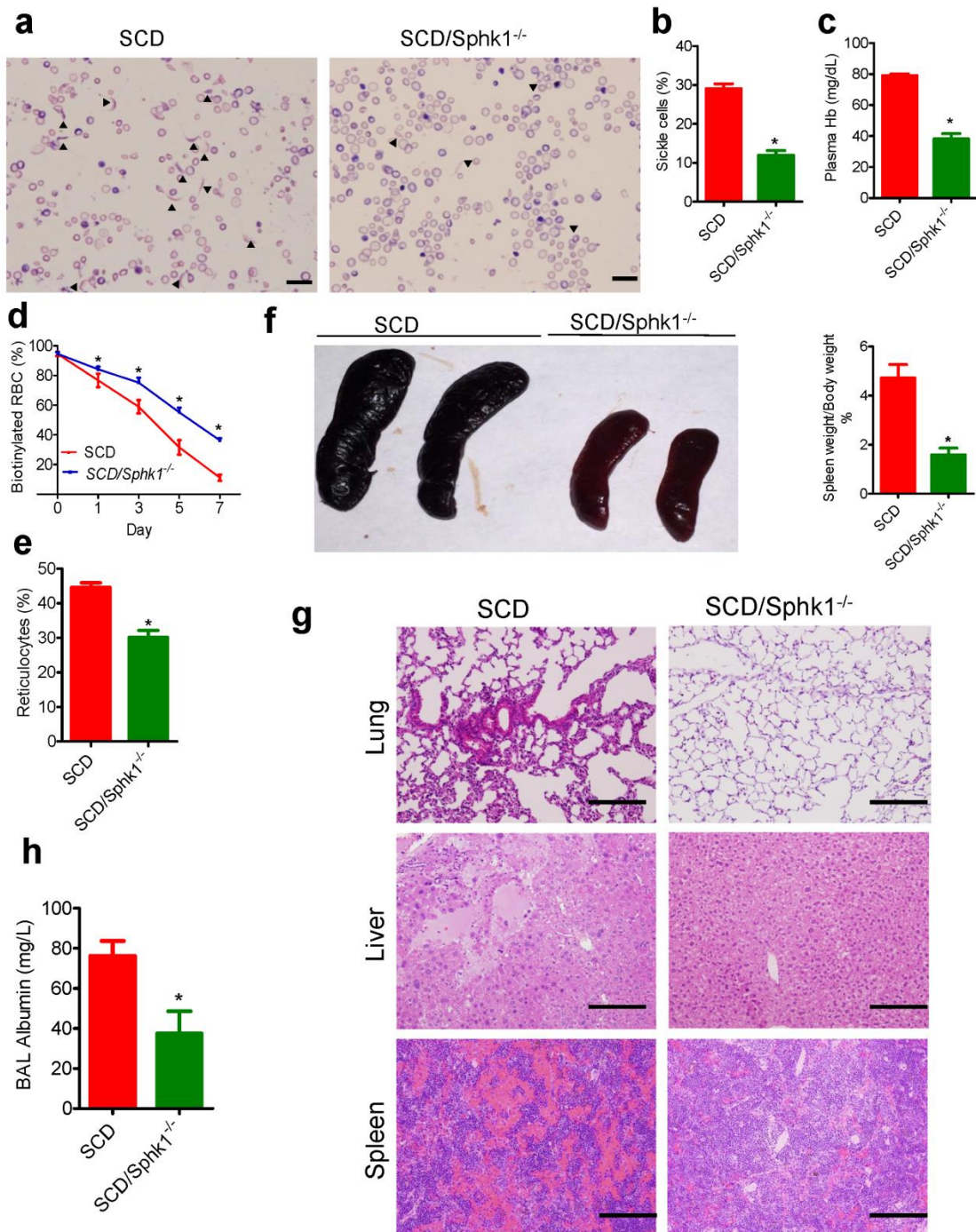


Figure 21. Genetic deletion of Sphk1 improves disease conditions in SCD Berkeley mice.

(a) Representative pictures of blood smears from SCD and *SCD/Sphk1*^{-/-} mice (magnification X400). Percentage of sickle cells (b), plasma Hb (c) and reticulocytes (e) were significantly reduced while erythrocyte lifespan was significantly prolonged (d) by genetic deletion of Sphk1. Spleen size, (f) H&E staining of spleens, livers, and lungs (g), and albumin concentrations in bronchial alveolar lavage (BAL)

fluid (h) collected from SCD and *SCD/Sphk1^{-/-}* mice. Values shown represent the mean \pm SEM (n = 5-10); **p* < 0.05 versus SCD, Student's *t*-test. Scale bar: 20 μ M in blood smear pictures; 200 μ M in H&E staining pictures. ▲ Indicates sickled RBCs.

3.3.2 Enhanced erythrocyte pentose phosphate pathway and anti-oxidation capacity in *SCD/Sphk1^{-/-}* mice

Next, because erythrocytes lack nuclei and organelles, metabolic adaptation has a key role in erythrocyte homeostasis[120], to further determine the molecular basis underlying such beneficial effects of Sphk1 deficiency in SCD, unbiased high-throughput metabolomics profiling was conducted to compare global metabolic changes in the erythrocytes among WT, SCD and *SCD/Sphk1^{-/-}* mice. Then, an unbiased pathway-enrichment analysis was performed in the results using MetaboAnalyst[121]. Among the 25 pathways identified, the top three metabolic pathways affected by genetic deletion of Sphk1 in SCD mice were the pentose phosphate pathway (PPP), glutathione metabolism, and sphingolipid metabolism (Figure 22a). Sphingolipid metabolism alteration validates the impact of Sphk1 deletion (Figure 20). Moreover, steady state levels of multiple intermediates of PPP including glucose 6-phosphate (G6P), gluconate-6-phosphate (6-P-gluconate), ribose 1-phosphate (R1P), erythrose 4-phosphate (E4P) and sedoheptulose 7-phosphate (S7P) substantially increased in the erythrocytes of *SCD/Sphk1^{-/-}* mice comparing to SCD mice (Figure 22b and c), suggesting that the PPP is significantly enhanced. In agreement with enhanced PPP, NADPH, an important byproduct of this pathway, increased as well (Figure 22d). As such, reduced glutathione (GSH), a key NADPH-dependent antioxidant, was substantially elevated (Figure 22e). Altogether, these data strongly suggest a decrease

in oxidative stress in *SCD/Sphk1^{-/-}* erythrocytes. Not surprisingly, ROS levels are significantly lower in *SCD/Sphk1^{-/-}* erythrocytes (Figure 22f). Many studies have indicated that excessive oxidative stress in SCD leads to hemolysis and erythrocyte destruction[64]. Thus, I sought to determine if deletion of Sphk1 increases resistance of SCD erythrocytes to hemolytic challenges induced by oxidative stress. After exposure to hydrogen peroxide (H_2O_2), *SCD/Sphk1^{-/-}* erythrocytes had a significantly lower osmotic fragility with increased half-maximal effective concentrations (EC50) (Figure 22g), consistent with increased GSH and NADPH-dependent antioxidant capacity.

Figure 22

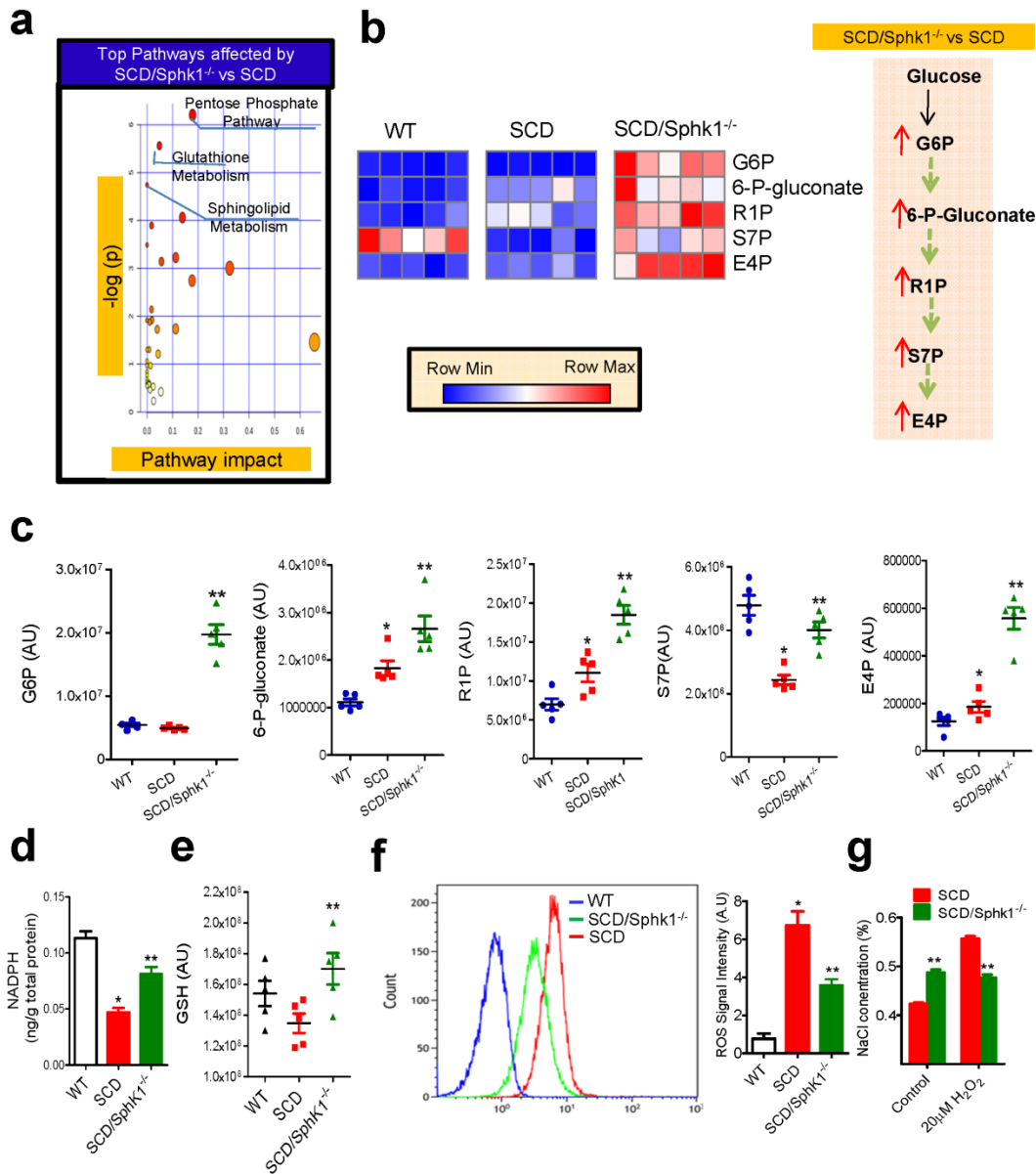


Figure 22. Enhanced pentose phosphate pathway and anti-oxidant capacity in *SCD/Sphk1*^{-/-} mouse erythrocytes.

(a) Top metabolic pathways affected by genetic deletion of *Sphk1* in SCD mice. (b) Relative abundance of selected PPP metabolites in erythrocytes from WT, SCD and *SCD/Sphk1*^{-/-} mice (left); PPP is significantly enhanced in erythrocytes of *SCD/Sphk1*^{-/-} mice comparing to SCD mice (right). (c) Intensity peak of selected PPP metabolites in erythrocytes from WT, SCD and *SCD/Sphk1*^{-/-} mice detected by metabolomics screening. Levels of NADPH (d), GSH (e) and ROS (f) in erythrocytes from WT, SCD and *SCD/Sphk1*^{-/-} mice. (g) Resistance of SCD and *SCD/Sphk1*^{-/-} erythrocytes to osmolality-induced hemolysis with or without oxidative stress challenge. Values shown represent the mean \pm SEM (n = 5); **p* < 0.05 versus WT; ***p* < 0.05 versus SCD; Student's *t*-test. G6P: Glucose 6-phosphate; 6-P-Gluconate: Gluconate-6-phosphate; R1P: Ribose 1-phosphate; E4P: Erythrose 4-phosphate; S7P: Sedoheptulose 7-

phosphate; GSH: reduced glutathione. (Figure 22 a and b drawn by Dr. Angelo D'Alessandro of The University of Colorado School of Medicine, use with permission)

3.3.3 Reduced erythrocyte glycolysis and Hb-O₂ binding affinity in

***SCD/Sphk1^{-/-}* mice**

Glucose in erythrocytes is metabolized through either PPP, to generate reducing equivalents to preserve redox homeostasis, or glycolysis, to produce ATP as an energy source[122]. Additionally, approximately 19~25% of the glucose is utilized to produce 2,3-BPG, a key allosteric regulator of Hb-O₂ affinity, which derives from the Rapoport-Luebering branch of glycolysis[123]. Under high O₂ saturation conditions, oxidative stress promotes PPP to generate NADPH. To deliver O₂ efficiently while neutralizing excessive oxidative stress caused by a heavy load of O₂, erythrocytes rely on a finely-tuned O₂-dependent modulation of glucose metabolism[113]. Based on the enhanced PPP and glutathione metabolism in the erythrocytes of *SCD/Sphk1^{-/-}* mice (Figure 22), I sought to test if increased steady state levels of PPP intermediates in *SCD/Sphk1^{-/-}* mouse erythrocytes correspond to a decline of metabolic flux through glycolysis. First, I observed significantly increased glycolytic intermediates including G6P, fructose 1,6-bisphosphate (FBP), glyceraldehyde 3-phosphate (G3P), 2/3-phosphoglyceric acid (2/3-PG), phosphoenolpyruvate (PEP) and pyruvate in SCD mouse erythrocytes compared to WT (Figure 54.a-b), confirming that glycolysis rather than the PPP is preferentially active in SCD mouse erythrocytes, which explains the compromised capacity to produce reducing equivalents and preserve glutathione homeostasis in SCD. Surprisingly, three upstream glycolysis metabolites including G6P, FBP and G3P increased in *SCD/Sphk1^{-/-}* erythrocytes compared to SCD (Figure 23a and b), suggesting a metabolic bottleneck downstream to G3P dehydrogenase (GAPDH)[124].

In contrast, the levels of three glycolytic intermediates downstream of G3P including 2/3-PG, PEP and pyruvate were significantly reduced in *SCD/Sphk1^{-/-}* erythrocytes (Figure 23a and b). More importantly, 2,3-BPG, also an intermediate downstream of G3P, increased in SCD erythrocyte but decreased in that of *SCD/Sphk1^{-/-}* mice (Figure 23c). The major reasons why elevated 2,3-BPG-mediated erythrocyte sickling is by decreasing HbS-O₂ binding affinity which leads to increased deoxyHbS and deoxyHbS polymerization[125, 126]. To determine if Sphk1 contributes to this process, I measured the O₂ equilibrium curve (OEC) indexed by calculating the partial pressure of O₂ required to produce 50% Hb-O₂ saturation (P50) and found increased Hb-O₂ binding affinity and thus reduced P50 in *SCD/Sphk1^{-/-}* mouse erythrocytes (Figure 23d). These findings indicate that decreased 2,3-BPG due to deficiency of Sphk1 results in Hb-O₂ binding affinity increase and deoxyHbS level decrease, which supports the observation of less sickling in *SCD/Sphk1^{-/-}* mouse. Altogether, the beneficial role of Sphk1 deficiency in anti-sickling and anti-hemolysis is strongly supported by metabolic rewiring in *SCD/Sphk1^{-/-}* erythrocytes.

Figure 23

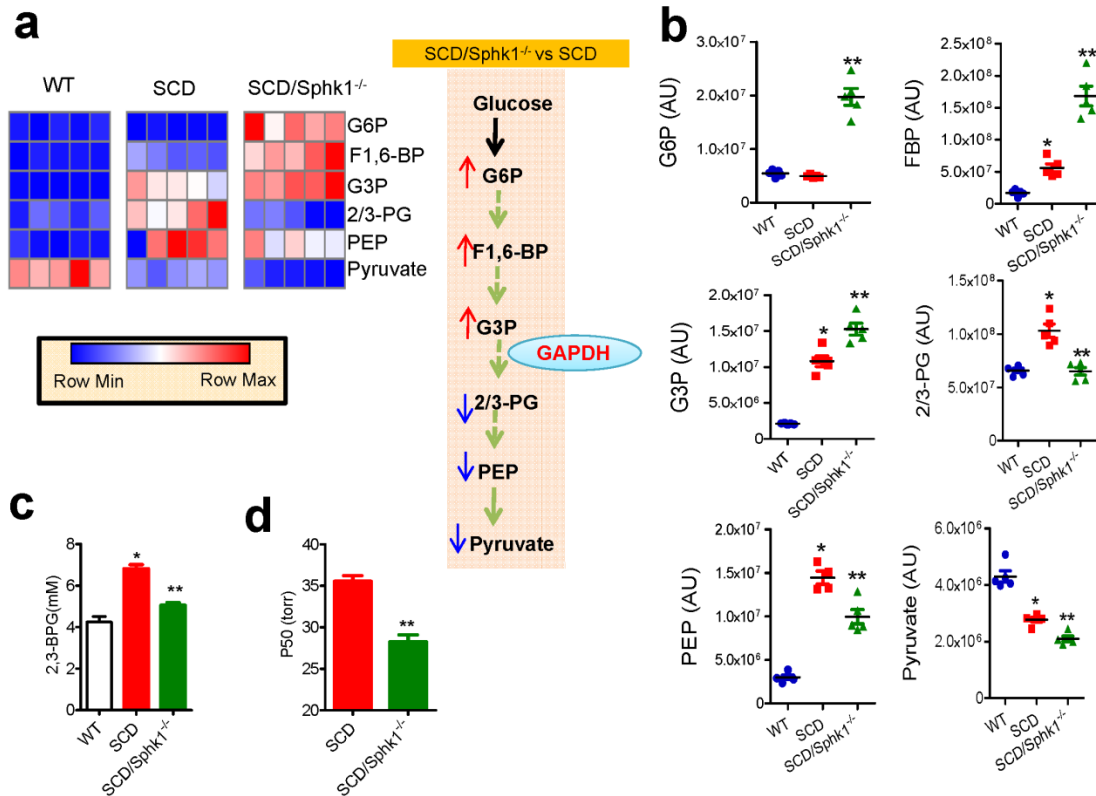


Figure 23. Genetic deletion of Sphk1 reduces glycolysis and O₂ release.

(a) Relative abundance of selected glycolysis metabolites in erythrocytes from WT, SCD and *SCD/Sphk1^{-/-}* mice (left); glycolysis is blocked at the step where G3P is metabolized by GAPDH in erythrocytes of *SCD/Sphk1^{-/-}* mice comparing to SCD mice (right). (b) Intensity peak of selected glycolysis metabolites in erythrocytes from WT, SCD and *SCD/Sphk1^{-/-}* mice detected by metabolomics screening. Reduced 2,3-BPG level (c) and P50 (d) in *SCD/Sphk1^{-/-}* mouse erythrocytes. Values shown represent the mean ± SEM (n = 5); **p* < 0.05 versus WT; ***p* < 0.05 versus SCD; Student's *t*-test. PPP: pentose phosphate pathway; G6P: Glucose 6-phosphate; FBP: Fructose 1,6-bisphosphate; G3P: Glyceraldehyde 3-phosphate; 2/3-PG: 2/3-Phosphoglyceric acid; PEP: Phosphoenolpyruvate. (Figure 23 a drawn by Dr. Angelo D'Alessandro of The University of Colorado School of Medicine, use with permission)

3.3.4 Genetic deletion of Sphk1 channels glucose fluxes to PPP in SCD erythrocytes

Next, to provide direct mechanistic insights into intracellular glucose flux, I used the stable ¹³C_{1,2,3}-glucose isotope to trace intracellular glucose metabolism through glycolysis and PPP in SCD and *SCD/Sphk1^{-/-}* erythrocytes at different time points. Specially, I investigated whether glycolysis or the PPP is the major contributor to the

accumulation of G3P in *SCD/Sphk1^{-/-}* mouse erythrocytes by determining the ratios of the isotopologues $^{13}\text{C}_{2,3}/^{13}\text{C}_{1,2,3}$ of G3P (Figure 24a). First, $^{13}\text{C}_{1,2,3}\text{-lactate}/^{13}\text{C}_{1,2,3}\text{-glucose}$ ratios were significantly increased in SCD but not in *SCD/Sphk1^{-/-}* mouse erythrocytes in a time-dependent manner, indicating significant increases in metabolic fluxes through PPP in SCD mouse erythrocytes (Figure 24b). As expected, ratios of $^{13}\text{C}_{2,3}\text{-G3P}/^{13}\text{C}_{1,2,3}\text{-G3P}$ isotopologues were significantly higher in erythrocytes from *SCD/Sphk1^{-/-}* erythrocytes (Figure 24c), indicating that glucose fluxes through the PPP are enhanced.

Figure 24

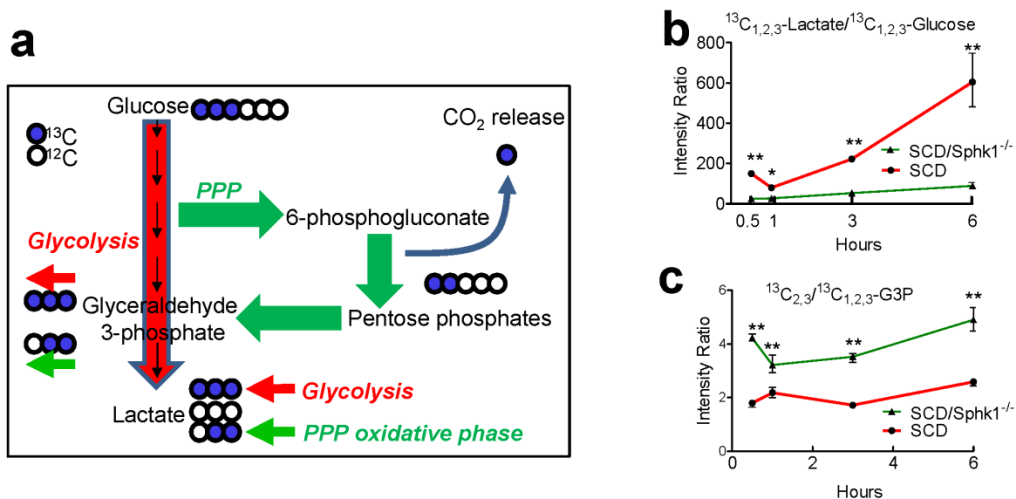


Figure 24. Genetic deletion of Sphk1 channels glucose flux to PPP in SCD erythrocytes. (a) Schematic illustration of glucose metabolism flux detection using $^{13}\text{C}_{1,2,3}\text{-Glucose}$. Ratios of $^{13}\text{C}_{1,2,3}\text{-Lactate}/^{13}\text{C}_{1,2,3}\text{-Glucose}$ (b) and $^{13}\text{C}_{2,3}/^{13}\text{C}_{1,2,3}\text{-G3P}$ (c) in SCD and *SCD/Sphk1^{-/-}* mouse erythrocytes. Values shown represent the mean \pm SEM (n = 5); ***p* < 0.05 versus SCD; Student's *t*-test. CO_2 : carbon dioxide. (Figure 24 a drawn by Dr. Angelo D'Alessandro of The University of Colorado School of Medicine, use with permission)

3.3.5 Sphk1 regulates GAPDH localization in SCD erythrocyte

Under normoxia, erythrocyte glucose flux through glycolysis is limited by the inhibitory sequestration of glycolytic enzymes, including GAPDH, to the membrane

protein Band3[78]. However, under hypoxia, deoxygenated Hb (deoxyHb) competes with glycolytic enzymes for binding to Band3, which results in the release of those enzymes, thereby promoting glycolysis[78]. Recent studies have revealed that deoxyHbS disturbs normal coupling among erythrocyte O₂ content, glycolysis and antioxidant capacity by increasing release of membrane anchored GAPDH to the cytosol[6]. Since the previous chapter revealed that S1P can regulate GAPDH localization in normal erythrocyte in hypoxia, I sought to test if such regulation also exists in SCD erythrocytes. Western blot results indicated no obvious difference in total amount of GAPDH (Figure 25a). However, a significantly larger percentage of GAPDH in *SCD/Sphk1*^{-/-} erythrocytes was found on the membrane (Figure 25a). Moreover, cytosolic GAPDH activity significantly reduced in *SCD/Sphk1*^{-/-} erythrocytes compared to *SCD* (Figure 25b). Thus, genetic and biochemical evidence demonstrate that Sphk1 enhances release of membrane anchored GAPDH and increases cytosolic GAPDH activity. Next, I isolated erythrocyte membrane ghosts from *SCD* and *SCD/Sphk1*^{-/-} mice and noticed that ghost membrane isolated from erythrocytes of *SCD* mice displayed much more intensive red color compared to *SCD/Sphk1*^{-/-} mice (Figure 25c left panel), indicative of increased membrane bound hemoglobin in the former. To dissect the influence of non-specifically bound HbS, I inverted the membrane ghost on silicon beads and washed for 8 times with low-salt buffer. Significantly higher heme can be seen anchored on the ghost membrane of erythrocytes from *SCD* (Figure 25c, right panel). These findings indicate that elevated Sphk1 is associated with enhanced HbS anchoring to membrane, and are consistent with the release of membrane bound GAPDH and increased cytosolic GAPDH activity.

Figure 25

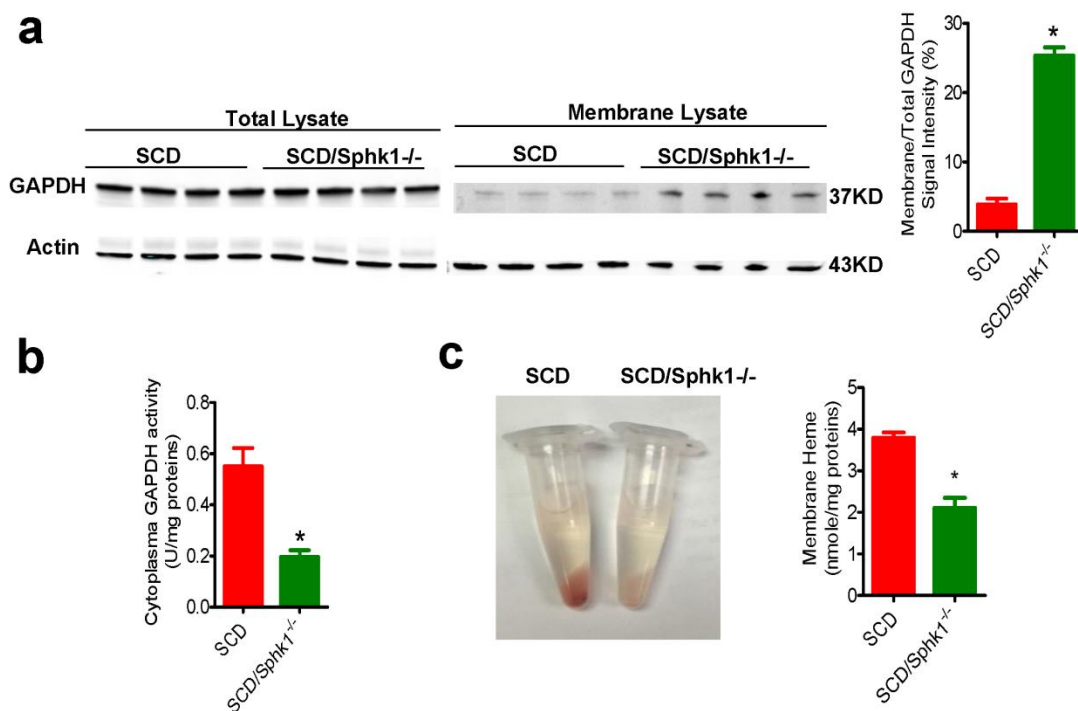


Figure 25. Sphk1-mediated production of S1P functions intracellularly to regulate GAPDH and Hb localization and subsequent metabolic consequences.

(a) Total and membrane bound GAPDH protein levels in SCD and *SCD/Sphk1^{-/-}* mouse erythrocytes detected by western blot. (b) Cytosolic GAPDH activity in SCD and *SCD/Sphk1^{-/-}* mouse erythrocytes. (c) Significantly decreased membrane bound heme in *SCD/Sphk1^{-/-}* mouse erythrocytes compared to SCD mouse erythrocytes. Values shown represent the mean \pm SEM (n = 5); **p* < 0.05 versus SCD; Student's *t*-test.

3.3.6 Co-binding of 2,3-BPG and S1P to Hb is required for S1P-induced decrease in Hb-O₂ affinity

Since S1P directly induces HbS anchoring to membrane, I speculated that S1P binds to HbS as it binds to HbA. Indeed, S1P-conjugated beads successfully pulled HbS from normal and SCD patients erythrocyte lysates, while sphingosine or lysophosphatidic acid beads cannot (Figure 26a), indicating that S1P directly and specifically binds to both human HbA and HbS in erythrocyte lysates. Next, to determine

if S1P regulates Hb-O₂ binding affinity, HbA and HbS O₂ binding equilibrium curves were measured in the absence or presence of different concentrations of S1P. To mimic the molar ratio of S1P to Hb from 1:2500 to 1:500 as seen in normal and sickle human erythrocytes, 10 μmole·l⁻¹ HbA or HbS were used with the concentrations of S1P ranging from 0 to 10 nmole·l⁻¹. Unexpectedly, S1P alone has no effect on Hb-O₂ binding affinity. Realizing that there is very abundant 2,3-BPG is in erythrocytes which binds to deoxyHb, 2,3-BPG was added to the system. P50 of purified HbA or HbS in the presence of 2,3-BPG along with S1P revealed that S1P decreased HbA and HbS-O₂ binding affinity in a dose-dependent manner (Figure 26b-c). Thus, biochemical and functional evidence demonstrate that S1P binds directly to Hb but requires co-binding of 2,3-BPG to decrease O₂ binding affinity, presumably by further stabilizing deoxyHb and increasing its T-state character.

Figure 26

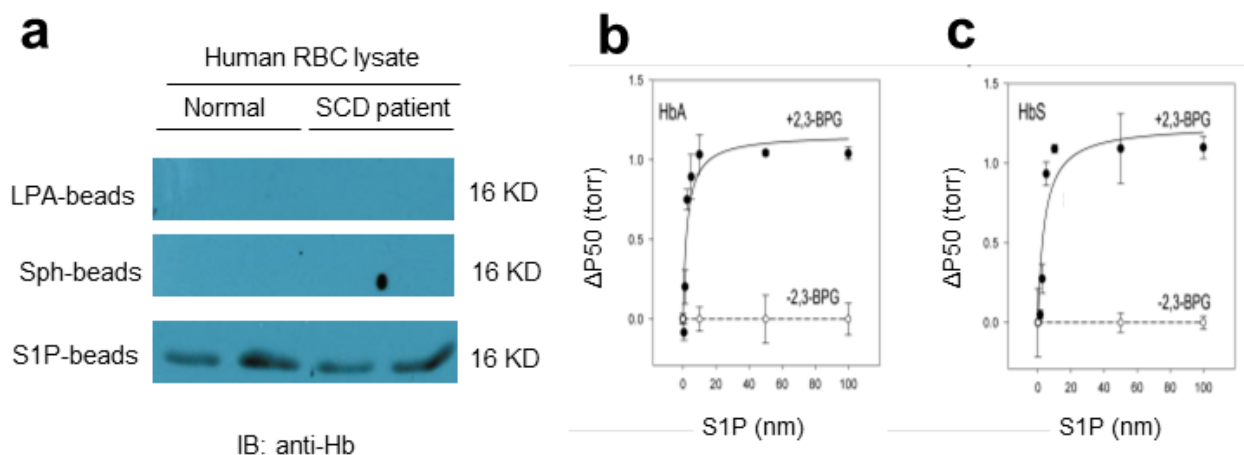


Figure 26. Functional evidence of S1P binding to Hb and stabilizing deoxyHb in T-state. (a) Pull-down of Hb by LPA, Sphingosine and S1P beads from normal human and SCD patient RBC lysates. S1P, at physiological and pathological molar ratios, induces further O₂ release from HbA (b) and HbS (c) in the presence of 2,3-BPG. (Data collected by Dr. Yujin Zhang and Dr. Anren Song, use with permission)

3.4 Chapter 4: X-ray crystallography reveals atomic level insight into S1P-Hb binding

Since chapter 2 and 3 revealed that S1P directly binds to Hb in the presence of 2,3-BPG and induces further O₂ release that stabilizes the deoxy-Hb in T-state, it is imperative to provide atomic level insight into the exact fashion of S1P-Hb binding. Given the fact that structures (both tertiary and quaternary) of bound or unbound normal HbA and sickle HbS are identical even at the pathogenic β Val6 mutation site[127, 128] and that it is easier to crystalize HbA, we chose to determine the crystal structures of deoxyHbA in complex with S1P alone (deoxyHbA-S1P) or in combination with 2,3-BPG (deoxyHbA-S1P-BPG) (subsequently solved at 2.4 Å and 1.8 Å) to gain structural insight into the above described S1P-mediated functional/biological effects. The structures were determined by molecular replacement using the high resolution native deoxyHbA structure (PDB code: 2DN2; details in Table 2)[88]. Expectedly, and consistent with published studies, we observed 2,3-BPG bound in two alternate conformations at the dyad axis of the β -cleft in the ternary deoxyHbA-S1P-2,3-BPG complex to tie together the two β -subunits via interactions with the residues β His2, β Lys82, β Asn139, and β His143 from both β -subunits (intermolecular interactions) in symmetry-related fashion (Figure 27a-b). In both the binary deoxyHbA-S1P and ternary deoxyHbA-S1P-2,3-BPG complexes, S1P was observed bound in the central water cavity, with the phosphate and the amide moieties located in a pocket formed by α 1Lys99, α 1His103, β 1Asn108, β 1Tyr35 and β 1Gln131, while the flexible aliphatic long chain snaked toward the β -cleft making hydrophobic interactions with α 1Phe36, α 1Ser35, β 1Lys132, β 1Gln131, β 1Ala135, β 1Val1 and β 1His2 (Figure 27c). However,

while the ternary complex showed S1P bound in a symmetry-related fashion (Figure 27c-d), the binding of S1P in the binary deoxyHbA-S1P complex was weak (Figure 27d), and only one S1P binding site could be unambiguously fitted in the complex ($\alpha 1\beta 1$ site). In the deoxyHbA-S1P complex, the side-chain of $\alpha 2\text{Lys}99$ was in a similar position as 2DN2, consistent with very weak S1P binding as opposed to the ternary deoxyHbA-S1P-2,3-BPG complex. Binding of 2,3-BPG might have increased the affinity of the protein for S1P in the central water cavity. Note that the same concentration of S1P was used during crystallization of both the binary and ternary complexes. Each S1P-associated interaction in the central water cavity was essentially intramolecular in nature (i.e. make interactions with only $\alpha 1\beta 1$ or $\alpha 2\beta 2$) and suggest that central-water cavity bound S1P might not contribute significantly to the stabilization of the T-state structure[129]. This observation indicates that although the affinity of S1P binding to central water cavity of the protein is increased by 2,3-BPG, it is unlikely to cause significant changes to the deoxyHbA conformation.

Interestingly, besides the central water cavity bound S1P as described above, we also found two additional S1P molecules bound in a symmetry-related fashion at the surface of the deoxyHbA-S1P-2,3-BPG complex but not in the deoxyHbA-S1P complex, indicating that 2,3-BPG binding most likely is required for S1P binding at the surface of the protein. Specifically, the phosphate moiety binds close to the $\alpha 1$ -heme and located in a highly positive environment formed by $\alpha 1\text{Arg}92$, $\beta 2\text{Arg}40$, $\alpha 1\text{His}45$, and $\alpha 1\text{Lys}90$, as well as with $\beta 2\text{Glu}43$; either making direct salt-bridge/hydrogen-bond interactions and/or water-mediated hydrogen-bond interactions with these residues (Figure 27e). The S1P amide nitrogen makes water-mediated interaction with $\alpha 1\text{Lys}90$ and the $\alpha 1$ -

heme propionate. The side-chains of both $\beta 2\text{Glu}43$ and $\alpha 1\text{Lys}90$ have moved from their native positions to make interactions with the S1P. The highly flexible aliphatic chain snaked along a shallow cavity wall making hydrophobic interactions with the so-called “switch region” residues of $\beta 2\text{Phe}41$, $\alpha 1\text{Thr}41$, $\alpha 1\text{Pro}44$, $\beta 2\text{Leu}96$, $\beta 2\text{His}97$, as well as with $\beta 2$ -heme, like a molecular sticky tape. The last 3-4 carbon atoms of the aliphatic chain project into the bulk solvent (Figure 27e-f). Similar symmetry related interactions are observed from the $\beta 2$ -heme site to the $\beta 1$ -heme site. As previously noted, the switch region is characterized by significant structural changes during the T to R transition[129, 130], and effectors that prevent these changes are known to decrease Hb affinity for O_2 [129]. These findings raise an intriguing possibility that the surface bound S1P makes several inter-subunit interactions that involve residues from the switch region serve to stabilize the T-state, and presumably further decrease the T-state affinity for O_2 .

Figure 27

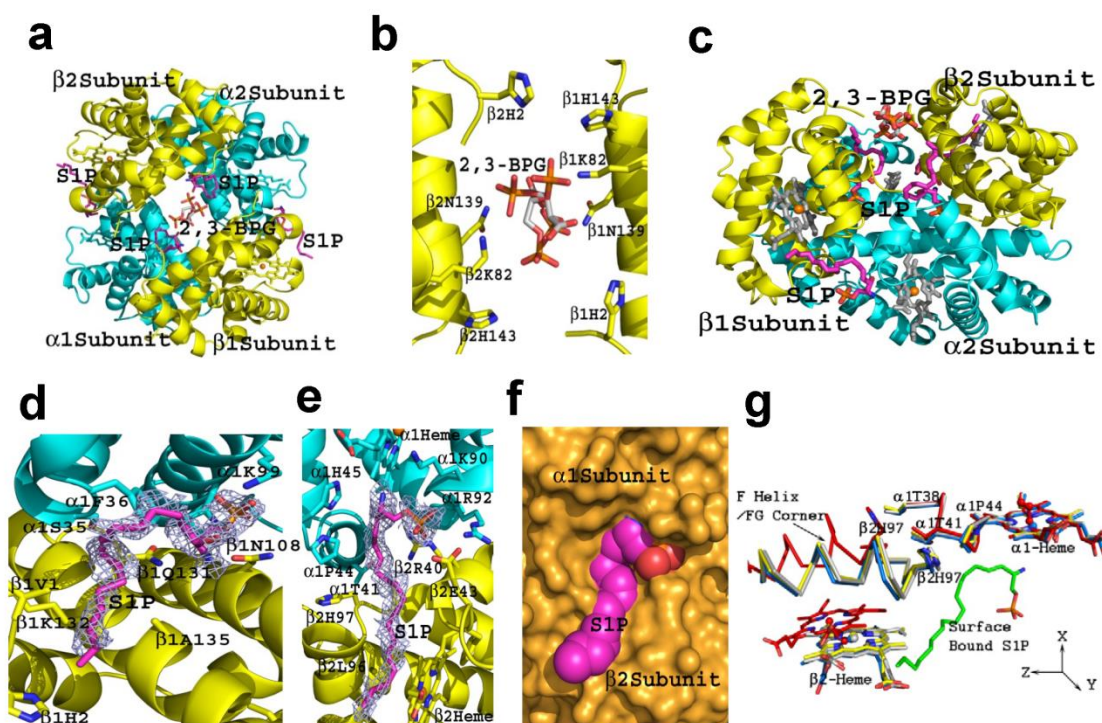


Figure 27. Structural evidence of S1P binding to Hb and stabilizing deoxyHb in T-state.

(a) Crystal structure of deoxyHbA in complex with 2,3-BPG (bound at the β -cleft), and S1P (bound both at the central water cavity and the protein surface). (b) Close view of 2,3-BPG binding at the β -cleft. (c) Ribbon diagram of tetrameric structure of Hb with bound 2,3-BPG at the β -cleft, 2 molecules of S1P bound in the central water cavity, and two other molecules of S1P bound at the surface of the protein. The α -subunits are colored in cyan and β -subunits in yellow. The small molecules are shown in sticks. (d) Binary structure of the central water-cavity bound S1P. (e-g) S1P binds to the surface of HbA in the presence of 2,3-BPG and induces further conformational change stabilizing the complex in T-state. (Data in this figure was collected by Drs. Mostafa H Ahmed and Martin K. Safo of Virginia Commonwealth University, use with permission)

To test this hypothesis, we compared the T-state structures deoxyHbA-S1P, deoxyHbA-S1P-2,3-BPG, native deoxyHbA (PDB code: 2DN2) and native R-state COHbA structure (PDB code: 2DN1)[88] by superposing their α 1 β 1 dimers (~ 0.3 Å) and then obtaining the screw rotation angles that are required to superpose the non-superposed α 2 β 2 Hb dimers as a quaternary measure[129, 130]. Notably, we found that deoxyHbA-S1P-BPG was further removed from the R-state (15.7°) more than

deoxyHbA-S1P (14.8°) and T-state HbA (PDB code: 2DN2) (14.2°). Consistently, the dimer interface β 2F helix/ β 2FG corner at the switch region show some significant positional differences, with that of deoxyHbA-S1P-BPG further removed from the R-state (Figure 27g). These observations support our conclusion that 2,3-BPG is required for S1P binding to the protein, especially to the surface of the protein which leads to the protein becoming more tense, and presumably lower affinity for O₂ compared to either the deoxyHbA or the binary deoxyHbA-S1P complex structures.

Table 2. Crystallographic data for deoxyHbA-S1P-2,3-BPG and deoxyHbA-S1P complex structures.

Values in parentheses refer to the outermost resolution bin. . (Data in this table was collected by Drs. Mostafa H Ahmed and Martin K. Safo of Virginia Commonwealth University, use with permission)

	deoxyHbA-S1P-2,3-BPG	deoxyHbA-S1P
Data Collection Statistics		
Space group	P2 ₁ 2 ₁ 2	P2 ₁ 2 ₁ 2
Cell dimensions (Å)	95.94, 98.08, 65.14	97.56, 95.15, 64.98
Molecules/asymmetric unit	1 tetramer	1 tetramer
Resolution (Å)	29.42-1.80 (1.86-1.80)	29.33-2.40 (2.49-2.40)
No. of measurements	221938 (21321)	119348 (10341)
Unique reflections	54124 (5483)	24236 (2293)
I/sigma I	11.5 (3.4)	9.4 (3.1)
Completeness (%)	93.9 (96.4)	96.6 (96.8)
Rmerge (%) ^a	7.6 (38.0)	12.0 (39.8)
Refinement Statistics		
Resolution limit (Å)	29.42-1.80 (1.88-1.80)	29.08-2.40 (2.51-2.40)
Sigma cutoff (F)	0.0	0.0
No. of reflections	54123 (6869)	24093 (2969)
Rfactor (%)	18.1 (29.6)	22.4 (34.3)
Rfree (%) ^b	21.8 (32.7)	27.9 (38.3)
Rmsd standard geometry		

Bond-lengths (Å)/ -angles (°)	0.010 /1.5	0.000/ 1.6
Dihedral angles		
Most favored /allowed regions	96.8/3.2	92.4/6.7
Average B-Factors		
All atoms/Protein/Heme	23.5/19.3/16.9	43.2/42.6/41.6
Water/S1P/2,3-BPG	40.4/73.5/58.9	47.5/96.2

^a $R_{\text{merge}} = \frac{\sum_{hkl} \sum_i |I_i(hkl) - \langle I(hkl) \rangle|}{\sum_{hkl} \sum_i I_i(hkl)}$. ^b R_{free} was calculated from 5% randomly selected reflection for cross-validation. All other measured reflections were used during refinement.

IV. Discussion

Sphingosine 1-phosphate was discovered two decades ago as a unique signaling molecule of the sphingolipids family. Since then, a large body of studies has characterized S1P as a versatile bioactive lipid playing various important roles both extracellularly and intracellularly. By binding to the five GPCRs on the membrane and to different proteins inside, S1P was found important in a myriad of physiological and pathological process including but not limited to immune responses, vascular integrity, cell proliferation and apoptosis, cell migration, neurogenesis, angiogenesis, hematopoiesis, etc. [10]. Since the discovery of S1P and the two S1P generating enzymes Sphk1 and Sphk2, erythrocytes have caught the attention of many researchers because of the high-level of S1P stored in erythrocytes and the ability to generate large amounts of S1P. However, erythrocyte was considered merely a primary reservoir supplying circulating S1P before a recent study from our lab reporting the detrimental role of elevated erythrocyte Sphk1 and S1P in SCD. Nonetheless, three major questions remained to be answered: 1) how erythrocyte S1P production is regulated; 2) the normal function of S1P in erythrocytes; 3) why elevated Sphk1 and S1P contributes to sickling and disease progression in SCD. Here in this thesis, I have provided solid answers to these three questions: 1) testing a series of hypoxia-related molecules and known molecules to induce Sphk1 activity in other cell types, I identified that adenosine signaling via ADORA2B is a previously unrecognized signaling pathway that stimulates Sphk1 activity in normal and sickle erythrocytes isolated from both humans and mice. Then, using a genetic approach I provided in vivo evidence that excess plasma adenosine induces erythrocyte Sphk1 activity in ADA-deficient mice.

ADA enzyme therapy or genetic deletion of ADORA2B completely abolishes excess adenosine-induced erythrocyte Sphk1 activity in ADA-deficient mice. Finally, I provided both human and mouse evidence that ADORA2B activation-mediated PKA signaling is responsible for adenosine-induced Sphk1 activity in an ERK1/2-dependent manner in both normal and sickle erythrocytes (Figure 28). 2) I identified that S1P is significantly induced in humans following ascent to high altitude or mice exposed to hypoxia. Functionally, I demonstrated the beneficial role of Sphk1-dependent elevation of erythrocyte S1P by promoting 2,3-BPG production and O₂ release to counteract tissue hypoxia. Mechanistically, I revealed that S1P functions intracellularly by binding directly to Hb, promoting deoxy-Hb anchoring to the membrane and subsequently enhancing the release of membrane bound glycolytic enzymes to the cytosol. As such, increased erythrocyte S1P leads to increased metabolic fluxes through glycolysis to generate more 2,3-BPG and thereby promoting O₂ release to protect against tissue hypoxia (Figure 29). 3) I found that: genetic deletion of Sphk1 in SCD has potent anti-sickling and anti-hemolysis effects by correcting pathogenic metabolic reprogramming, channeling glucose to pentose phosphate pathway relative to glycolysis, lowering 2,3-BPG production and rewiring NADPH/glutathione-mediated detoxification. In collaboration with structural biologists, we found that S1P as erythrocyte enriched biolipid works collaboratively with 2,3-BPG to cause further conformational changes and stabilize 2,3-BPG-bound deoxyHbS and HbA to a more enhanced T-state deoxyHbA or deoxyHbS that bind to the membrane mediated by the 3-4 tail carbon atoms of S1P, promote release of GAPDH to cytosol and thus channel glucose to glycolysis relative to PPP (Figure 30). Altogether, I have discovered previously unknown functions of S1P in

erythrocytes of normal and SCD and demonstrated the signaling pathway that regulates its production. These findings not only significantly extend our understanding of the function of S1P, erythrocyte metabolism and regulation, and the molecular basis of SCD pathology, but also provide novel therapeutic possibilities for hypoxia-related illness including but not limited to high-altitude sickness and SCD (Figure 31).

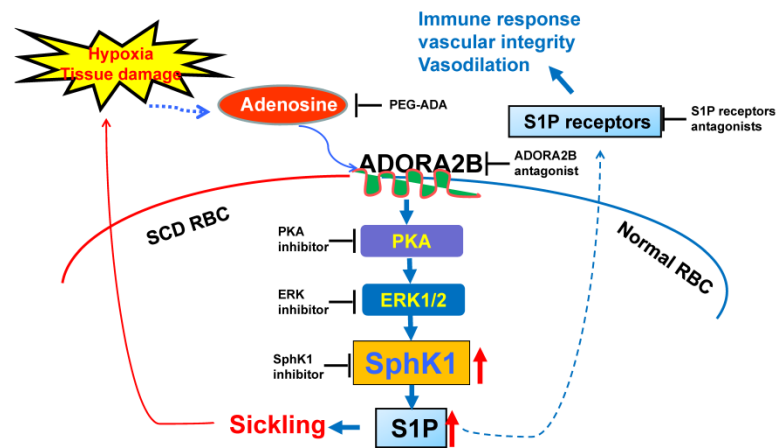


Figure 28. Regulation of erythrocyte Sphk1 activity by adenosine signaling. Hypoxia or tissue damage leads to increased plasma adenosine which signals through ADORA2B and subsequent PKA and ERK1/2 pathways to activate SphK1 and produce more S1P in erythrocyte.

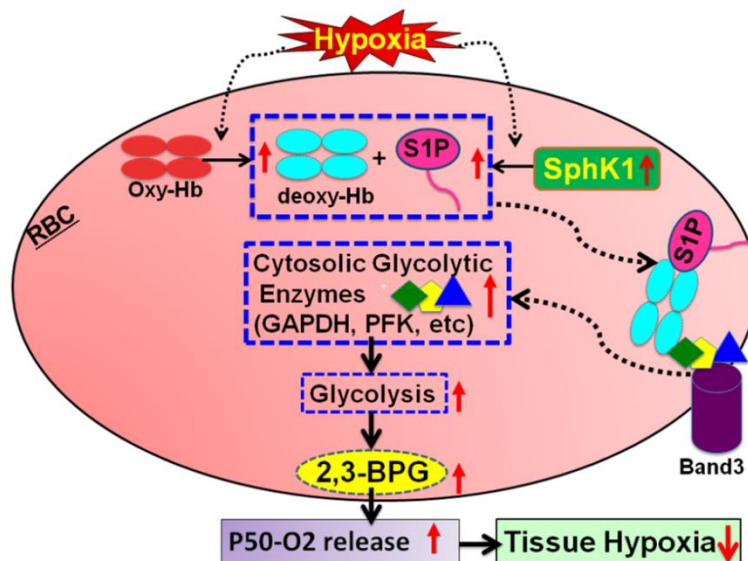


Figure 29. Hypoxia-induced S1P promotes glycolysis for hypoxia adaptation.

Hypoxia-mediated elevation of erythrocyte Sphk1 activity increases S1P level, which binds to deoxy-Hb and facilitates binding of deoxy-Hb to membrane and release of GAPDH; increased cytosolic GAPDH accelerates glycolysis and shifts glucose metabolism in favor of 2,3-BPG production which in turn leads to more O₂ release to counteract tissue hypoxia.

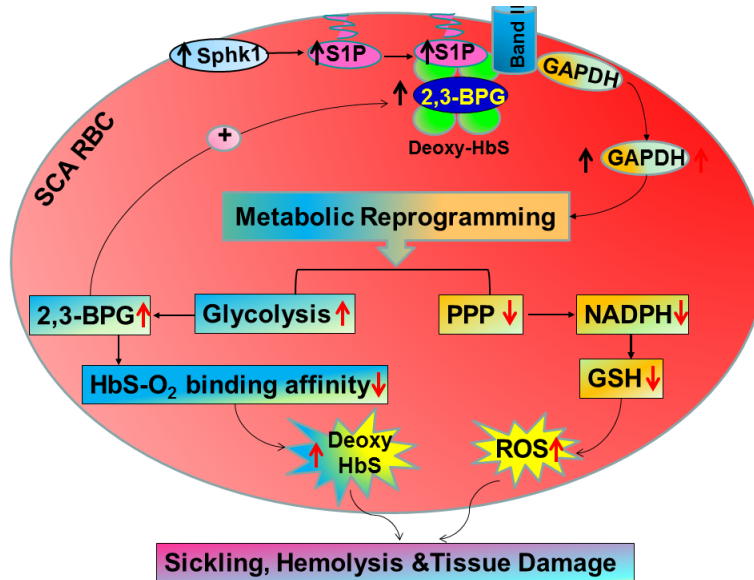


Figure 30. Erythrocyte Sphk1/S1P induces impaired metabolic reprogramming in SCD. Elevated erythrocyte Sphk1 activity increases production of S1P, which binds to deoxyHbS and facilitates deoxyHbS anchoring to membrane and release of GAPDH. Increased cytosolic GAPDH accelerates glycolysis and 2,3-BPG production while decreasing PPP and antioxidant production. Increased 2,3-BPG leads to more deoxyHbS and more sickling while decreased antioxidant causes more oxidative stress (ROS) and more hemolysis. Altogether, erythrocyte S1P induced by elevated Sphk1 activity leads to impaired metabolic reprogramming and thus underlies sickling, hemolysis and disease progression in SCD.

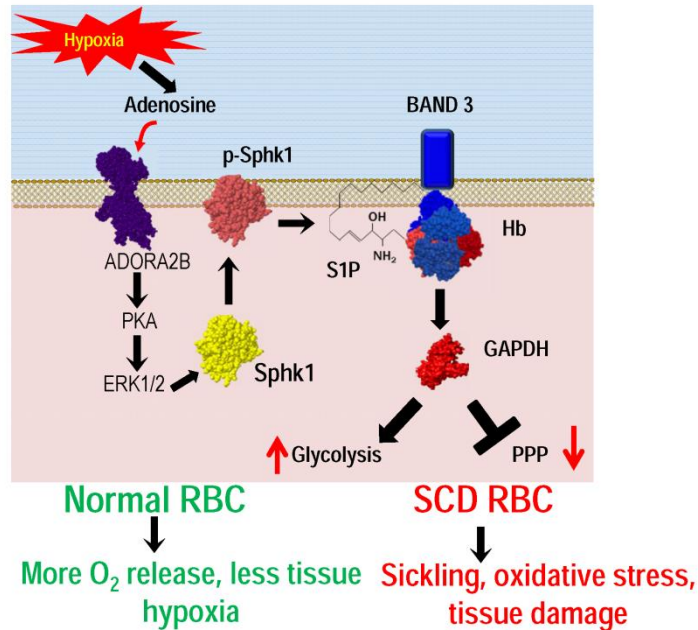


Figure 31. Role and Regulation of Erythrocyte Sphingosine 1-phosphate

Hypoxia induced adenosine signaling activates Sphk1 through ADORA2B and downstream PKA and ERK1/2. Activated Sphk1 increases erythrocyte S1P level. S1P binds to deoxyHb and increases binding of deoxyHb to the membrane and release of GAPDH, which facilitates glycolysis while inhibits PPP. This signaling pathway is beneficial in normal erythrocytes to boost oxygen release but becomes detrimental in SCD erythrocytes due to increased sickling and oxidative stress.

4.1 Hypoxic Regulation of Sphk1

Many previous studies have reported activation of Sphk1 in various nucleated cells in response to hypoxia. It has been found in U87MG glioma cells [131], and endothelial cells[132] that both HIF-1 and HIF-2 transcription factors can compete for binding to putative hypoxia response elements (HREs) located in the promoter region of *Sphk1* gene. Sphk1 mRNA was also found increased in vascular smooth muscle cells[133] and pulmonary smooth muscle cells[134] exposed to hypoxia, though via unknown mechanisms. Besides the transcriptional regulations, a diverse range of growth factors, cytokines and other external stimuli such as tumor necrosis factor-alpha (TNF- α), interleukin-1 β , PDGF, VEGF, Endothelin-1 and phorbol esters could increase

cellular SphK1 activity rapidly and transiently[31]. These external factors may induce Sphk1 phosphorylation[32], phosphatidylserine binding to Sphk1[135] and calcium mobilization[136] which directly affect Sphk1 activity. Other studies also indicate that Sphk1 has a substantial basal activity, and stimulation with agonists leads to less than two fold increase in catalytic activity. Therefore, Sphk1 activity might rather be regulated by cellular localization[137]. The results presented in this thesis demonstrate that adenosine signaling can regulate both Sphk1 phosphorylation and membrane translocalization, suggesting a dual mechanism of Sphk1 activity regulation. Taking into consideration the prevalent expression of adenosine-ADORA2B and Sphk1, it is reasonable to speculate that the adenosine signaling mediated Sphk1 activation may likely exist in other cell types susceptible to hypoxia, such as endothelial cells, vascular smooth muscle cells, and cancer cells. The adenosine-ADORA2B-Sphk1-S1P axis could also play a big part in the response of these cells to hypoxia. Hypoxic responses of endothelial cells and vascular smooth muscle cells are key to blood flow regulation; whereas hypoxia is an important factor promoting cancer cell proliferation.

4.2 Role of Sphk1/S1P in Hypoxia

As an important member of the sphingolipids family that constitutes the plasma membrane structure, S1P is widely expressed in every tissue and organ. Previous studies conducted in nucleated cells have revealed strong connections between S1P production and the oxygen-sensitive transcription factors HIFs, particularly HIF-1[138]. HIF-1 consists of the oxygen-sensitive regulatory subunit HIF-1 α and the constitutively expressed HIF-1 β . Although constantly synthesized, HIF-1 α is prolyl hydroxylated, ubiquitinated by the von Hippel Lindau (pVHL) E3 ligase complex and degraded in

proteasomes under normoxic conditions. However, prolyl hydroxylase activity is attenuated by low oxygen availability in hypoxia and HIF-1 α protein becomes stabilized. HIF-1 can induce the expression of genes that regulate glucose metabolism, angiogenesis, survival and invasion and in turn contribute to the adaptation to low oxygen levels. Various studies have reported that physiological concentrations of S1P are enough to induce the stabilization of HIF-1 α in normoxic conditions in different cells including thyroid follicular carcinoma cells[139], vascular endothelial and smooth muscle cells[140], mouse T cells[141] and macrophages[142], human HepG2 liver cell line[143], and distinct tumor cell models (glioblastoma, prostate, breast, lung, kidney)[144]. More importantly, rapid activation of SphK1 activity was observed in various tumor cells under hypoxic conditions, indicating a likely post-translational effect that may relate to the adenosine signaling since adenosine is a potent hypoxia indicator. Of note, the Sphk1 activation invariably precedes HIF-1 α stabilization and accumulation, which again confirms that Sphk1/S1P signaling works upstream of HIF-1 α .

Besides the regulation of HIF which causes transcriptional and translational activation of certain genes, S1P signaling can directly activate various cellular processes. In cardiomyocytes, S1P can enhance survival during hypoxia by triggering the S1P1 receptor signaling [145, 146]. In vascular smooth muscle cells, S1P induce cell proliferation in hypoxic conditions[133]. In pulmonary smooth muscle cells, chronic (10 days) hypoxia increased SphK1 mRNA and triggered the ability of S1P to act as a mitogen by stimulating the ERK1/2 pathway in these cells, contributing to arterial remodeling in patients with hypertension[134]. Through the activation of HIFs and other

signaling cascades in various cell types, the Sphk1/S1P signaling plays important roles in angiogenesis, cell migration and proliferation, and cellular glucose/energy metabolism.

Taking a different perspective from these studies that focused on the influence of Sphk1/S1P in hypoxic response of the oxygen-consuming cells, I have demonstrated the novel function of Sphk1/S1P in regulating the metabolism of the oxygen-delivering cells. Upon activation by hypoxia-induced adenosine signaling, erythrocyte Sphk1 generates more S1P which can do two things: on the one hand, elevated S1P switches erythrocyte glucose metabolism towards glycolysis which leads to the elevation of 2,3-BPG resulting more oxygen release; on the other hand, elevated erythrocyte S1P can be released outside and activate S1P receptors on the peripheral cells and thereby inducing the hypoxia responses including HIF stabilization and the activation of the various signaling components. Therefore, imperative future endeavors are needed to dig deeper into the functional role of erythrocyte Sphk1/S1P in various hypoxia conditions, including ischemia, extreme athletic activities, cardiac diseases and various tumor. In addition, erythrocytes have long been recognized as the major contributor of circulating S1P. However, it is yet unclear how S1P is released from erythrocytes, especially in hypoxia. Although an S1P specific transporter Sphs2 was characterized as the major S1P transporter in endothelial cells, it is not expressed in mature erythrocytes[147]. An early study claimed that an ATP dependent transporter mediates S1P release from erythrocyte[148], but that transporter has not been well-characterized, not to mention its response to hypoxia. Studies also showed that RBC lysis contributes to increased plasma S1P and underlies the circadian rhythm of circulation S1P concentration[149, 150], but this is apparently not the major mechanism of S1P release

in healthy individuals. Therefore, understanding the release of S1P from erythrocyte requires further investigation.

4.3 S1P Regulates Erythrocyte Metabolism

Early studies showed that under hypoxia, deoxy-Hb binds to cytosolic domain of Band 3 (cdB3) on the membrane to cause release of glycolytic enzymes such as GAPDH from membrane to cytosol to enhance glycolysis and 2,3-BPG production[112, 151-153]. However, the specific molecules mediating the binding of cytosolic deoxy-Hb binding to cdB3 and subsequent elevation of glycolysis under hypoxia remains unidentified. Studies presented in this thesis demonstrated for the first time that hypoxia directly induces switch of glucose fluxes through glycolysis from PPP in erythrocytes and this switch is Sphk1/S1P dependent. Because the T state of deoxy-Hb is stabilized by binding of organic phosphate including 2,3-BPG[105], it has long been speculated that anchoring of deoxy-Hb to the membrane may be mediated by binding of phosphate-containing lipophilic signaling molecules targeting the membrane. Here, I report that S1P is such a phosphate that can bind directly to Hb and promote deoxy-Hb anchoring to the membrane. The binding affinity of 2,3-BPG to deoxygenated Hb is at $\mu\text{mole}\cdot\text{l}^{-1}$ range, while at $\text{mmole}\cdot\text{l}^{-1}$ to oxygenated Hb[42]. Thus, the $\sim 2\text{-}3\text{ mmole}\cdot\text{l}^{-1}$ elevation of 2,3-BPG under hypoxia condition observed in humans in high-altitude and mouse in hypoxia chamber can likely convert $2\text{-}3\text{ mmole}\cdot\text{l}^{-1}$ of oxyHb (1:1 molar ratio) to deoxyHb.

Although intracellular S1P binds and regulates the function of multiple important proteins including histone deacetylases[11], TNF receptor-associated factor 2 (TRAF2)[12], and Prohibitin 2 (PHB2)[154], interaction of S1P and Hb is identified for

the first time. Moreover, S1P binds to both normal and sickle Hb. It is indeed interesting that intracellular S1P at $\mu\text{mole}\cdot\text{l}^{-1}$ concentrations can mediate metabolic reprogramming in SCD by regulating binding of deoxyHb to cdB3. Due to the molar ratio of about 1:300 between cdB3 and Hb[6], cdB3 (present at $\mu\text{mole}\cdot\text{l}^{-1}$ concentrations), not deoxyHb (present at $\text{mmole}\cdot\text{l}^{-1}$ concentrations), is the rate-limiting factor in deoxyHb-cdB3 interaction. Interestingly, S1P has an approximately 1:1 molar ratio with cdB3 in normal erythrocytes and an even higher ratio in SCD erythrocytes. Thus, although deoxyHb is expected to be present at a much higher concentration than S1P, it is the concentration of S1P that controls the amount of deoxyHb that binds to cdB3. Besides regulating the sequestration of glycolytic enzymes, it is reasonable to speculate that increased S1P in SCD erythrocytes may also play a role in other cdB3-mediated effect including the binding of S-nitrosohemoglobin and spectrin to cdB3. The former is involved in the nitric oxide (NO) metabolism[155, 156] in erythrocytes while the latter plays a key role in erythrocyte deformability[157], both of which are important in the pathophysiology of SCD[158-160].

The crystal structure data indicate that S1P binds to the surface of 2,3-BPG-Hb and leads to considerable additional conformational change of deoxyHb (by making hydrophobic interactions at the switch interface) to a more T-state character that in part should explain the decreased Hb-O₂ affinity. It is also notable that the surface-bound S1P could sterically impede diffusion of diatomic ligands (O₂) into the heme, and in part also decreased Hb-O₂ affinity. Similar studies have been reported for allosteric effectors that bind and block the heme access to the bulk solvent[129, 161]. Although S1P was also observed bound in the central water cavity, the water cavity is known to be a “sink”

for several compounds especially those with anionic groups and not all of these compounds show allosteric effect[129]. Since in the absence of 2,3-BPG, we observed weak binding of S1P at the water cavity and no apparent effect on the protein's allosteric activity, it is possible that the central water cavity S1P binding is non-specific. Another interesting structural observation is that the last 3-4 carbon atoms of the surface bound S1P do not make any interaction with the protein residue but project in the bulk solvent, which could possibly mediate hydrophobic interactions with other proteins, akin to the hydrophobic β Val6 pathogenic mutation involvement in HbS polymerization[118]. S1P, like other effectors of Hb binds to multiple residues. Mutation of one or multiple residues may result in uncooperative function of Hb tetramer. Such study is thus rarely used to ascertain the binding of an effector, but instead structural and/or O₂ equilibrium studies (Hb-O₂ binding studies) have been the norm. Importantly, the structural study that show surface S1P binding only in the presence of 2,3-BPG binding in the central water cavity is highly suggestive that the surface binding is specific. There are similar reported studies where binding of allosteric effectors to Hb lead to subtle but significant tertiary and/or quaternary structural changes at the heme environment, α 1 β 2 interface, α -cleft or β -cleft[162],^{32,47}. Such changes have been used to explain the differences in the allosteric activities of these effectors. Notably, effectors that lead to increase in Hb affinity of O₂ show more relaxed Hb structural features, while the opposite is true for effectors that bind to Hb and decrease its O₂ affinity for oxygen[129].

4.4 Regulation of Erythrocyte Oxygen Release in Hypoxia

Ever since the emergence of multicellular systems, hypoxia has become a common environmental stress to living organisms. To cope with such stress, all vertebrates but also some cold-blood fishes, rely on the packed Hb molecules in erythrocytes to deliver oxygen to peripheral tissues. Failure of erythrocytes in delivering enough oxygen in a timely manner underlies a myriad of life-threatening conditions including trauma shock, anemia, and various poisonings including arsenic and CO. The regulation of erythrocyte oxygen delivery ability is at two aspects: i) regulating Hb-O₂ binding affinity; ii) regulating the transport of erythrocytes in blood vessels. The studies presented in this thesis demonstrate for the first time that erythrocyte Sphk1/S1P plays an important role in regulating Hb-O₂ binding affinity by increasing glycolysis and 2,3-BPG production. It is also reasonable to speculate the Sphk1/S1P is also involved in regulating blood vessel tone and thereby controlling the flow of erythrocytes.

With Hb accounting for over 90% of the dry weight, mature erythrocytes have no room for a nucleus, mitochondria and other cellular apparatuses. Therefore, lipid and protein metabolism is absent in erythrocytes and glucose metabolism dictates the vast majority of cellular activities. Glucose is not merely the sole energy source for erythrocytes, it also generates antioxidant and 2,3-BPG. It has been known for over two decades that hypoxia regulates erythrocyte glucose metabolism in favoring of the production of energy and 2,3-BPG while limiting the generation of antioxidant[43]. However, besides deoxyHb, S1P is the first identified factor that also regulates such metabolic change. There are also many other small molecules with elevated levels

identified in metabolomics screenings conducted in various erythrocyte samples with altered oxygen release capacity [7, 76, 104]. It is possible that some of these hypoxia-induced molecules can also directly or indirectly regulate erythrocyte oxygen release capacity, similar to that of S1P and adenosine. Therefore, further investigation may uncover more available therapeutic targets for the treatments of hypoxia-related illness.

Besides enhancing O₂ off-loading, erythrocytes can regulate their own distribution by releasing vasodilatory compounds that increase blood flow in hypoxic tissues. The main mechanisms include: i) release of ATP that activates P2 receptors on endothelial cells to generate more NO; ii) release of NO that is synthesized from the reduction of nitrate by deoxyHb[163]. Interestingly, the release of ATP from erythrocytes also depends on the binding of deoxyHb with Band3[164], which is regulated by S1P as proved here. This indicates that S1P, by binding to deoxyHb and mediating deoxyHb-band3 interaction, can on the one hand increase ATP by facilitating glycolysis, and on the other hand enhance ATP release. In these ways, S1P induces vasodilation and increases blood flow to the hypoxic tissues. Moreover, S1P directly activates endothelial NO synthase (eNOS)[165]. Therefore, it is highly possible that S1P released from erythrocytes during hypoxia activate eNOS in the endothelial cells and generate NO to cause vasodilation. More importantly, eNOS has also been located inside of erythrocytes[166]. Although it is unknown how this eNOS behaves in hypoxic condition, we can reasonably hypothesize that the localization of erythrocyte eNOS, much like the other erythrocyte enzymes such as the glycolytic

enzymes, is regulated by S1P-mediated deoxyHb-Band3 interaction. In this way, S1P may directly regulate NO produced in erythrocytes.

4.5 Regulation of GAPDH Activity and Localization

GAPDH is an evolutionarily conserved enzyme that controls the rate-limiting step in the glycolysis pathway of glucose metabolism. It comprises ~10–20% of the total cellular protein content [167]. Because it is highly conservative across species, GAPDH has been used as a control in protein and gene studies, as well as a standard in Northern and Western blots [167, 168]. Besides, various studies have revealed many diverse and non-glycolytic functions of GAPDH. GAPDH can bind DNA and RNA, catalyze microtubule formation and polymerization, facilitate vesicular transport, and bind integral membrane ion pumps associated with calcium release [169]. It also interacts with a number of small molecules, including tumor necrosis factor (TNF)- α ribozymes, glutathione, p53, and nitric oxide (NO) [169].

With so many diversified catalytic and non-catalytic functions, GAPDH regulation plays an important role in many cellular processes. GAPDH is regulated in two ways: cellular localization and post-translational modification. Sequence motifs for intracellular localization of a protein were found on GAPDH through protein sequence analysis. One motif has the sequence KKVVK (residues 259-263), which is partially homologous to the nuclear localization signal (NLS), and the other is ALQNIJP (residues 202-208), which is partially homologous to a nuclear export domain [167, 170]. In non-nucleated cells, such as mature erythrocytes, GAPDH also binds to membrane proteins, which is the cytosolic domain of band3 in the case of erythrocytes [151]. Unlike nuclear localization, binding of GAPDH to erythrocyte

membrane protein band3 involves the modification of G3P-binding site residues, Lys-191 and Lys-212, presumably by oxidation [171]. Recently, proteomics analyses conducted in stored erythrocytes revealed a storage-dependent oxidation of GAPDH at functional Cys152, 156, 247, and His179, which leads to the decrease of GAPDH activity and thereby disturbance of erythrocyte metabolism[172]. These studies suggest the oxidation of certain residues on GAPDH regulates both the cellular localization and the catalytic activity of GAPDH. Besides oxidation, Nitric Oxide (NO)-mediated S-nitrosylation of GAPDH is responsible for reversible enzyme inhibition[173]. Moreover, recent studies have shown that GAPDH can also be phosphorylated by protein kinase C delta [174] and AMP-activated protein kinase [175] and play important roles in ischemia-reoxygenation-induced injury and autophagy, respectively. So far, no direct evidence suggests phosphorylation of GAPDH affects the catalytic activity in addition to its cellular localization. Research presented in this thesis demonstrated an additional regulatory mechanism of GAPDH location by S1P mediated deoxyHb-Band3 binding in erythrocytes. However, whether additional steps are needed to fully activate the GAPDH released from erythrocyte membrane is unknown and awaits further investigation.

4.6 Targeting Adenosine-ADORA2B-Sphk1-S1P Axis for Therapeutics

Development

The studies presented above have discovered the Adenosine-ADORA2B-Sphk1-S1P axis that plays a detrimental role in SCD but is beneficial in helping normal individuals adapt to hypoxia. Targeting this axis is therefore promising to treat various diseases including SCD, anemia, and acute mountain sickness and even boosting

athletic performance. First, adenosine level can be lowered by administration of the FDA-approved enzyme therapy PEG-ADA. PEG-ADA treatment has been shown to be very successful in lowering the plasma adenosine levels in patients with ADA deficiency[176]. Therefore, treat SCD patients with PEG-ADA is possible. However, caution should be applied since other studies also indicate beneficial role of adenosine in SCD through ADORA2A, though in different animal models[177]. Second, various ADORA2B antagonist and agonist have been developed and test it in vivo and even in human as treatments for other diseases and conditions. For example, GS 6201 (CVT 6883), a selective and highly potent ADORA2B antagonist, has been evaluated in phase I clinical trial for the treatment of asthma[178]; whereas BAY 60-6583, a potent ADORA2B agonist, has demonstrated cardioprotective role by attenuating infarct size in a mouse model of myocardial ischemia[179]. These two drugs can be used for testing in SCD and hypoxia adaptation, respectively.

In comparison to adenosine and ADORA2B, Sphk1 and S1P have drawn more attention from drug developers because of their great potential in treating cancer and inflammatory disorders. A plethora of Sphk1 inhibitors, including SKI-I[180-183], Safingol[184], SKI-II[185], and PF-543[186] decreases cancer progression, angiogenesis, lymphangiogenesis and airway hyper-responsiveness. Moreover, PF-543 has been used previously by our lab in treating SCD Berkeley mice and was effective in inhibiting sickling and disease progression [7]. It was also used in a hypoxic model of pulmonary arterial hypertension and proven effective in reducing post-myocardial infarction cardiac remodeling and dysfunction in a most recent study[187], suggesting that PF-543 could be used for clinical applications. In addition, testing PF-543 and other

Sphk1 inhibitors in other SCD animal models, such as the Townes SCD mice[188], is also necessary to provide more solid conclusion.

Since the discovery of the strong immune-regulatory functions of S1P signaling through its receptors particularly S1P1, S1P and its five receptors have become hot therapeutic targets for immune and cancer drug developers. In 2010, fingolimod (FTY720), an S1PR1 agonist and functional antagonist, was approved by FDA as the first oral disease-modifying drug for the treatment of relapses and delay disability progression in patients with relapsing forms of multiple sclerosis[189]. Moreover, it can also suppress experimental autoimmune encephalomyelitis, inhibit lymphocyte trafficking, prevent transplant rejection and decreases colitis and cancer progression[190-194]. Although S1P1 was not detected in mature erythrocytes (data not shown), targeting S1P1 with fingolimod to treat SCD has been examined in our lab and demonstrated effectiveness in decreasing inflammation and tissue damage in the Berkeley SCD mouse model (Zhao et al, manuscript under review). Considering that inflammation is a serious complication facing SCD patients and that circulating S1P is highly elevated in SCD, fingolimod may become a second FDA-approved treatment for SCD adding to the only approved drug hydroxyurea. Besides targeting S1P receptors, decreasing S1P availability by neutralization it with specific antibodies offers a new therapeutic angle. In fact, S1P neutralizing antibodies have been successfully developed and tested in preclinical and clinical studies for multiple cancer and angiogenic disorders including renal carcinoma and age-related macular degeneration[19, 195]. These studies have shown that S1P neutralizing antibody can successfully block S1P receptor activation and subsequent angiogenesis and cancer

proliferation. It is reasonable to speculate that S1P neutralizing antibody can also be helpful in ameliorating the elevated S1P signaling induced inflammation, leukocyte infiltration and adhesion and end-organ damage[8]. In collaboration with the biotech company that has generated this S1P neutralizing antibody, our lab is currently investigating the treatment effects in the SCD Berkeley mouse model. Preliminary results have indicated significantly lowered white blood cell numbers in SCD mice treated with the S1P antibody in comparison to the control group that were treated with control IgG only, suggesting very promising therapeutic possibilities.

4.7 Future Directions

To summarize the future research directions discussed above, further research efforts should be taken to investigate: 1) the regulation of Sphk1 activity by adenosine in other cells and systems; 2) release of S1P from erythrocytes; 3) other small metabolites and signaling molecules in erythrocytes with similar functions as S1P; 4) regulation of cytosolic GAPDH by post-translational modification; 5) developing treatments for SCD and other hypoxia-related diseases with the therapeutic targets identified.

V. References

1. Spiegel S, Milstien S: **Sphingosine-1-phosphate: an enigmatic signalling lipid.** *Nat Rev Mol Cell Biol* 2003, **4**(5):397-407.
2. Takabe K, Paugh SW, Milstien S, Spiegel S: **"Inside-out" signaling of sphingosine-1-phosphate: therapeutic targets.** *Pharmacol Rev* 2008, **60**(2):181-195.
3. Schwab SR, Cyster JG: **Finding a way out: lymphocyte egress from lymphoid organs.** *Nat Immunol* 2007, **8**(12):1295-1301.
4. Hanel P, Andreani P, Graler MH: **Erythrocytes store and release sphingosine 1-phosphate in blood.** *FASEB J* 2007, **21**(4):1202-1209.
5. Darghouth D, Koehl B, Madalinski G, Heilier JF, Bovee P, Xu Y, Olivier MF, Bartolucci P, Benkerrou M, Pissard S, Colin Y, Galacteros F, Bosman G, Junot C, Romeo PH: **Pathophysiology of sickle cell disease is mirrored by the red blood cell metabolome.** *Blood* 2011, **117**(6):e57-66.
6. Rogers SC, Ross JG, d'Avignon A, Gibbons LB, Gazit V, Hassan MN, McLaughlin D, Griffin S, Neumayr T, Debaun M, DeBaun MR, Doctor A: **Sickle hemoglobin disturbs normal coupling among erythrocyte O₂ content, glycolysis, and antioxidant capacity.** *Blood* 2013, **121**(9):1651-1662.
7. Zhang Y, Dai Y, Wen J, Zhang W, Grenz A, Sun H, Tao L, Lu G, Alexander DC, Milburn MV, Carter-Dawson L, Lewis DE, Eltzschig HK, Kellems RE, Blackburn MR, Juneja HS, Xia Y: **Detrimental effects of adenosine signaling in sickle cell disease.** *Nat Med* 2011, **17**(1):79-86.
8. Zhang Y, Berka V, Song A, Sun K, Wang W, Zhang W, Ning C, Li C, Zhang Q, Bogdanov M, Alexander DC, Milburn MV, Ahmed MH, Lin H, Idowu M, Zhang J, Kato GJ, Abdulmalik OY, Dowhan W, Kellems RE, Zhang P, Jin J, Safo M, Tsai AL, Juneja HS, Xia Y: **Elevated sphingosine-1-phosphate promotes sickling and sickle cell disease progression.** *J Clin Invest* 2014, **124**(6):2750-2761.

9. Sun K, Zhang Y, D'Alessandro A, Nemkov T, Song A, Wu H, Liu H, Adebiyi M, Huang A, Wen YE, Bogdanov MV, Vila A, O'Brien J, Kellems RE, Dowhan W, Subudhi AW, Jameson-Van Houten S, Julian CG, Lovering AT, Safo M, Hansen KC, Roach RC, Xia Y: **Sphingosine-1-phosphate promotes erythrocyte glycolysis and oxygen release for adaptation to high-altitude hypoxia.** *Nat Commun* 2016, **7**:12086.
10. Maceyka M, Harikumar KB, Milstien S, Spiegel S: **Sphingosine-1-phosphate signaling and its role in disease.** *Trends Cell Biol* 2012, **22**(1):50-60.
11. Hait NC, Allegood J, Maceyka M, Strub GM, Harikumar KB, Singh SK, Luo C, Marmorstein R, Kordula T, Milstien S, Spiegel S: **Regulation of histone acetylation in the nucleus by sphingosine-1-phosphate.** *Science* 2009, **325**(5945):1254-1257.
12. Alvarez SE, Harikumar KB, Hait NC, Allegood J, Strub GM, Kim EY, Maceyka M, Jiang H, Luo C, Kordula T, Milstien S, Spiegel S: **Sphingosine-1-phosphate is a missing cofactor for the E3 ubiquitin ligase TRAF2.** *Nature* 2010, **465**(7301):1084-1088.
13. Murata N, Sato K, Kon J, Tomura H, Okajima F: **Quantitative measurement of sphingosine 1-phosphate by radioreceptor-binding assay.** *Anal Biochem* 2000, **282**(1):115-120.
14. Sensken SC, Bode C, Nagarajan M, Peest U, Pabst O, Graler MH: **Redistribution of sphingosine 1-phosphate by sphingosine kinase 2 contributes to lymphopenia.** *J Immunol* 2010, **184**(8):4133-4142.
15. Andreani P, Graler MH: **Comparative quantification of sphingolipids and analogs in biological samples by high-performance liquid chromatography after chloroform extraction.** *Anal Biochem* 2006, **358**(2):239-246.
16. Pappu R, Schwab SR, Cornelissen I, Pereira JP, Regard JB, Xu Y, Camerer E, Zheng YW, Huang Y, Cyster JG, Coughlin SR: **Promotion of lymphocyte egress into blood and lymph by distinct sources of sphingosine-1-phosphate.** *Science* 2007, **316**(5822):295-298.

17. Camerer E, Regard JB, Cornelissen I, Srinivasan Y, Duong DN, Palmer D, Pham TH, Wong JS, Pappu R, Coughlin SR: **Sphingosine-1-phosphate in the plasma compartment regulates basal and inflammation-induced vascular leak in mice.** *J Clin Invest* 2009, **119**(7):1871-1879.
18. Ishii M, Egen JG, Klauschen F, Meier-Schellersheim M, Saeki Y, Vacher J, Proia RL, Germain RN: **Sphingosine-1-phosphate mobilizes osteoclast precursors and regulates bone homeostasis.** *Nature* 2009, **458**(7237):524-528.
19. Visentin B, Vekich JA, Sibbald BJ, Cavalli AL, Moreno KM, Matteo RG, Garland WA, Lu Y, Yu S, Hall HS, Kundra V, Mills GB, Sabbadini RA: **Validation of an anti-sphingosine-1-phosphate antibody as a potential therapeutic in reducing growth, invasion, and angiogenesis in multiple tumor lineages.** *Cancer Cell* 2006, **9**(3):225-238.
20. Cinamon G, Zachariah MA, Lam OM, Foss FW, Jr., Cyster JG: **Follicular shuttling of marginal zone B cells facilitates antigen transport.** *Nat Immunol* 2008, **9**(1):54-62.
21. Bode C, Sensken SC, Peest U, Beutel G, Thol F, Levkau B, Li Z, Bittman R, Huang T, Tolle M, van der Giet M, Graler MH: **Erythrocytes serve as a reservoir for cellular and extracellular sphingosine 1-phosphate.** *J Cell Biochem* 2010, **109**(6):1232-1243.
22. Xiong Y, Yang P, Proia RL, Hla T: **Erythrocyte-derived sphingosine 1-phosphate is essential for vascular development.** *J Clin Invest* 2014, **124**(11):4823-4828.
23. Mizugishi K, Yamashita T, Olivera A, Miller GF, Spiegel S, Proia RL: **Essential role for sphingosine kinases in neural and vascular development.** *Mol Cell Biol* 2005, **25**(24):11113-11121.
24. Maceyka M, Sankala H, Hait NC, Le Stunff H, Liu H, Toman R, Collier C, Zhang M, Satin LS, Merrill AH, Jr., Milstien S, Spiegel S: **SphK1 and SphK2, sphingosine kinase isoenzymes with opposing functions in sphingolipid metabolism.** *J Biol Chem* 2005, **280**(44):37118-37129.
25. Taha TA, Hannun YA, Obeid LM: **Sphingosine kinase: biochemical and cellular regulation and role in disease.** *J Biochem Mol Biol* 2006, **39**(2):113-131.

26. Liu H, Sugiura M, Nava VE, Edsall LC, Kono K, Poulton S, Milstien S, Kohama T, Spiegel S: **Molecular cloning and functional characterization of a novel mammalian sphingosine kinase type 2 isoform.** *J Biol Chem* 2000, **275**(26):19513-19520.
27. Kihara A, Anada Y, Igarashi Y: **Mouse sphingosine kinase isoforms SPHK1a and SPHK1b differ in enzymatic traits including stability, localization, modification, and oligomerization.** *J Biol Chem* 2006, **281**(7):4532-4539.
28. Billich A, Bornancin F, Devay P, Mechtcheriakova D, Urtz N, Baumruker T: **Phosphorylation of the immunomodulatory drug FTY720 by sphingosine kinases.** *J Biol Chem* 2003, **278**(48):47408-47415.
29. Wang Z, Min X, Xiao SH, Johnstone S, Romanow W, Meininger D, Xu H, Liu J, Dai J, An S, Thibault S, Walker N: **Molecular basis of sphingosine kinase 1 substrate recognition and catalysis.** *Structure* 2013, **21**(5):798-809.
30. Chen J, Tang H, Sysol JR, Moreno-Vinasco L, Shioura KM, Chen T, Gorshkova I, Wang L, Huang LS, Usatyuk PV, Sammani S, Zhou G, Raj JU, Garcia JG, Berdyshev E, Yuan JX, Natarajan V, Machado RF: **The sphingosine kinase 1/sphingosine-1-phosphate pathway in pulmonary arterial hypertension.** *Am J Respir Crit Care Med* 2014, **190**(9):1032-1043.
31. Pitson SM, Moretti PA, Zebol JR, Xia P, Gamble JR, Vadas MA, D'Andrea RJ, Wattenberg BW: **Expression of a catalytically inactive sphingosine kinase mutant blocks agonist-induced sphingosine kinase activation. A dominant-negative sphingosine kinase.** *J Biol Chem* 2000, **275**(43):33945-33950.
32. Pitson SM, Moretti PA, Zebol JR, Lynn HE, Xia P, Vadas MA, Wattenberg BW: **Activation of sphingosine kinase 1 by ERK1/2-mediated phosphorylation.** *EMBO J* 2003, **22**(20):5491-5500.

33. Pitson SM, Xia P, Leclercq TM, Moretti PA, Zebol JR, Lynn HE, Wattenberg BW, Vadas MA: **Phosphorylation-dependent translocation of sphingosine kinase to the plasma membrane drives its oncogenic signalling.** *J Exp Med* 2005, **201**(1):49-54.
34. Lin CS, Lim SK, D'Agati V, Costantini F: **Differential effects of an erythropoietin receptor gene disruption on primitive and definitive erythropoiesis.** *Genes Dev* 1996, **10**(2):154-164.
35. Fraser ST, Isern J, Baron MH: **Maturation and enucleation of primitive erythroblasts during mouse embryogenesis is accompanied by changes in cell-surface antigen expression.** *Blood* 2007, **109**(1):343-352.
36. Socolovsky M: **Molecular insights into stress erythropoiesis.** *Curr Opin Hematol* 2007, **14**(3):215-224.
37. Dzierzak E, Philipsen S: **Erythropoiesis: development and differentiation.** *Cold Spring Harb Perspect Med* 2013, **3**(4):a011601.
38. Mebius RE, Kraal G: **Structure and function of the spleen.** *Nat Rev Immunol* 2005, **5**(8):606-616.
39. Lang KS, Lang PA, Bauer C, Duranton C, Wieder T, Huber SM, Lang F: **Mechanisms of suicidal erythrocyte death.** *Cell Physiol Biochem* 2005, **15**(5):195-202.
40. de Back DZ, Kostova EB, van Kraaij M, van den Berg TK, van Bruggen R: **Of macrophages and red blood cells; a complex love story.** *Front Physiol* 2014, **5**:9.
41. Gonzalez-Cinca N, Perez de la Ossa P, Carreras J, Climent F: **Effects of thyroid hormone and hypoxia on 2,3-bisphosphoglycerate, bisphosphoglycerate synthase and phosphoglycerate mutase in rabbit erythroblasts and reticulocytes in vivo.** *Horm Res* 2004, **62**(4):191-196.
42. Benesch R, Benesch RE: **The effect of organic phosphates from the human erythrocyte on the allosteric properties of hemoglobin.** *Biochem Biophys Res Commun* 1967, **26**(2):162-167.
43. Castagnola M, Messana I, Sanna MT, Giardina B: **Oxygen-linked modulation of erythrocyte metabolism: state of the art.** *Blood Transfus* 2010, **8 Suppl 3**:s53-58.

44. Bartsch P, Gibbs JS: **Effect of altitude on the heart and the lungs.** *Circulation* 2007, **116**(19):2191-2202.
45. West JB: **The physiologic basis of high-altitude diseases.** *Ann Intern Med* 2004, **141**(10):789-800.
46. Luks AM, Swenson ER, Bartsch P: **Acute high-altitude sickness.** *Eur Respir Rev* 2017, **26**(143).
47. Petousi N, Robbins PA: **Human adaptation to the hypoxia of high altitude: the Tibetan paradigm from the pregenomic to the postgenomic era.** *J Appl Physiol (1985)* 2014, **116**(7):875-884.
48. Storz JF, Scott GR, Cheviron ZA: **Phenotypic plasticity and genetic adaptation to high-altitude hypoxia in vertebrates.** *J Exp Biol* 2010, **213**(Pt 24):4125-4136.
49. Frisancho AR: **Developmental functional adaptation to high altitude: review.** *Am J Hum Biol* 2013, **25**(2):151-168.
50. Anderson JD, Honigman B: **The effect of altitude-induced hypoxia on heart disease: do acute, intermittent, and chronic exposures provide cardioprotection?** *High Alt Med Biol* 2011, **12**(1):45-55.
51. Bartsch P, Swenson ER: **Acute high-altitude illnesses.** *N Engl J Med* 2013, **369**(17):1666-1667.
52. Semenza GL: **Hypoxia-inducible factor 1 and cardiovascular disease.** *Annu Rev Physiol* 2014, **76**:39-56.
53. Giordano FJ: **Oxygen, oxidative stress, hypoxia, and heart failure.** *J Clin Invest* 2005, **115**(3):500-508.
54. Weissmann N, Grimminger F, Seeger W: **Hypoxia in lung vascular biology and disease.** *Cardiovasc Res* 2006, **71**(4):618-619.
55. Tuder RM, Yun JH, Bhunia A, Fijalkowska I: **Hypoxia and chronic lung disease.** *J Mol Med (Berl)* 2007, **85**(12):1317-1324.

56. Sun K, Xia Y: **New insights into sickle cell disease: a disease of hypoxia.** *Curr Opin Hematol* 2013, **20**(3):215-221.
57. Greer SN, Metcalf JL, Wang Y, Ohh M: **The updated biology of hypoxia-inducible factor.** *EMBO J* 2012, **31**(11):2448-2460.
58. Simonson TS: **Altitude Adaptation: A Glimpse Through Various Lenses.** *High Alt Med Biol* 2015, **16**(2):125-137.
59. Colgan SP, Eltzschig HK, Eckle T, Thompson LF: **Physiological roles for ecto-5'-nucleotidase (CD73).** *Purinergic Signal* 2006, **2**(2):351-360.
60. Idzko M, Ferrari D, Eltzschig HK: **Nucleotide signalling during inflammation.** *Nature* 2014, **509**(7500):310-317.
61. Blackburn MR, Datta SK, Kellems RE: **Adenosine deaminase-deficient mice generated using a two-stage genetic engineering strategy exhibit a combined immunodeficiency.** *J Biol Chem* 1998, **273**(9):5093-5100.
62. Parise LV, Berliner N: **Sickle cell disease: challenges and progress.** *Blood* 2016, **127**(7):789.
63. Pauling L, Itano HA, et al.: **Sickle cell anemia a molecular disease.** *Science* 1949, **110**(2865):543-548.
64. Silva DG, Belini Junior E, de Almeida EA, Bonini-Domingos CR: **Oxidative stress in sickle cell disease: an overview of erythrocyte redox metabolism and current antioxidant therapeutic strategies.** *Free Radic Biol Med* 2013, **65**:1101-1109.
65. Subudhi AW, Bourdillon N, Bucher J, Davis C, Elliott JE, Eutermoster M, Evero O, Fan JL, Jameson-Van Houten S, Julian CG, Kark J, Kark S, Kayser B, Kern JP, Kim SE, Lathan C, Laurie SS, Lovering AT, Paterson R, Polaner DM, Ryan BJ, Spira JL, Tsao JW, Wachsmuth NB, Roach RC: **AltitudeOmics: the integrative physiology of human acclimatization to hypobaric hypoxia and its retention upon reascent.** *PLoS One* 2014, **9**(3):e92191.

66. Blackburn MR, Datta SK, Wakamiya M, Vartabedian BS, Kellems RE: **Metabolic and immunologic consequences of limited adenosine deaminase expression in mice.** *J Biol Chem* 1996, **271**(25):15203-15210.
67. Zhou Y, Mohsenin A, Morschl E, Young HW, Molina JG, Ma W, Sun CX, Martinez-Valdez H, Blackburn MR: **Enhanced airway inflammation and remodeling in adenosine deaminase-deficient mice lacking the A2B adenosine receptor.** *J Immunol* 2009, **182**(12):8037-8046.
68. Paszty C, Brion CM, Mancini E, Witkowska HE, Stevens ME, Mohandas N, Rubin EM: **Transgenic knockout mice with exclusively human sickle hemoglobin and sickle cell disease.** *Science* 1997, **278**(5339):876-878.
69. Chunn JL, Mohsenin A, Young HW, Lee CG, Elias JA, Kellems RE, Blackburn MR: **Partially adenosine deaminase-deficient mice develop pulmonary fibrosis in association with adenosine elevations.** *Am J Physiol Lung Cell Mol Physiol* 2006, **290**(3):L579-587.
70. Chunn JL, Molina JG, Mi T, Xia Y, Kellems RE, Blackburn MR: **Adenosine-dependent pulmonary fibrosis in adenosine deaminase-deficient mice.** *J Immunol* 2005, **175**(3):1937-1946.
71. Chunn JL, Young HW, Banerjee SK, Colasurdo GN, Blackburn MR: **Adenosine-dependent airway inflammation and hyperresponsiveness in partially adenosine deaminase-deficient mice.** *J Immunol* 2001, **167**(8):4676-4685.
72. Zhang Y, Dai Y, Wen J, Zhang W, Grenz A, Sun H, Tao L, Lu G, Alexander DC, Milburn MV, Carter-Dawson L, Lewis DE, Zhang W, Eltzschig HK, Kellems RE, Blackburn MR, Juneja HS, Xia Y: **Detrimental effects of adenosine signaling in sickle cell disease.** *Nat Med* 2011, **17**(1):79-86.
73. Aldrich MB, Blackburn MR, Datta SK, Kellems RE: **Adenosine deaminase-deficient mice: models for the study of lymphocyte development and adenosine signaling.** *Adv Exp Med Biol* 2000, **486**:57-63.

74. Olivera A, Kohama T, Tu Z, Milstien S, Spiegel S: **Purification and characterization of rat kidney sphingosine kinase.** *J Biol Chem* 1998, **273**(20):12576-12583.
75. Johnson KR, Becker KP, Facchinetti MM, Hannun YA, Obeid LM: **PKC-dependent activation of sphingosine kinase 1 and translocation to the plasma membrane. Extracellular release of sphingosine-1-phosphate induced by phorbol 12-myristate 13-acetate (PMA).** *J Biol Chem* 2002, **277**(38):35257-35262.
76. D'Alessandro A, Hansen KC, Silliman CC, Moore EE, Kelher M, Banerjee A: **Metabolomics of AS-5 RBC supernatants following routine storage.** *Vox Sang* 2015, **108**(2):131-140.
77. D'Alessandro A, Amelio I, Berkers CR, Antonov A, Vousden KH, Melino G, Zolla L: **Metabolic effect of TAp63alpha: enhanced glycolysis and pentose phosphate pathway, resulting in increased antioxidant defense.** *Oncotarget* 2014, **5**(17):7722-7733.
78. Lewis IA, Campanella ME, Markley JL, Low PS: **Role of band 3 in regulating metabolic flux of red blood cells.** *Proc Natl Acad Sci U S A* 2009, **106**(44):18515-18520.
79. Raleigh JA, Calkins-Adams DP, Rinker LH, Ballenger CA, Weissler MC, Fowler WC, Jr., Novotny DB, Varia MA: **Hypoxia and vascular endothelial growth factor expression in human squamous cell carcinomas using pimonidazole as a hypoxia marker.** *Cancer Res* 1998, **58**(17):3765-3768.
80. Aguilera KY, Rivera LB, Hur H, Carbon JG, Toombs JE, Goldstein CD, Dellinger MT, Castrillon DH, Brekken RA: **Collagen signaling enhances tumor progression after anti-VEGF therapy in a murine model of pancreatic ductal adenocarcinoma.** *Cancer Res* 2014, **74**(4):1032-1044.
81. Ericson A, de Verdier CH: **A modified method for the determination of 2,3-diphosphoglycerate in erythrocytes.** *Scand J Clin Lab Invest* 1972, **29**(1):84-90.
82. Lichtman MA, Murphy MS, Adamson JW: **Detection of mutant hemoglobins with altered affinity for oxygen. A simplified technique.** *Ann Intern Med* 1976, **84**(5):517-520.

83. Lin YL, Jiang G, Zhang Z, Nor JE, ElSayed ME: **Silencing bcl-2 expression in epithelial cancer cells using "smart" particles.** *J Funct Biomater* 2014, **5**(3):167-182.
84. Kuross SA, Rank BH, Hebbel RP: **Excess heme in sickle erythrocyte inside-out membranes: possible role in thiol oxidation.** *Blood* 1988, **71**(4):876-882.
85. Safo MK, Abraham DJ: **X-ray crystallography of hemoglobins.** *Methods Mol Med* 2003, **82**:1-19.
86. Winn MD, Ballard CC, Cowtan KD, Dodson EJ, Emsley P, Evans PR, Keegan RM, Krissinel EB, Leslie AG, McCoy A, McNicholas SJ, Murshudov GN, Pannu NS, Potterton EA, Powell HR, Read RJ, Vagin A, Wilson KS: **Overview of the CCP4 suite and current developments.** *Acta Crystallogr D Biol Crystallogr* 2011, **67**(Pt 4):235-242.
87. Adams PD, Afonine PV, Bunkoczi G, Chen VB, Echols N, Headd JJ, Hung LW, Jain S, Kapral GJ, Grosse Kunstleve RW, McCoy AJ, Moriarty NW, Oeffner RD, Read RJ, Richardson DC, Richardson JS, Terwilliger TC, Zwart PH: **The Phenix software for automated determination of macromolecular structures.** *Methods* 2011, **55**(1):94-106.
88. Park SY, Yokoyama T, Shibayama N, Shiro Y, Tame JR: **1.25 Å resolution crystal structures of human haemoglobin in the oxy, deoxy and carbonmonoxy forms.** *J Mol Biol* 2006, **360**(3):690-701.
89. Brunger AT, Adams PD, Clore GM, DeLano WL, Gros P, Grosse-Kunstleve RW, Jiang JS, Kuszewski J, Nilges M, Pannu NS, Read RJ, Rice LM, Simonson T, Warren GL: **Crystallography & NMR system: A new software suite for macromolecular structure determination.** *Acta Crystallogr D Biol Crystallogr* 1998, **54**(Pt 5):905-921.
90. Emsley P, Lohkamp B, Scott WG, Cowtan K: **Features and development of Coot.** *Acta Crystallogr D Biol Crystallogr* 2010, **66**(Pt 4):486-501.
91. Sun K, Zhang Y, Bogdanov MV, Wu H, Song A, Li J, Dowhan W, Idowu M, Juneja HS, Molina JG, Blackburn MR, Kellems RE, Xia Y: **Elevated adenosine signaling via adenosine A2B receptor**

- induces normal and sickle erythrocyte sphingosine kinase 1 activity.** *Blood* 2015, **125**(10):1643-1652.
92. Mulders AC, Hendriks-Balk MC, Mathy MJ, Michel MC, Alewijnse AE, Peters SL: **Sphingosine kinase-dependent activation of endothelial nitric oxide synthase by angiotensin II.** *Arterioscler Thromb Vasc Biol* 2006, **26**(9):2043-2048.
93. Pettus BJ, Bielawski J, Porcelli AM, Reames DL, Johnson KR, Morrow J, Chalfant CE, Obeid LM, Hannun YA: **The sphingosine kinase 1/sphingosine-1-phosphate pathway mediates COX-2 induction and PGE2 production in response to TNF-alpha.** *FASEB J* 2003, **17**(11):1411-1421.
94. Zhi L, Leung BP, Melendez AJ: **Sphingosine kinase 1 regulates pro-inflammatory responses triggered by TNFalpha in primary human monocytes.** *J Cell Physiol* 2006, **208**(1):109-115.
95. Raymond MN, Bole-Feysot C, Banno Y, Tanfin Z, Robin P: **Endothelin-1 inhibits apoptosis through a sphingosine kinase 1-dependent mechanism in uterine leiomyoma ELT3 cells.** *Endocrinology* 2006, **147**(12):5873-5882.
96. Leiber D, Banno Y, Tanfin Z: **Exogenous sphingosine 1-phosphate and sphingosine kinase activated by endothelin-1 induced myometrial contraction through differential mechanisms.** *Am J Physiol Cell Physiol* 2007, **292**(1):C240-250.
97. Pitson SM: **Regulation of sphingosine kinase and sphingolipid signaling.** *Trends Biochem Sci* 2011, **36**(2):97-107.
98. Jacobson KA, Gao ZG: **Adenosine receptors as therapeutic targets.** *Nat Rev Drug Discov* 2006, **5**(3):247-264.
99. Fredholm BB, AP IJ, Jacobson KA, Linden J, Muller CE: **International Union of Basic and Clinical Pharmacology. LXXXI. Nomenclature and classification of adenosine receptors--an update.** *Pharmacol Rev* 2011, **63**(1):1-34.

100. Fredholm BB, AP IJ, Jacobson KA, Klotz KN, Linden J: **International Union of Pharmacology. XXV. Nomenclature and classification of adenosine receptors.** *Pharmacol Rev* 2001, **53**(4):527-552.
101. Wen J, Grenz A, Zhang Y, Dai Y, Kellems RE, Blackburn MR, Eltzhig HK, Xia Y: **A2B adenosine receptor contributes to penile erection via PI3K/AKT signaling cascade-mediated eNOS activation.** *Faseb J* 2011, **25**(8):2823-2830.
102. Dai Y, Zhang W, Wen J, Zhang Y, Kellems RE, Xia Y: **A2B Adenosine Receptor-Mediated Induction of IL-6 Promotes CKD.** *J Am Soc Nephrol* 2011, **22**(5):890-901.
103. Grant MB, Davis MI, Caballero S, Feoktistov I, Biaggioni I, Belardinelli L: **Proliferation, migration, and ERK activation in human retinal endothelial cells through A(2B) adenosine receptor stimulation.** *Invest Ophthalmol Vis Sci* 2001, **42**(9):2068-2073.
104. D'Alessandro A, Nemkov T, Sun K, Liu H, Song A, Monte AA, Subudhi AW, Lovering AT, Dvorkin D, Julian CG, Kevil CG, Kolluru GK, Shiva S, Gladwin MT, Xia Y, Hansen KC, Roach RC: **AltitudeOmics: Red Blood Cell Metabolic Adaptation to High Altitude Hypoxia.** *J Proteome Res* 2016, **15**(10):3883-3895.
105. Lenfant C, Torrance J, English E, Finch CA, Reynafarje C, Ramos J, Faura J: **Effect of altitude on oxygen binding by hemoglobin and on organic phosphate levels.** *J Clin Invest* 1968, **47**(12):2652-2656.
106. Xiong Y, Hla T: **S1P control of endothelial integrity.** *Curr Top Microbiol Immunol* 2014, **378**:85-105.
107. Allende ML, Sasaki T, Kawai H, Olivera A, Mi Y, van Echten-Deckert G, Hajdu R, Rosenbach M, Keohane CA, Mandala S, Spiegel S, Proia RL: **Mice deficient in sphingosine kinase 1 are rendered lymphopenic by FTY720.** *J Biol Chem* 2004, **279**(50):52487-52492.
108. Eckardt KU, Bernhardt WM, Weidemann A, Warnecke C, Rosenberger C, Wiesener MS, Willam C: **Role of hypoxia in the pathogenesis of renal disease.** *Kidney Int Suppl* 2005(99):S46-51.

109. Blaho VA, Hla T: **An update on the biology of sphingosine 1-phosphate receptors.** *J Lipid Res* 2014, **55**(8):1596-1608.
110. Berg JM, Tymoczko JL, Stryer L: **Biochemistry**, 5th edn. New York: W.H. Freeman; 2002.
111. Giardina B, Messina I, Scatena R, Castagnola M: **The multiple functions of hemoglobin.** *Crit Rev Biochem Mol Biol* 1995, **30**(3):165-196.
112. Messina I, Orlando M, Cassiano L, Pennacchietti L, Zuppi C, Castagnola M, Giardina B: **Human erythrocyte metabolism is modulated by the O₂-linked transition of hemoglobin.** *FEBS Lett* 1996, **390**(1):25-28.
113. Rogers SC, Said A, Corcuera D, McLaughlin D, Kell P, Doctor A: **Hypoxia limits antioxidant capacity in red blood cells by altering glycolytic pathway dominance.** *FASEB J* 2009, **23**(9):3159-3170.
114. Benesch R, Benesch RE: **Intracellular organic phosphates as regulators of oxygen release by haemoglobin.** *Nature* 1969, **221**(5181):618-622.
115. Benesch R, Benesch RE, Enoki Y: **The interaction of hemoglobin and its subunits with 2,3-diphosphoglycerate.** *Proc Natl Acad Sci U S A* 1968, **61**(3):1102-1106.
116. Benesch R, Macduff G, Benesch RE: **Determination of Oxygen Equilibria with a Versatile New Tonometer.** *Anal Biochem* 1965, **11**:81-87.
117. Bansil R, Herzfeld J, Stanley HE: **Hemoglobin kinetics and the effect of organic phosphates.** *Science* 1974, **186**(4167):929-932.
118. Madigan C, Malik P: **Pathophysiology and therapy for haemoglobinopathies. Part I: sickle cell disease.** *Expert Rev Mol Med* 2006, **8**(9):1-23.
119. Spiegel S, Milstien S: **The outs and the ins of sphingosine-1-phosphate in immunity.** *Nat Rev Immunol* 2011, **11**(6):403-415.

120. Bosman GJ: **The involvement of erythrocyte metabolism in organismal homeostasis in health and disease.** *Proteomics Clin Appl* 2016.
121. Xia J, Sinelnikov IV, Han B, Wishart DS: **MetaboAnalyst 3.0--making metabolomics more meaningful.** *Nucleic Acids Res* 2015, **43**(W1):W251-257.
122. van Wijk R, van Solinge WW: **The energy-less red blood cell is lost: erythrocyte enzyme abnormalities of glycolysis.** *Blood* 2005, **106**(13):4034-4042.
123. Mulquiney PJ, Bubb WA, Kuchel PW: **Model of 2,3-bisphosphoglycerate metabolism in the human erythrocyte based on detailed enzyme kinetic equations: in vivo kinetic characterization of 2,3-bisphosphoglycerate synthase/phosphatase using ¹³C and ³¹P NMR.** *Biochem J* 1999, **342 Pt 3**:567-580.
124. Campanella ME, Chu H, Wandersee NJ, Peters LL, Mohandas N, Gilligan DM, Low PS: **Characterization of glycolytic enzyme interactions with murine erythrocyte membranes in wild-type and membrane protein knockout mice.** *Blood* 2008, **112**(9):3900-3906.
125. Charache S, Grisolia S, Fiedler AJ, Hellegers AE: **Effect of 2,3-diphosphoglycerate on oxygen affinity of blood in sickle cell anemia.** *J Clin Invest* 1970, **49**(4):806-812.
126. Poillon WN, Kim BC, Labotka RJ, Hicks CU, Kark JA: **Antisickling effects of 2,3-diphosphoglycerate depletion.** *Blood* 1995, **85**(11):3289-3296.
127. Ghatge MS, Ahmed MH, Omar AS, Pagare PP, Rosef S, Kellogg GE, Abdulmalik O, Safo MK: **Crystal structure of carbonmonoxy sickle hemoglobin in R-state conformation.** *J Struct Biol* 2016, **194**(3):446-450.
128. Harrington DJ, Adachi K, Royer WE, Jr.: **The high resolution crystal structure of deoxyhemoglobin S.** *J Mol Biol* 1997, **272**(3):398-407.
129. Safo MK, Ahmed MH, Ghatge MS, Boyiri T: **Hemoglobin-ligand binding: understanding Hb function and allostery on atomic level.** *Biochim Biophys Acta* 2011, **1814**(6):797-809.

130. Baldwin J, Chothia C: **Haemoglobin: the structural changes related to ligand binding and its allosteric mechanism.** *J Mol Biol* 1979, **129**(2):175-220.
131. Anelli V, Gault CR, Cheng AB, Obeid LM: **Sphingosine kinase 1 is up-regulated during hypoxia in U87MG glioma cells. Role of hypoxia-inducible factors 1 and 2.** *J Biol Chem* 2008, **283**(6):3365-3375.
132. Schwalm S, Doll F, Romer I, Bubnova S, Pfeilschifter J, Huwiler A: **Sphingosine kinase-1 is a hypoxia-regulated gene that stimulates migration of human endothelial cells.** *Biochem Biophys Res Commun* 2008, **368**(4):1020-1025.
133. Yun JK, Kester M: **Regulatory role of sphingomyelin metabolites in hypoxia-induced vascular smooth muscle cell proliferation.** *Arch Biochem Biophys* 2002, **408**(1):78-86.
134. Ahmad M, Long JS, Pyne NJ, Pyne S: **The effect of hypoxia on lipid phosphate receptor and sphingosine kinase expression and mitogen-activated protein kinase signaling in human pulmonary smooth muscle cells.** *Prostaglandins Other Lipid Mediat* 2006, **79**(3-4):278-286.
135. Stahelin RV, Hwang JH, Kim JH, Park ZY, Johnson KR, Obeid LM, Cho W: **The mechanism of membrane targeting of human sphingosine kinase 1.** *J Biol Chem* 2005, **280**(52):43030-43038.
136. Alemany R, Sichelschmidt B, zu Heringdorf DM, Lass H, van Koppen CJ, Jakobs KH: **Stimulation of sphingosine-1-phosphate formation by the P2Y(2) receptor in HL-60 cells: Ca(2+) requirement and implication in receptor-mediated Ca(2+) mobilization, but not MAP kinase activation.** *Mol Pharmacol* 2000, **58**(3):491-497.
137. Wattenberg BW, Pitson SM, Raben DM: **The sphingosine and diacylglycerol kinase superfamily of signaling kinases: localization as a key to signaling function.** *J Lipid Res* 2006, **47**(6):1128-1139.
138. Cuvillier O, Ader I: **Hypoxia-inducible factors and sphingosine 1-phosphate signaling.** *Anticancer Agents Med Chem* 2011, **11**(9):854-862.

139. Kalhori V, Kemppainen K, Asghar MY, Bergelin N, Jaakkola P, Tornquist K: **Sphingosine-1-Phosphate as a Regulator of Hypoxia-Induced Factor-1alpha in Thyroid Follicular Carcinoma Cells.** *PLoS One* 2013, **8**(6):e66189.
140. Michaud MD, Robitaille GA, Gratton JP, Richard DE: **Sphingosine-1-phosphate: a novel nonhypoxic activator of hypoxia-inducible factor-1 in vascular cells.** *Arterioscler Thromb Vasc Biol* 2009, **29**(6):902-908.
141. Srinivasan S, Bolick DT, Lukashev D, Lappas C, Sitkovsky M, Lynch KR, Hedrick CC: **Sphingosine-1-phosphate reduces CD4+ T-cell activation in type 1 diabetes through regulation of hypoxia-inducible factor short isoform I.1 and CD69.** *Diabetes* 2008, **57**(2):484-493.
142. Herr B, Zhou J, Werno C, Menrad H, Namgaladze D, Weigert A, Dehne N, Brune B: **The supernatant of apoptotic cells causes transcriptional activation of hypoxia-inducible factor-1alpha in macrophages via sphingosine-1-phosphate and transforming growth factor-beta.** *Blood* 2009, **114**(10):2140-2148.
143. Sanagawa A, Iwaki S, Asai M, Sakakibara D, Norimoto H, Sobel BE, Fujii S: **Sphingosine 1phosphate induced by hypoxia increases the expression of PAI1 in HepG2 cells via HIF1alpha.** *Mol Med Rep* 2016, **14**(2):1841-1848.
144. Ader I, Brizuela L, Bouquerel P, Malavaud B, Cu villier O: **Sphingosine kinase 1: a new modulator of hypoxia inducible factor 1alpha during hypoxia in human cancer cells.** *Cancer Res* 2008, **68**(20):8635-8642.
145. Karliner JS, Honbo N, Summers K, Gray MO, Goetzl EJ: **The lysophospholipids sphingosine-1-phosphate and lysophosphatidic acid enhance survival during hypoxia in neonatal rat cardiac myocytes.** *J Mol Cell Cardiol* 2001, **33**(9):1713-1717.

146. Zhang J, Honbo N, Goetzl EJ, Chatterjee K, Karliner JS, Gray MO: **Signals from type 1 sphingosine 1-phosphate receptors enhance adult mouse cardiac myocyte survival during hypoxia.** *Am J Physiol Heart Circ Physiol* 2007, **293**(5):H3150-3158.
147. Hisano Y, Kobayashi N, Yamaguchi A, Nishi T: **Mouse SPNS2 functions as a sphingosine-1-phosphate transporter in vascular endothelial cells.** *PLoS One* 2012, **7**(6):e38941.
148. Kobayashi N, Yamaguchi A, Nishi T: **Characterization of the ATP-dependent sphingosine 1-phosphate transporter in rat erythrocytes.** *J Biol Chem* 2009, **284**(32):21192-21200.
149. Golan K, Kollet O, Lapidot T: **Dynamic Cross Talk between S1P and CXCL12 Regulates Hematopoietic Stem Cells Migration, Development and Bone Remodeling.** *Pharmaceuticals (Basel)* 2013, **6**(9):1145-1169.
150. Ratajczak MZ, Lee H, Wysoczynski M, Wan W, Marlicz W, Laughlin MJ, Kucia M, Janowska-Wieczorek A, Ratajczak J: **Novel insight into stem cell mobilization-plasma sphingosine-1-phosphate is a major chemoattractant that directs the egress of hematopoietic stem progenitor cells from the bone marrow and its level in peripheral blood increases during mobilization due to activation of complement cascade/membrane attack complex.** *Leukemia* 2010, **24**(5):976-985.
151. Harrison ML, Rathinavelu P, Arese P, Geahlen RL, Low PS: **Role of band 3 tyrosine phosphorylation in the regulation of erythrocyte glycolysis.** *J Biol Chem* 1991, **266**(7):4106-4111.
152. Low PS, Rathinavelu P, Harrison ML: **Regulation of glycolysis via reversible enzyme binding to the membrane protein, band 3.** *J Biol Chem* 1993, **268**(20):14627-14631.
153. Tsuneshige A, Imai K, Tyuma I: **The binding of hemoglobin to red cell membrane lowers its oxygen affinity.** *J Biochem* 1987, **101**(3):695-704.

154. Strub GM, Paillard M, Liang J, Gomez L, Allegood JC, Hait NC, Maceyka M, Price MM, Chen Q, Simpson DC, Kordula T, Milstien S, Lesnefsky EJ, Spiegel S: **Sphingosine-1-phosphate produced by sphingosine kinase 2 in mitochondria interacts with prohibitin 2 to regulate complex IV assembly and respiration.** *FASEB J* 2011, **25**(2):600-612.
155. Doctor A, Spinella P: **Effect of processing and storage on red blood cell function in vivo.** *Semin Perinatol* 2012, **36**(4):248-259.
156. Pawloski JR, Hess DT, Stamler JS: **Export by red blood cells of nitric oxide bioactivity.** *Nature* 2001, **409**(6820):622-626.
157. Bruce LJ, Beckmann R, Ribeiro ML, Peters LL, Chasis JA, Delaunay J, Mohandas N, Anstee DJ, Tanner MJ: **A band 3-based macrocomplex of integral and peripheral proteins in the RBC membrane.** *Blood* 2003, **101**(10):4180-4188.
158. Mack AK, Kato GJ: **Sickle cell disease and nitric oxide: a paradigm shift?** *Int J Biochem Cell Biol* 2006, **38**(8):1237-1243.
159. Belanger AM, Keggi C, Kaniias T, Gladwin MT, Kim-Shapiro DB: **Effects of nitric oxide and its congeners on sickle red blood cell deformability.** *Transfusion* 2015, **55**(10):2464-2472.
160. Chang TL, Kakhniashvili DG, Goodman SR: **Spectrin's E2/E3 ubiquitin conjugating/ligating activity is diminished in sickle cells.** *Am J Hematol* 2005, **79**(2):89-96.
161. Shibayama N, Miura S, Tame JR, Yonetani T, Park SY: **Crystal structure of horse carbonmonoxyhemoglobin-bezafibrate complex at 1.55-A resolution. A novel allosteric binding site in R-state hemoglobin.** *J Biol Chem* 2002, **277**(41):38791-38796.
162. Yokoyama T, Neya S, Tsuneshige A, Yonetani T, Park SY, Tame JR: **R-state haemoglobin with low oxygen affinity: crystal structures of deoxy human and carbonmonoxy horse haemoglobin bound to the effector molecule L35.** *J Mol Biol* 2006, **356**(3):790-801.

163. Jensen FB: **The dual roles of red blood cells in tissue oxygen delivery: oxygen carriers and regulators of local blood flow.** *J Exp Biol* 2009, **212**(Pt 21):3387-3393.
164. Jagger JE, Bateman RM, Ellsworth ML, Ellis CG: **Role of erythrocyte in regulating local O₂ delivery mediated by hemoglobin oxygenation.** *Am J Physiol Heart Circ Physiol* 2001, **280**(6):H2833-2839.
165. Igarashi J, Bernier SG, Michel T: **Sphingosine 1-phosphate and activation of endothelial nitric-oxide synthase. differential regulation of Akt and MAP kinase pathways by EDG and bradykinin receptors in vascular endothelial cells.** *J Biol Chem* 2001, **276**(15):12420-12426.
166. Kleinbongard P, Schulz R, Rassaf T, Lauer T, Dejam A, Jax T, Kumara I, Gharini P, Kabanova S, Ozuyaman B, Schnurch HG, Godecke A, Weber AA, Robenek M, Robenek H, Bloch W, Rosen P, Kelm M: **Red blood cells express a functional endothelial nitric oxide synthase.** *Blood* 2006, **107**(7):2943-2951.
167. Sirover MA: **New insights into an old protein: the functional diversity of mammalian glyceraldehyde-3-phosphate dehydrogenase.** *Biochim Biophys Acta* 1999, **1432**(2):159-184.
168. Branlant G, Branlant C: **Nucleotide sequence of the Escherichia coli gap gene. Different evolutionary behavior of the NAD⁺-binding domain and of the catalytic domain of D-glyceraldehyde-3-phosphate dehydrogenase.** *Eur J Biochem* 1985, **150**(1):61-66.
169. Butterfield DA, Hardas SS, Lange ML: **Oxidatively modified glyceraldehyde-3-phosphate dehydrogenase (GAPDH) and Alzheimer's disease: many pathways to neurodegeneration.** *J Alzheimers Dis* 2010, **20**(2):369-393.
170. Fukuda M, Gotoh I, Gotoh Y, Nishida E: **Cytoplasmic localization of mitogen-activated protein kinase kinase directed by its NH₂-terminal, leucine-rich short amino acid sequence, which acts as a nuclear export signal.** *J Biol Chem* 1996, **271**(33):20024-20028.

171. Eby D, Kirtley ME: **Role of lysine residues in the binding of glyceraldehyde-3-phosphate dehydrogenase to human erythrocyte membranes.** *Biochem Biophys Res Commun* 1983, **116**(2):423-427.
172. Reisz JA, Wither MJ, Dzieciatkowska M, Nemkov T, Issaian A, Yoshida T, Dunham AJ, Hill RC, Hansen KC, D'Alessandro A: **Oxidative modifications of glyceraldehyde 3-phosphate dehydrogenase regulate metabolic reprogramming of stored red blood cells.** *Blood* 2016, **128**(12):e32-42.
173. Mohr S, Stamler JS, Brune B: **Posttranslational modification of glyceraldehyde-3-phosphate dehydrogenase by S-nitrosylation and subsequent NADH attachment.** *J Biol Chem* 1996, **271**(8):4209-4214.
174. Yogalingam G, Hwang S, Ferreira JC, Mochly-Rosen D: **Glyceraldehyde-3-phosphate dehydrogenase (GAPDH) phosphorylation by protein kinase Cdelta (PKCdelta) inhibits mitochondria elimination by lysosomal-like structures following ischemia and reoxygenation-induced injury.** *J Biol Chem* 2013, **288**(26):18947-18960.
175. Chang C, Su H, Zhang D, Wang Y, Shen Q, Liu B, Huang R, Zhou T, Peng C, Wong CC, Shen HM, Lippincott-Schwartz J, Liu W: **AMPK-Dependent Phosphorylation of GAPDH Triggers Sirt1 Activation and Is Necessary for Autophagy upon Glucose Starvation.** *Mol Cell* 2015, **60**(6):930-940.
176. Hershfield MS: **PEG-ADA: an alternative to haploidentical bone marrow transplantation and an adjunct to gene therapy for adenosine deaminase deficiency.** *Hum Mutat* 1995, **5**(2):107-112.
177. Field JJ, Nathan DG, Linden J: **Targeting iNKT cells for the treatment of sickle cell disease.** *Clin Immunol* 2011, **140**(2):177-183.
178. Muller CE, Jacobson KA: **Recent developments in adenosine receptor ligands and their potential as novel drugs.** *Biochim Biophys Acta* 2011, **1808**(5):1290-1308.

179. Eckle T, Krahn T, Grenz A, Kohler D, Mittelbronn M, Ledent C, Jacobson MA, Osswald H, Thompson LF, Unertl K, Eltzschig HK: **Cardioprotection by ecto-5'-nucleotidase (CD73) and A2B adenosine receptors.** *Circulation* 2007, **115**(12):1581-1590.
180. Nagahashi M, Ramachandran S, Kim EY, Allegood JC, Rashid OM, Yamada A, Zhao R, Milstien S, Zhou H, Spiegel S, Takabe K: **Sphingosine-1-phosphate produced by sphingosine kinase 1 promotes breast cancer progression by stimulating angiogenesis and lymphangiogenesis.** *Cancer Res* 2012, **72**(3):726-735.
181. Paugh SW, Paugh BS, Rahmani M, Kapitonov D, Almenara JA, Kordula T, Milstien S, Adams JK, Zipkin RE, Grant S, Spiegel S: **A selective sphingosine kinase 1 inhibitor integrates multiple molecular therapeutic targets in human leukemia.** *Blood* 2008, **112**(4):1382-1391.
182. Kapitonov D, Allegood JC, Mitchell C, Hait NC, Almenara JA, Adams JK, Zipkin RE, Dent P, Kordula T, Milstien S, Spiegel S: **Targeting sphingosine kinase 1 inhibits Akt signaling, induces apoptosis, and suppresses growth of human glioblastoma cells and xenografts.** *Cancer Res* 2009, **69**(17):6915-6923.
183. Price MM, Oskeritzian CA, Falanga YT, Harikumar KB, Allegood JC, Alvarez SE, Conrad D, Ryan JJ, Milstien S, Spiegel S: **A specific sphingosine kinase 1 inhibitor attenuates airway hyperresponsiveness and inflammation in a mast cell-dependent murine model of allergic asthma.** *J Allergy Clin Immunol* 2013, **131**(2):501-511 e501.
184. Dickson MA, Carvajal RD, Merrill AH, Jr., Gonen M, Cane LM, Schwartz GK: **A phase I clinical trial of safingol in combination with cisplatin in advanced solid tumors.** *Clin Cancer Res* 2011, **17**(8):2484-2492.
185. Gao P, Peterson YK, Smith RA, Smith CD: **Characterization of isoenzyme-selective inhibitors of human sphingosine kinases.** *PLoS One* 2012, **7**(9):e44543.

186. Schnute ME, McReynolds MD, Kasten T, Yates M, Jerome G, Rains JW, Hall T, Chrencik J, Kraus M, Cronin CN, Saabye M, Highkin MK, Broadus R, Ogawa S, Cukyne K, Zawadzke LE, Peterkin V, Iyanar K, Scholten JA, Wendling J, Fujiwara H, Nemirovskiy O, Wittwer AJ, Nagiec MM: **Modulation of cellular S1P levels with a novel, potent and specific inhibitor of sphingosine kinase-1.** *Biochem J* 2012, **444**(1):79-88.
187. MacRitchie N, Volpert G, Al Washih M, Watson DG, Futerman AH, Kennedy S, Pyne S, Pyne NJ: **Effect of the sphingosine kinase 1 selective inhibitor, PF-543 on arterial and cardiac remodelling in a hypoxic model of pulmonary arterial hypertension.** *Cell Signal* 2016, **28**(8):946-955.
188. Ryan TM, Ciavatta DJ, Townes TM: **Knockout-transgenic mouse model of sickle cell disease.** *Science* 1997, **278**(5339):873-876.
189. Sanford M: **Fingolimod: a review of its use in relapsing-remitting multiple sclerosis.** *Drugs* 2014, **74**(12):1411-1433.
190. Brinkmann V, Billich A, Baumruker T, Heining P, Schmouder R, Francis G, Aradhye S, Burtin P: **Fingolimod (FTY720): discovery and development of an oral drug to treat multiple sclerosis.** *Nat Rev Drug Discov* 2010, **9**(11):883-897.
191. Liang J, Nagahashi M, Kim EY, Harikumar KB, Yamada A, Huang WC, Hait NC, Allegood JC, Price MM, Avni D, Takabe K, Kordula T, Milstien S, Spiegel S: **Sphingosine-1-phosphate links persistent STAT3 activation, chronic intestinal inflammation, and development of colitis-associated cancer.** *Cancer Cell* 2013, **23**(1):107-120.
192. Lee H, Deng J, Kujawski M, Yang C, Liu Y, Herrmann A, Kortylewski M, Horne D, Somlo G, Forman S, Jove R, Yu H: **STAT3-induced S1PR1 expression is crucial for persistent STAT3 activation in tumors.** *Nat Med* 2010, **16**(12):1421-1428.

193. Mandala S, Hajdu R, Bergstrom J, Quackenbush E, Xie J, Milligan J, Thornton R, Shei GJ, Card D, Keohane C, Rosenbach M, Hale J, Lynch CL, Rupprecht K, Parsons W, Rosen H: **Alteration of lymphocyte trafficking by sphingosine-1-phosphate receptor agonists.** *Science* 2002, **296**(5566):346-349.
194. Saddoughi SA, Gencer S, Peterson YK, Ward KE, Mukhopadhyay A, Oaks J, Bielawski J, Szulc ZM, Thomas RJ, Selvam SP, Senkal CE, Garrett-Mayer E, De Palma RM, Fedarovich D, Liu A, Habib AA, Stahelin RV, Perrotti D, Ogretmen B: **Sphingosine analogue drug FTY720 targets I2PP2A/SET and mediates lung tumour suppression via activation of PP2A-RIPK1-dependent necroptosis.** *EMBO Mol Med* 2013, **5**(1):105-121.
195. Sabbadini RA: **Sphingosine-1-phosphate antibodies as potential agents in the treatment of cancer and age-related macular degeneration.** *Br J Pharmacol* 2011, **162**(6):1225-1238.

Bibliography

NAME

KAIQI SUN

PRESENT POSITION AND ADDRESS

Ph.D candidate in Biochemistry and Molecular Biology
UT MD Anderson Cancer Center UT Health Graduate School of
Biomedical Science
6431 Fannin Street, MSB 6.014, Houston TX 77030
Mobile: 1-281-793-8025
Office: 1-713-500-6063
Fax: 1-713-500-0652
E-mail: Kaiqi.sun@uth.tmc.edu

EDUCATION

- | | |
|-----------------|--|
| 12/2013-present | Ph.D candidate in Biochemistry and Molecular Biology, UT MD Anderson Cancer Center UT Health Graduate School of Biomedical Science, Houston TX |
| 8/2011-12/2013 | Doctoral student, UT MD Anderson Cancer Center UT Health Graduate School of Biomedical Science, Houston TX |
| 9/2007-6/2011 | B.Sc in Biological Sciences, Central South University-Xiang Ya School of Medicine, Changsha China. |

RESEARCH SUMMARY

My research focuses on understanding how erythrocytes oxygen delivery ability is regulated by physiological and pathological stimuli. In particular, I am interested in the role and regulation of a bioactive signaling lipid-Sphingosine 1-phosphate, which is highly enriched in erythrocytes. My academic training and research experiences to date have provided me with an excellent background in biochemistry and translational medicine. As an undergraduate at Xiang-ya School of Medicine, Central South University in China, I conducted research with Dr. Rong Xiang on endothelial cell migration, proliferation and apoptosis, which resulted in two co-authorship publications, as well as the first prize award to my undergraduate thesis work. In my graduate training at the UT MD Anderson Cancer Center UT Health Graduate School of Biomedical Science, I study erythrocyte physiology and pathology under the supervisory of Dr. Yang Xia. Dr. Xia is an internationally recognized expert in the field of erythrocyte metabolism, Sickle Cell Diseases and cardiovascular diseases. So far, my research has led to two first

author research publications in the prestigious journal *Blood* and *Nature Communications*, one review paper published in *Current Opinion of Hematology* and seven co-author publications in other high-profile journals including *Circulation*, *Journal of Clinical Investigation*, *Circulation Research*, *Scientific Reports* and *Cell Reports*. I have another three manuscripts in preparation or under review as of Feb 2017.

RESEARCH EXPERIENCES

- 8/2012-present Graduate Research Assistant in Dr. Yang Xia's lab, Dept. of Biochemistry and Molecular Biology, UT Health McGovern Medical School, Houston TX
- 9/2009-1/2011 Undergraduate Research Assistant in Dr. Rong Xiang's lab, Dept. of Cell Biology, Central South University-Xiang Ya School of Medicine, Changsha China
- 6-8/2008 Summer research fellow, Biomass Energy Research Center, Central South University, Changsha, China

PUBLICATIONS

1. **Sun K***, Zhang Y*, D'Alessandro A*, et al. Sphingosine 1 Phosphate Promotes Erythrocyte Glycolysis and Oxygen Release for Adaptation to High Altitude Hypoxia. *Nat Commun*. 2016 Jul 15;7:12086.
2. **Sun K**, Zhang Y, Bogdanov MV, et al. Elevated adenosine signaling via adenosine A2B receptor induces normal and sickle erythrocyte sphingosine kinase 1 activity. *Blood*. Mar 5 2015;125(10):1643-1652.
3. **Sun K**, Xia Y. New insights into sickle cell disease: a disease of hypoxia. *Curr Opin Hematol*. May 2013;20(3):215-221.
4. Iriyama T, **Sun K**, Parchim NF, et al. Elevated placental adenosine signaling contributes to the pathogenesis of preeclampsia. *Circulation*. Feb 24 2015;131(8):730-741.
5. Song A, Zhang Y, Han L, Yegutkin GG, Liu H, **Sun K**, D'Alessandro A, Li J, Karmouty-Quintana H, Iriyama T et al: Erythrocytes retain hypoxic adenosine response for faster acclimatization upon re-ascent. *Nat Commun* 2017, 8:14108.
6. Zhang Y, Berka V, Song A, **Sun K** et al. Elevated sphingosine-1-phosphate promotes sickling and sickle cell disease progression. *J Clin Invest*. Jun 2 2014;124(6):2750-2761.
7. Wu H, Bogdanov M, Zhang Y, **Sun K**, Zhao S, Song A, Luo R, Parchim NF, Liu H, Huang A et al: Hypoxia-mediated impaired erythrocyte Lands' Cycle is pathogenic for sickle cell disease. *Sci Rep* 2016, 6:29637.
8. Hu X, Adebisi MG, Luo J, **Sun K**, Le TT, Zhang Y, Wu H, Zhao S, Karmouty-Quintana H, Liu H et al: Sustained Elevated Adenosine via ADORA2B Promotes Chronic Pain through Neuro-immune Interaction. *Cell Rep* 2016, 16(1):106-119..
9. Liu H, Zhang Y, Wu H, D'Alessandro A, Yegutkin GG, Song A, **Sun K**, Li J, Cheng NY, Huang A et al: Beneficial Role of Erythrocyte Adenosine A2B Receptor-Mediated AMP-

- Activated Protein Kinase Activation in High-Altitude Hypoxia. *Circulation* 2016, 134(5):405-421.
10. Wang M, ... **Sun K**,... Xia Y, Lai Y. Iron overload correlates with serum liver fibrotic markers and liver dysfunction: Potential new methods to predict iron overload-related liver fibrosis in thalassemia patients. *United European Gastroenterology Journal*. April 28, 2016 2050640616646525.
 11. Zhang W, Zhang Y, Wang W, Dai Y, Ning C, Luo R, **Sun K**, Glover L, Grenz A, Sun H et al: Elevated ecto-5'-nucleotidase-mediated increased renal adenosine signaling via A2B adenosine receptor contributes to chronic hypertension. *Circ Res* 2013, 112(11):1466-1478.
 12. XIANG Rong, **SUN Kai-qi**, ZhONG E-ryun. Recent development of Cell Surface Molecule and Atherosclerosis. *International Journal of Genetics* [Chinese], 2010 33(3):171-174.
 13. Rong Xiang, Hong-Shan Guo, **Kai-Qi Sun**. Platelets: The Initiator and Promoter of Atherosclerosis. *Chinese Journal of Histochemistry and Cytochemistry* [Chinese], 2010 32(5): 777-780.

MANUSCRIPTS

14. **Sun K**, D'Alessandro A, Ahmed M ... Xia Y. Structural and Functional Insight of Sphingosine 1-Phosphate-Mediated Pathogenic Metabolic Reprogramming in Sickle Cell Disease. *Blood*. Under review.
15. **Sun K**, Xia Y. Erythrocyte Purinergic Signaling Components Underlies Hypoxia Adaptation. *Journal of Applied Physiology*. Under review.
16. **Sun K**, D'Alessandro A, Xia Y. Purinergic Control of Red Blood Cell Metabolism: novel strategies to improve red cell storage quality. *Blood Transfusion*. Under review

HONORS & AWARDS:

8/2016	President's Research Scholarship Award
5/2016	Highest Award-The Alexander Yeu-Ming Wang Memorial Scholarship award of the 30 th annual meeting of the Society of Chinese Bio-scientist in American (SCBA)-Texas Chapter
3/2016	First place in student oral presentation of the 2016 Biochemistry and Molecular Biology program retreat
7/2015	Dean's Research Scholarship
5/2015	Third-prize in oral presentation of the 29 th annual meeting of the Society of Chinese Bio-scientist in American (SCBA)-Texas Chapter
3/2015	Harry S. & Isabel C. Cameron Foundation Fellowship
6/2014	Outstanding student alumni of Xiang-ya Overseas Alumni Association
3/2014	First place in student poster presentation of the 2014 Biochemistry and Molecular Biology program retreat
12/2013	University of Texas Graduate School of Biomedical Science student travel award
12/2013	Abstract achievement award of the 55 th American Society of Hematology annual meeting
8/2013	University of Texas Graduate School of Biomedical Science program of

	Biochemistry and Molecular Biology student travel award
5/2013	Highest Award-The Alexander Yeu-Ming Wang Memorial Scholarship award of the 27 th annual meeting of the Society of Chinese Bio-scientist in American (SCBA)-Texas Chapter
3/2012	Third prize in oral presentation of the 2013 Biochemistry and Molecular Biology program annual retreat
3/2012	Third prize in poster presentation of the 2012 Biochemistry and Molecular Biology program annual retreat
6/2011	First Prize of Undergraduate thesis Award of Central South University
9/2010	Second Prize of Outstanding Student Scholarship of Central South University
9/2010	First Prize of Yale-China Scholarship
9/2009	Outstanding Undergraduate Student Award of Central South University
9/2009	Second Prize of Outstanding Student Scholarship of Central South University
4/2009	Second Prize in National English Contest for College Students

PRESENTATIONS:

1. Jun 2016 Student Research Day of The University of Texas Graduate School of Biomedical Sciences, Houston TX, oral presentation "Red Blood Cell Metabolic Reprogramming by Sphingosine 1-phosphate: Good, Bad, and Beyond"
2. May 2016 the 30th annual meeting of the Society of Chinese Bio-scientist in American (SCBA) Texas-Chapter, Houston TX, oral presentation "Structural and Functional Insight of Sphingosine 1-Phosphate-Mediated Pathogenic Metabolic Reprogramming in Sickle Cell Disease"
3. November 2015 UT Health-Medical School Retreat poster presentation "Erythrocyte sphingosine 1 phosphate: a key intracellular modulator for adaptation to high altitude hypoxia"
4. May 2015 the 29th annual meeting of the Society of Chinese Bio-scientist in American (SCBA) Texas-Chapter, Houston TX, oral presentation "Erythrocyte sphingosine 1 phosphate: a key intracellular modulator for adaptation to high altitude hypoxia"
5. December 2014 the 56th American Society of Hematology annual meeting, San Francisco, CA.
6. Poster presentation "Elevated Adenosine Signaling via Adenosine A2B Receptor Induces Normal and Sickle Erythrocyte Sphingosine Kinase 1 Activity in Human and Mice"
7. March 2014 Biochemistry and Molecular Biology Spring Retreat, New Braunfels, TX-Poster presentation
8. December 2013 the 55th American Society of Hematology annual meeting, New Orleans LA, oral presentation "Role and Regulation of Erythrocyte Sphingosine Kinase 1 in Normal and Sickle Cell Disease"
9. May 2013 the 27th annual meeting of the Society of Chinese Bio-scientist in American (SCBA) Texas-Chapter, Houston TX, oral presentation "Regulation of

Sphingosine Kinase 1 (Sphk1) Activity by Adenosine through ADOA2B Receptor in Normal and Sickle Erythrocyte”

10. March 2013 Biochemistry and Molecular Biology Spring Retreat, Camp Allen, TX-Oral presentation, “Regulation of Sphingosine Kinase 1 activity by adenosine through ADOA2B receptor in normal and Sickle Cell Disease erythrocyte”

11. March 2012 Biochemistry and Molecular Biology Spring Retreat, Camp Allen, TX-Poster presentation, “Sphingosine 1-Phosphate Receptors Expression Profiles in Sickle and Normal Human Erythrocytes”

OTHER EXPERIENCE AND PROFESSIONAL MEMBERSHIPS

1/2016-1/2017	Vice President of the Consulting Club at the Texas Medical Center
6-8/2015	Program Management PhD Intern at Regeneron Pharmaceuticals, Inc.
9/2014-1/2016	One of the two student representatives in the Program Coordinating Committee of The University of Texas Graduate School of Biomedical Science
2/2014-4/2015	Post-candidacy student liaison of the Biochemistry and Molecular Biology Program, University of Texas Graduate School of Biomedical Science
12/2013-present	Student/Trainee Membership, American Heart Association/American Stroke Association
11/2013-present	Graduate/Medical Student Member, American Society of Hematology
2/2011-6/2011	Teaching assistant, Dept. of Cell Biology, Xiangya School of Medicine, Central South University, Changsha, China

CONTACT PERSON

- Ph.D advisor: Yang Xia, M.D, Ph.D, Professor, McGovern Scholar, Dept. of Biochemistry and Molecular Biology, UT Health. Email: yang.xia@uth.tmc.edu, Phone: +1 (713) 500-5039
- Advisory committee member: Rodney E. Kellems, Ph.D, Professor and Chairman, Dept. of Biochemistry and Molecular Biology, UT Health. Email: rodney.e.kellems@uth.tmc.edu, Phone: +1 (713) 500-6124
- Advisory & Candidacy Examination Committees member: Zheng (Jake) Chen, Ph.D, Assistant Professor, Dept. of Biochemistry and Molecular Biology, UT Health. Email: Zheng.Chen.1@uth.tmc.edu, Phone: +1 (713) 500-6809
- Advisory & Candidacy Examination Committee member: Dorothy E. Lewis, Ph.D, Professor, Dept. of Internal Medicine, UT Health. Email: dorothy.e.lewis@uth.tmc.edu, Phone: +1 (713) 500-6809
- Undergraduate thesis adviser: Rong Xiang, Ph.D, Professor, Associate Dean, Dept. of Cell Biology, School of Life Science, Central South University. Email: rongxiang@csu.edu.cn, Phone: +86 (731) 8265-0230

Vita

Kaiqi Sun was born in Lu'An, Anhui, P.R. China, on February 7, 1990, the son of Hong Jiang and Hong Sun. After completing his education at NO.2 Middle School, Lu'An, Anhui, P.R. China in 2007, he entered Xiangya School of Medicine, Central South University, Changsha, Hunan, P. R. China. He received the degree of Bachelor of Science with a major in Biological Sciences from Central South University in June, 2011. In August of 2011 he entered The University of Texas MD Anderson Cancer Center UT Health Graduate School of Biomedical Sciences.

Permanent address:

Fuhe Village, Jinzhai County

Lu'An, Anhui, P. R. China 237322